



Universidade do Minho
Escola de Engenharia

Helena Prado Felgueiras

**MG63 osteoblast-like cells response to
surface modified commercially pure titanium**



Universidade do Minho

Escola de Engenharia

Helena Prado Felgueiras

Mg63 osteoblast-like cells response to surface modified commercially pure titanium

Master Degree in Biomedical Engineering
Area of Biomaterials, Biomechanics and Rehabilitation

Supervisor:

Professor Luís Augusto Rocha

Co-supervisors:

Professor Véronique Migonney

Professor Didier Lutomski

Professor Mariana Contente Rangel Henriques

July 2011

AUTHOR: Helena Prado Felgueiras

EMAIL: felgueiras.helena@gmail.com

TITLE OF THE THESIS: MG63 osteoblast-like cells response to surface modified commercially pure titanium

SUPERVISOR:

Professor Luís Augusto Rocha

CO-SUPERVISORS:

Professor Véronique Migonney

Professor Didier Lutomski

Professor Mariana Contente Rangel Henriques

THESIS CONCLUDED IN: July 2011

Master Degree in Biomedical Engineering

Area of Biomaterials, Biomechanics and Rehabilitation

THE INTEGRAL REPRODUCTION OF THIS THESIS/REPORT IS ONLY AUTHORIZED FOR RESEARCH PURPOSES, PROVIDED PROPER COMMITMENT AND WRITTEN DECLARATION OF THE INTERESTED PART.

University of Minho, 2011

ACKNOWLEDGEMENTS

I sincerely thank my supervisor Professor Luís Rocha from University of Minho for the management of my master project as well as my Erasmus program. I also want to thank him for all his involvement and support during my time abroad.

I would like to thank my co-supervisor Professor Véronique Migonney for all the valuable suggestions and for giving me the opportunity of developing this project in her research group.

I also thank Professor Didier Lutomski for all the support and enthusiasm during my time in Campus de Bobigny, which motivated me to improve and to develop a better work.

A special thank to Professor Mariana Henriques from University of Minho and to Doctor Sylvie Changotade from Université Paris XIII for all their guidance and support. Their dynamics, insight view and pertinent suggestions helped me greatly during this investigation. They were excellent mentors with endless patience to discuss my doubts.

To Professor Ponthiaux from École Centrale de Paris and to Professor Celis from Katholieke Universiteit Leuven for their insightful view and pertinent questions during the discussion meetings.

To Soucunda Lessin, Sophiane Oughlis, Florence Poirier and the rest of the group of the Laboratory of Biomaterials and Special Polymers, from Campus de Bobigny, for their prompt help and great atmosphere at work.

To Alexandra Alves and Fernando Oliveira from the CT2M group for their collaboration on the titanium samples production.

To my family and to all my friends for their unconditional support and constant motivation.

ABSTRACT

The interaction between implanted materials and surrounding tissue, osseointegration, is the critical factor for the successful restoration and reconstruction of damaged body parts. Since the biological response is strongly influenced by the properties of the biomaterials outermost layer, after few minutes of contact a protein film will be formed on the implant surface and its stability will determine the long-term success of the implant. Attending to all the problems related to implantation, it has becoming essential to analyze in detail the response of the human body to different and modified biomaterials surfaces.

In this project, the interaction between the osteoblasts and the commercially pure titanium (CP Ti) was investigated. CP Ti samples were modified by anodic treatment, with calcium (Ca) and phosphorus (P), and all phases involved in the tissue restoration were carefully followed and examined. In parallel, tribocorrosion tests were conducted on that samples, prior to osteoblasts culture, to verify the influence of the chemical and physical properties of the surface on their development and with that extrapolate the possible response of the human body after some time of implantation.

As a result, it was proven that anodic treatment can be effective and can incite osteoblasts MG63 development on titanium surfaces. The adhesion and morphologic tests showed that, even after small periods of time, these cells found their way to interact with the surface and create a bond, which can prevail for longest periods of culture (proliferation). Regarding osteoblasts MG63 differentiation, the results showed a very distinct line of evolution, exposing some important traces of the osteoblasts maturation, with a small but perceptive improvement in the levels of calcium and phosphate, proportioned by the bioactive properties of the anodic film. On the tribocorroded surfaces, it was clear the cells adhesion and progression, although in a slower rate compared to the regular surfaces. Additionally, through this test, it was also verified the MG63 osteoblasts preference for rougher surfaces.

For future investigations, however, the anodic treatment conditions should be changed, starting for instance in the electrolyte composition, in order to achieve a much more significant improvement in the cells behaviour.

RESUMO

A interacção entre o implante e o tecido subjacente, osteointegração, é o factor crítico para uma restauração e reconstrução de regiões do corpo danificadas bem sucedida. Uma vez que a resposta biológica é fortemente influenciada pelas propriedades da camada mais externa dos biomateriais, após alguns minutos em contacto um filme proteico é formado à superfície do biomaterial e a sua estabilidade irá determinar o sucesso a longo prazo do implante. Tendo em consideração todos os problemas associados à colocação de um implante, a análise cuidadosa e detalhada da resposta do corpo humano a alterações na superfície dos biomateriais tem-se tornado essencial.

Neste projecto, a interacção entre os osteoblastos e o titânio comercialmente puro (Ti CP) foi investigada. A superfície das amostras de Ti CP foi modificada por tratamento anódico, com cálcio (Ca) e fósforo (P), e todas as fases envolvidas na restauração do tecido ósseo foram meticolosamente seguidas e examinadas. Em paralelo, testes tribocorrosivos foram conduzidos sobre as amostras, num período prévio à cultura celular, de modo a verificar a influência das propriedades físicas e químicas da superfície no desenvolvimento das células ósseas. Com isto pretendeu-se inferir acerca da resposta do corpo humano após algum tempo de implantação.

A partir dos resultados foi provada a eficácia do tratamento anódico e a sua influência positiva sobre o desenvolvimento dos osteoblastos MG63 em superfícies de Ti. Os ensaios de adesão e morfologia comprovaram que, mesmo após curtos períodos de tempo em contacto, as células são capazes de interagir e criar fortes ligações, capazes de prevalecer por longos períodos de cultura (proliferação). Relativamente à diferenciação celular dos osteoblasts MG63, os resultados demonstraram, com grande detalhe, a evolução do desenvolvimento osteoblástico, sendo, ainda, perceptiva uma pequena melhoria nos níveis de cálcio e fosfato proporcionado pelas propriedades bioactivas do filme anódico. Quanto às superfícies tribologicamente modificadas, foi evidente a adesão e progressão celular, contudo de uma forma mais lenta do que nas superfícies consideradas normais. Além disso, foi comprovada a preferência dos osteoblastos MG63 por superfícies mais rugosas.

Porém, em investigações futuras, as condições do tratamento anódico deverão ser mudados, começando por exemplo pela composição do electrólito. Deste modo, melhorias mais significativas no comportamento celular poderão ser alcançadas.

CONTENT

Scope and Structure of the Thesis	ix
List of Figures.....	x
List of Tables	xiii
List of Abbreviations/ Nomenclature	xiv
Chapter 1	1
General Introduction.....	2
Chapter 2	4
1. History: A Quick Overview.....	5
2. Dental Implants	5
2.1 Constitution	6
2.2 Implant Systems	7
2.3 Success and Failure	8
3. The Human Bone.....	9
3.1 Composition	9
3.2 Organization	10
3.3 Biological Dynamics	15
3.4 The Healing Process	17
4. Bone-Implant Interaction.....	18
4.1 Biological Mechanisms of Bone Formation in the Interface.....	18
4.2 Bone Adhesion	21
5. Biomaterials.....	22
5.1 Biocompatibility	23
5.2 Classes of Biomaterials	24
5.3 Dental Implants Materials	25
6. Titanium as a Biomaterial.....	26
6.1 Passive Film.....	28
7. Surface Modification	30
7.1 The Anodic Treatment.....	31
7.2 Titanium Surface Modifications: Characterization	32
8. Summary.....	39
Chapter 3	41

1. Samples Preparation	42
2. Surface Characterization.....	42
2.1 Surface Morphology and Chemical Composition	43
2.2 Surface Topography	44
2.3 Contact Angle and Surface Free Energy	45
3. Sterilization.....	47
4. Osteoblasts Culture.....	48
4.1 Culture Expansion	48
4.2 Adhesion.....	49
4.3 Spreading and Morphology	50
4.4 Proliferation.....	51
4.5 Alkaline Phosphatase Activity	52
4.6 Mineralization.....	53
5. Osteoblasts response to tribologically modified surfaces	55
6. Statistical Analysis	56
Chapter 4	57
1. Surface Characterization.....	58
1.1 Surface Morphology and Chemical Composition	58
1.2 Surface Topography	61
1.3 Contact Angles and Surface Free Energy.....	62
2. Osteoblasts Culture.....	63
2.1 Adhesion.....	64
2.2 Spreading and Morphology	67
2.3 Proliferation.....	73
2.4 Alkaline Phosphatase (ALP) Activity.....	77
2.5 Mineralization.....	78
3. Osteoblasts response to tribologically modified surfaces	80
Chapter 5	86
Conclusions	87
Future Perspectives.....	89
Bibliography	90

SCOPE AND STRUCTURE OF THE THESIS

The interaction between implanted materials and surrounding tissue was always taken as a concerning issue, since it defines the success or falling of an implant. In this investigation the main objective was to study this interaction.

Adhesion, proliferation and differentiation assays were conducted to observe the response of MG63 osteoblasts when in contact with different types of surfaces: anodized and etched treatments. Besides that, the influences of bioactive anodized surfaces on the osteoblasts behaviour were also taken into consideration and followed in detail, with an especial attention to the calcium and phosphate levels (mineralization). This thesis also contributes for a better understanding of the influence of tribocorrosion tests on commercially pure titanium samples and how their changes affect the osteoblasts development.

This thesis is divided in 5 chapters. The Chapter 1 corresponds to the general introduction. Here a small overview over all main subjects involved on this investigation is made and the objectives clearly defined.

Chapter 2 includes a complete literature review about all subjects related to the main theme. The knowledge transmitted in this chapter follows a hierarchical orientation that goes from the simplest aspects about dental implantation to the most complex details.

In the following chapter, Chapter 3, a description of the materials and methods employed in this project is provided. This includes all the steps involved in the development of the bone cells, their proliferation and levels of attachment to the surface as well as differentiation and their response to tribocorrosion modified surfaces.

Chapter 4 deals with the results from all the experiments/assays and each one of them is accompanied by insightful overviews and discussions.

Finally, Chapter 5 is devoted to the main conclusions of this work and to new perspectives for future researches.

LIST OF FIGURES

Figure 1. Basic constitution of a dental implant (10).	6
Figure 2. Schematic representation of an (A) endosteal and a (B) subperiosteal implant (9).	7
Figure 3. Schematic representation of the collagen molecules arrangement to form gap regions for hydroxyapatite deposition, during mineralization (21).	10
Figure 4. Representative diagram of the bone tissue organization (22).	11
Figure 5. Bone tissue cellular composition: osteoblasts, osteoclasts and osteocytes and lining cells. Totality of cells involved in the bone formation and in the regeneration process (25).	12
Figure 6. Stages of bone remodelling (adapted from (31)).	16
Figure 7. Osteointegration development on dental implants: (A) Time 0; (B) 1 week; (C) 2 months; (D) 1 year; (E) 10 years (46).	20
Figure 8. Mechanisms controlling cell adhesion (adapted from (57)).	22
Figure 9. Pourbaix diagram for the titanium-water system (89).	29
Figure 10. Simple schematic representation of an electrochemical cell (adapted from (103)).	32
Figure 11. Possible classification for contact angles (122).	38
Figure 12. Aspect of a CP Ti sample, after anodic treatment application.	42
Figure 13. Schematic representation of a contact angle between a liquid and a solid surface. θ = contact angle; γ_{sl} = solid-liquid interface free energy; γ_{lv} = liquid free energy; γ_{sv} = solid free energy (134).	45
Figure 14. Osteoblasts culture in a polystyrene culture flask (T ₇₅) (CANON A480). ...	48
Figure 15. Six wells plate prepared for culture. A1 and A2 – Anodized samples; E1 and E2 – Etched samples; and O1 and O2 – Control (without sample). To each well, 2 ml of medium with a total of 4×10^4 osteoblasts was added.	49
Figure 16. Side view, schematic representation of a plate well with culture medium and sample, showing the three main parts from where the cells are removed and afterwards counted.	50
Figure 17. (A) Unidirectional <i>pin-on-disc</i> approach on the samples surface (136). (B) 1. Anodized sample, 0.8 N; 2. Etched sample, 0.8 N.	55

Figure 18. SEM micrographies of the (A) etched and (B) anodized surface morphology. Magnification of 500X.	58
Figure 19. Spectra representative of the (A) etched and (B) anodic surface chemical composition – EDS analysis.	59
Figure 20. Evolution of the osteoblasts MG63 adhesion to (A) etched and (B) anodized surfaces from 0.5, 2 and 4 h of culture. (C) Control results obtained by the direct culture on the well (without any sample).	64
Figure 21. Evolution of the number of osteoblasts MG63 adhered to the anodized and etched surfaces with time. Trial followed from 0.5 to 4 h of incubation at 37°C and 5% CO ₂ in air (p < 0.05 for 0.5 and 4 h).	66
Figure 22. Osteoblasts MG63 morphology and geometry after adhesion on etched and anodized samples after 0.5, 2 and 4 h of culture. The images were obtained by fluorescent microscopy using <i>Phalloidin</i> to colour the actin fibres (resolution of 40X and scale = 40 µm).	68
Figure 23. SEM micrographies of osteoblasts MG63 on (A) etched and (B) anodized samples with 2000x of magnification. These are representative of the osteoblasts dispersion above the samples' surface after 4 h of culture.	70
Figure 24. (A) Osteoblasts conformation and spreading after 4 h of culture above an anodized surface. Image taken using Fluorescent Microscopy and <i>Phalloidin</i> as marker (resolution of 10X and scale = 10 µm). (B) Conversion of the image B to format <i>.tif</i> for shape and size analysis.	71
Figure 25. Osteoblasts dimension after (A) 0.5 h, (B) 2 h and (C) 4 h of incubation onto anodized and etched Ti surfaces.	71
Figure 26. Evolution of the osteoblasts MG63 dimension on the anodized and etched samples, with time.	72
Figure 27. Evolution of the osteoblasts MG63 proliferation on (A) etched and (B) anodized surfaces from 1 to 14 days of culture (5 periods of time). (C) Control results obtained by the direct culture on the plate (without any sample), for the same periods of time.	73
Figure 28. Evolution of the number of osteoblasts MG63 on the anodized and etched surfaces, with time. Trial followed from 1 to 14 days of incubation at 37°C and 5% CO ₂ in air (no significant differences p > 0.05).	75

Figure 29. Osteoblasts MG63 confluence on etched and anodized samples after 7 and 14 days of culture. The images were obtained by fluorescent microscopy using <i>Phalloidin</i> , to colour the actin fibres (resolution of 10X and scale = 10 μm).	76
Figure 30. Evolution of the ALP activity with time (from 7 to 28 days of culture; control = culture directly on the plate surface, without sample) – significant results were detected for 14 and 21 days of culture, $p < 0.05$	77
Figure 31. Evolution of the (A) calcium and (B) phosphate levels with time (from 7 to 28 days of culture).	79
Figure 32. SEM micrographies representative of osteoblasts MG63 dispersion on the etched samples after 4 hours of culture (2000x of magnification). (A) and (B) images on the normal surface, and the (C) and (D) on the wear track (centre of the samples).	81
Figure 33. SEM micrographies representative of osteoblasts MG63 dispersion on the anodized samples after 4 hours of culture (2000x of magnification). (A) and (B) images on the normal surface, and the (C) and (D) on the wear track (centre of the samples)..	82
Figure 34. SEM micrographies of osteoblasts MG63 cultured on etched and anodized surfaces, for 3 and 7 days (magnification 1000 X). The designation “TRIBO Surface” indicates the visualization on the wear track (→ assembly of osteoblasts).	85

LIST OF TABLES

Table 1. Mechanical properties of commercially pure titanium (grade 1 to 4), titanium alloy Ti6Al4V and cortical bone (78).....	28
Table 2. Composition of the mediums used in the sterilization process.	47
Table 3. p-Nitrophenol (p-NP) range of concentrations in the buffer AMP.	53
Table 4. BSA range of concentrations in TBS-Triton.	53
Table 5. Calcium range of concentrations in TCA (15% (m/v)).	54
Table 6. Phosphate range of concentrations in TCA (15% (m/v)).	54
Table 7. 2D and 3D topographic (roughness) evaluations of etched and anodized titanium surfaces using Microtopography and Interferometry as techniques.....	61
Table 8. Contact angles of water (θ_w), formamide (θ_f) and bromonaphtalene (θ_b) of the etched and the anodized surfaces, measured using a Goniometre, and determination of the total surface free energy (ΔG).....	63
Table 9. Total number of cells presents on each well, considering medium (M), surface of the plate (P) and sample (S), according to the trial duration (0.5, 2 and 4 h).	65
Table 10. Analogy between the osteoblasts aspect after 0.5, 2 and 4 h of culture and the cell division introduced by Zhu X. et al (81).....	70
Table 11. Total number of cells presents on each well, considering medium (M), surface of the plate (P) and sample (S), according to the trial duration (1 to 14 days).....	74

LIST OF ABBREVIATIONS/NOMENCLATURE

CP Ti: commercially pure titanium;	Ti ²⁺ /Ti ⁴⁺ : titanium ions;
SEM: scanning electron microscopy;	PO ₄ ³⁻ : orthophosphate or phosphate ion;
w/w: weight per weight;	Ca: calcium;
v/v: volume per volume;	P: phosphorus;
%: percentage;	XRD: X-ray diffraction;
mm: millimetres;	EPMA: electron probe micro analyser;
min: minute;	XPS: X-ray photoelectron spectroscopy;
h: hour;	FE-SEM: field-emission scanning electron microscopy;
m ² : square metre;	TEM: transmission electron microscopy;
BMPs: bone morphogenetic proteins;	AFM: atomic force microscopy;
FGF: fibroblast growth factor;	hMSCs: human bone marrow mesenchymal stem cells;
ALP: alkaline phosphatase;	EIS: electrochemical impedance spectroscopy;
mm ² : square millimetre;	DCA: dynamic contact angle;
BMU: basic multicellular unit;	EDS: energy dispersive x-ray spectroscopy;
H ⁺ : hydrogen proton;	HF: hydrofluoric acid;
ECM: extracellular matrix;	HNO ₃ : nitric acid;
nm: nanometre;	H ₂ O: water;
MPa: megapascal;	mol/l: mole per litre;
g: grams;	V: volts;
g/cm ³ : grams per cubic centimetre;	DC: current continuous;
°C: degree Celsius;	2D: bi-dimensional;
ASTM: American Society for Testing and Materials;	3D: tri-dimensional;
Ti6Al4V: titanium, aluminium and vanadium alloy;	µl: microlitre;
TiO ₂ : titanium dioxide;	µm: micrometre;
GPa: gigapascal;	M: molar mass;
Ti ₂ O ₃ : titanium oxide/rioxide;	NaCl: sodium chloride;
Ti ₃ O ₄ : titanium oxide;	
OH ⁻ : hydroxide ion;	
O ⁻ /O ²⁻ : oxygen ions;	

PBS: phosphate buffered saline;
UV: ultra-violet;
DMEM: Dulbeco's Modified Eagle Medium;
FBS: Fetal Bovine Serum;
CO₂: carbon dioxide;
g/l; grams per litre;
DMSO: dimethyl sulfoxide;
EDTA: ethylenediaminetetraacetic acid;
BSA: bovine serum albumin;
TBS: tampon tris buffered saline;
mM: milimolar mass;
TCA: trichloroacetic acid;
CaCl₂: calcium chloride;
Na₂HPO₄: (di) sodium hydrogenophosphate;
rpm: rotations per minute;
N: newton;
cm²: centimetre square
Θ_w: contact angle of water;
Θ_f: contact angle of formamide;
Θ_b: contact angle of bromonaftalene;
ΔG: total surface free energy or Gibbs energy;
mJ/m²: mili-Joules per metre square.

CHAPTER 1:

GENERAL INTRODUCTION

GENERAL INTRODUCTION

The technological progresses and advances that characterize our society have led to an outstanding improvement in the dental field. New surgical techniques, instruments and equipments emerged with time and consequently dental implants were developed. Nowadays, they are considered an important strategy (globally) in dental medicine, with approximately one million implantations per year (statistical analysis of the past 20 years) (1).

Premature dental loss or bone defects are some of the most recurrent reasons for dental implantation. In the past, the existing tools only allowed limited esthetical and function recover. Now, with the introduction of the biomaterials, the success rates were enhanced, reaching about 96% (for the year of 2009) (2).

The chemical, physical and mechanical properties of the implantable material have an important role in the implant success, since they influence the behaviour of the bone cells (adhesion, morphology, proliferation and differentiation) and the global response of the human body. Considering that, the material should not produce an abnormal biological response (local or systemic) and suffer degradation when exposed to the surrounding tissues and body fluids.

Currently, there are several options available, namely, metals, polymers, ceramics and composites (most common categories), for tooth replacement. However, the ones that exhibit the best group of properties for this specific application are the metals. Their mechanical and physical properties, their corrosion resistance and their biocompatibility are the main points that confer them a grade of excellence for the production of artificial teeth. In the last few years, the titanium has been distinguished, among the metals category, as the best choice for dental implants.

One of the most important aspects about titanium is its ability to react with water and air and to produce a thin oxide layer on the surface, which works as a protective barrier against corrosion and ions release (responsible for inflammatory responses and implant failure). It is also in this film that relies the ability of titanium to interact with the surrounding cells and bone tissue without causing an adverse host response.

Since biocompatibility is determinant for a positive host response, in the last few years different treatments and techniques have been employed to modify the chemistry and tribology of the implantable materials' surface to enhance this property. Between the alternatives, anodization has been recently reported as the preferred one to form rough, porous

and thick oxide films on titanium surfaces, using simple and cheap approaches (3). Due to this technique, it is possible, for instance, to incorporate calcium and phosphate onto the implantable surface or control its roughness or wettability to increase the osteoconductivity and osteointegration, which facilitate the attachment and development of the osteoblasts, responsible for the bone formation at the interface. This way the implant is incorporated without any risks for the human life.

The aim of this project was to investigate the interaction of human osteoblast-like cells (from the cell line MG63) with commercially pure titanium (CP Ti) surfaces, with and without a bioactive anodic treatment. It was intended to observe how the osteoblasts adhesion, morphology, proliferation and maturation was affected by this specific surface treatment and, at the same time, verify the influence of the surface bioactivity on the MG63 differentiation.

CHAPTER 2:

LITERATURE REVIEW

1. HISTORY: A QUICK OVERVIEW

The foundations of the dentistry science (tooth replacement) were only established during the period from 1600 to 1840 (4). In these early days, minerals or animals' parts shaped to resemble the lost region, teeth extracted from living persons or even from cadavers were the most common choice for teeth replacement (4; 5). Little attention was given to the basic properties of the implant material or their interaction with the tissue surrounding (5).

With the beginning of the twentieth century many refinements and improvements in the quality of various materials and processes used in restorative dentistry were introduced. For the first time a concentrated effort was made to develop and improve products with specific properties and shape (4). This provided the basis for the in-depth considerations of booth design and biomaterials for dental implantation.

The evolution of the dentistry science till nowadays was enormous. In the past 20 years, the number of dental implant procedures has increased steadily worldwide, reaching about one million dental implantations per year (1). The progress and advances introduced in this science have led to an outstanding recognition of the field and to its establishment in our society (5). In a near future, it is hoped that the interactions between different sciences, like biology, tribology, mechanics, physics or chemistry, conduct to new and improved solutions for tooth replacement (4; 6).

2. DENTAL IMPLANTS

Few years ago a long term goal of dentistry was the ability to anchor a foreign material into the jaw to replace an entire tooth. Nowadays the goal is to improve this replacement by testing new and improved materials and designs and increasing the success of the biological interactions. The replication of the natural function and appearance of a lost tooth can be very difficult to accomplish. Although, thanks to the optimization of manufacturing tools and to the conciliation of different science fields, dental implants express now high levels of similarity (5).

Dental implants are small, inert and alloplastic¹ (7) structures embedded in the maxilla and/or mandible, and are used for the management of tooth loss and to aid replacement of lost

¹ Alloplastic: consisting of inorganic material implanted in living tissue, or involving the implantation of inorganic material into living tissue (7).

orofacial structures as a result of trauma, neoplasia and congenital defects. These implants are very durable and can last a lifetime. However, as natural teeth they require maintenance: brushing, flossing and regular dental check-up (4).

2.1 Constitution

A dental implant is composed of three main parts (Figure 1):

- **Implant**: anchor or foundation for the restoration. It is screwed into the jawbone providing a fixed platform for the abutment. The bone tissue can grow around the implant allowing the regeneration and strengthening of the jaw.
- **Abutment**: this structure fits over the portion of the implant that protrudes from the gum line (abutment screw) and provides support for the crown.
- **Crown**: responsible for the replication of the natural teeth appearance and for providing a biting surface. This is the top part of the restoration and the one we see inside the mouth. The crowns are usually cemented or screwed onto the abutment (8; 9; 10).

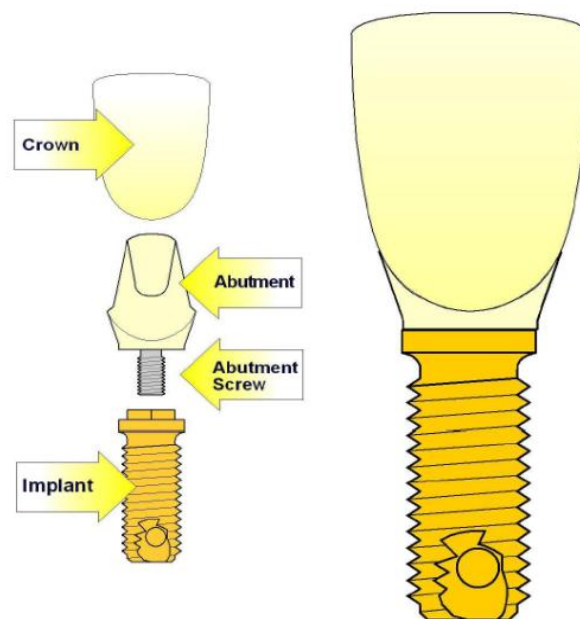


Figure 1. Basic constitution of a dental implant (10).

2.2 Implant Systems

There are several kinds of dental implant systems available, which are categorized according to their shape and relation to the bone tissue: endosteal (or endosseous) (Figure 2A) and subperiosteal implants (Figure 2B).

The first type, like the name suggests, is usually placed directly into the jawbone resembling the natural tooth roots. It is the most common type of dental implants used in dentistry (11). Endosseous implant systems include a range of sizes, shapes, coatings and prosthetic components – the choice is dependent on the available bone (2).

The process involved in the endosseous implantation requires surgery, in one or two steps. In the two steps surgery, firstly a hole is drilled into the bone and then the root part of the implant is inserted. Before continuing, it is necessary to make sure that the implant is properly fused with the bone and the tissue is healed (these can take some days or weeks). If the evaluation is positive the second step can be preformed. It consists in a small incision in the gums, which exposes the implant, allowing the attachment of the abutment as well as the crown. Some dentists use a single step surgery; however the only difference is that the implant is left above the gum margin, so the abutment and the crown can be connected without any incision (2; 8; 12; 13).

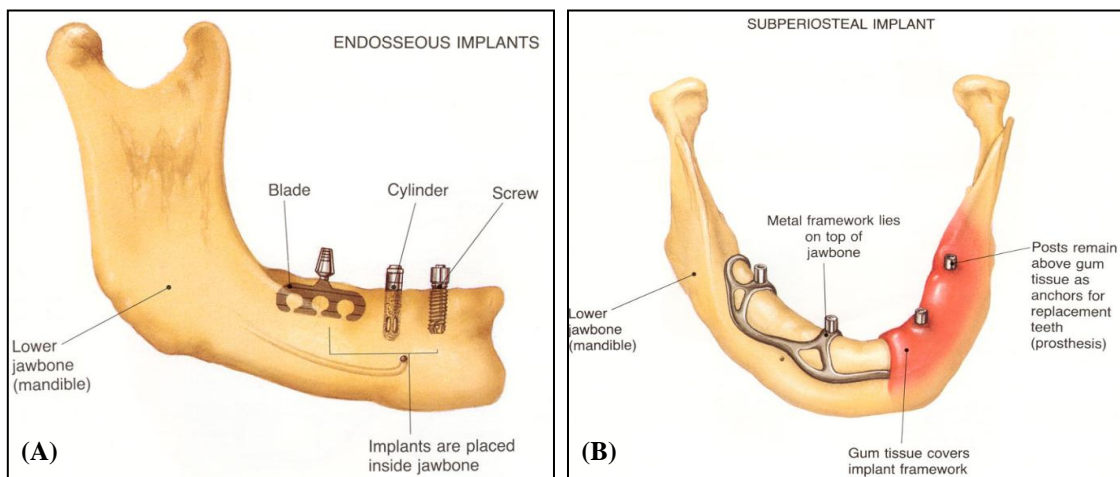


Figure 2. Schematic representation of an (A) endosteal and a (B) subperiosteal implant (9).

In contrast to the endosteal implants, the subperiosteal are fitted to the bone surface as customize shapes while bone plates are placed onto the bone, under the periosteum, and fixed with endosteal screws. These are mostly used when the bone presents atrophies and/or the jaw structure is limited. In this case, a metal framework, individually designed and very light

weight, is fitted over the jawbone providing the equivalent of multiple tooth roots. Nowadays, thanks to sophisticated and accurate technologies, modern CAT scan equipments and advanced computer modelling software, it is possible to produce precise models from a patient jawbone. In this case only one surgery is required, the one necessary to insert the subperiosteal dental implant (8; 9).

2.3 Success and Failure

The success and failure of an implant is defined by its interactions with the tissue surrounding and by the intrinsic response generated. In spite of the recent technological and scientific advances and the remarkable progress in the design and surgical techniques, failures in dental implantation still occur. A review study conducted in the year 2000 showed that approximately 2% of implants failed to achieve osseointegration after placement (14).

One of the most cited reasons for implant removal is fixture failure, also known as “loosening” (11; 15; 16). This problem is usually associated to a deficient integration of the implant by the host tissue, which is unable to establish or maintain the connection, or to an inflammatory response that may lead to the loss of the supporting bone (11; 17).

Besides that, the release and presence of particles/ions, derived from the implant, in the human body is also an important issue that could dictate the implant failure (18). In the oral cavity the materials are subjected to wide changes in the pH and temperature and to the action of acid or alkaline solutions as well as certain chemicals. All of these factors contribute in a high or low level to the materials degradation (particles liberation) and, consequently, to the decrease of their resistance. In this situation two things can happen: inflammatory response and fracture. The most common is the inflammatory response. The free particles are phagocytised by macrophages, which stimulate the release of cytokines (inflammatory mediators) towards bone surface contributing to its resorption by osteoblasts activation. Because of this the osteoblasts function is inhibited, resulting in an eventual osteolysis and in the implant's loss (11; 18; 19). The other possibility, more extreme and rare, is the fracture of the implant due to the degradation and reduction of the fatigue resistance (20).

Despite these problems the clinical success of oral implantation is real with an estimated rate of 96%, for the year of 2009 (2).

3. THE HUMAN BONE

The skeletal system is a collective of many individual bones joined by connective tissues. This structure is responsible for both metabolic supply and biomechanical support for the entire body, including the oral cavity (21).

The bone tissue is formed by inorganic salts embedded in an organic matrix that provides a greatly rigidity and hardness to the bone, when compared to other connective tissues (4; 21; 22). One of the most interesting aspects about bone is that it has the ability of self-repair, which is of extreme importance for a patient recovery after a surgical intervention as well as for the successful integration of an implant into the human body (4).

3.1 Composition

Bone tissue is composed of organic (30% w/w) and inorganic (60% w/w) phases and water (10% w/w).

The organic phase consists predominantly of type I collagen (86%), which gives elastic and viscoelastic qualities to the bone, with a small quantity of types III, V and X collagen. This phase is responsible for the formation and stability of the bone matrix. The collagen molecules (tropocollagens) are organized in fibres, which are further aligned in parallel to each other to produce a lamella sheet. Then, between the ends of these fibres, interfibrillar cross-links are formed providing more stability to the matrix, although numerous gap regions are evident (Figure 3) – during mineralization, the hydroxyapatite crystals (inorganic phase) are firstly deposited into those gaps and then they are extended into other intermolecular spaces resulting in a mineralized fibril. The three-dimensional arrangement of the collagen molecules within a fibril is not yet well understood. However, it is suggested that there are 200 to 800 collagen molecules in the cross section of a fibril with a diameter between 20 and 40 nm. In certain stages of bone matrix formation, the trace amounts of type III, V and X collagen are involved in the regulation of the diameter of the collagen fibrils (21; 22; 23; 24).

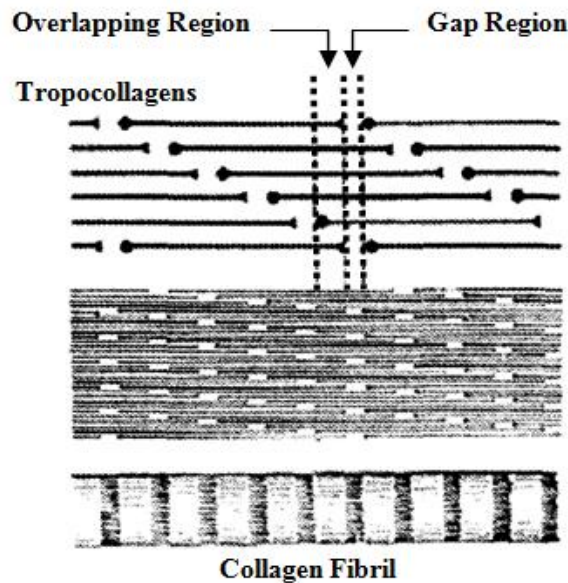


Figure 3. Schematic representation of the collagen molecules arrangement to form gap regions for hydroxyapatite deposition, during mineralization (21).

On its turn, the inorganic phase is composed by a ceramic crystalline-type mineral, commonly known as hydroxyapatite. The bone hydroxyapatite contains many impurities such as potassium, magnesium, strontium or sodium (in place of the calcium ions), carbonate (in place of the phosphate ions), and chloride or fluoride (in place of the hydroxyl ions). These impurities can be either incorporated into the crystal lattice or absorbed onto the crystal surface. Since these imperfect crystals are very soluble, the bone is able to re-solubilise and release its calcium, phosphate or magnesium ions into the extracellular fluid as needed – during mineralization, substances that have high bone affinity can also be incorporated into the bone matrix, promoting the equilibrium of the ions (21; 22).

3.2 Organization

The human bone (Figure 4) is divided in two main types: the cortical bone, also known as compact bone, and the trabecular bone, also known as cancellous or spongy bone. The basis for this classification relies on their porosity and microstructure unity and not on their cellular constituents, once they are basically the same (21; 22; 23; 24).

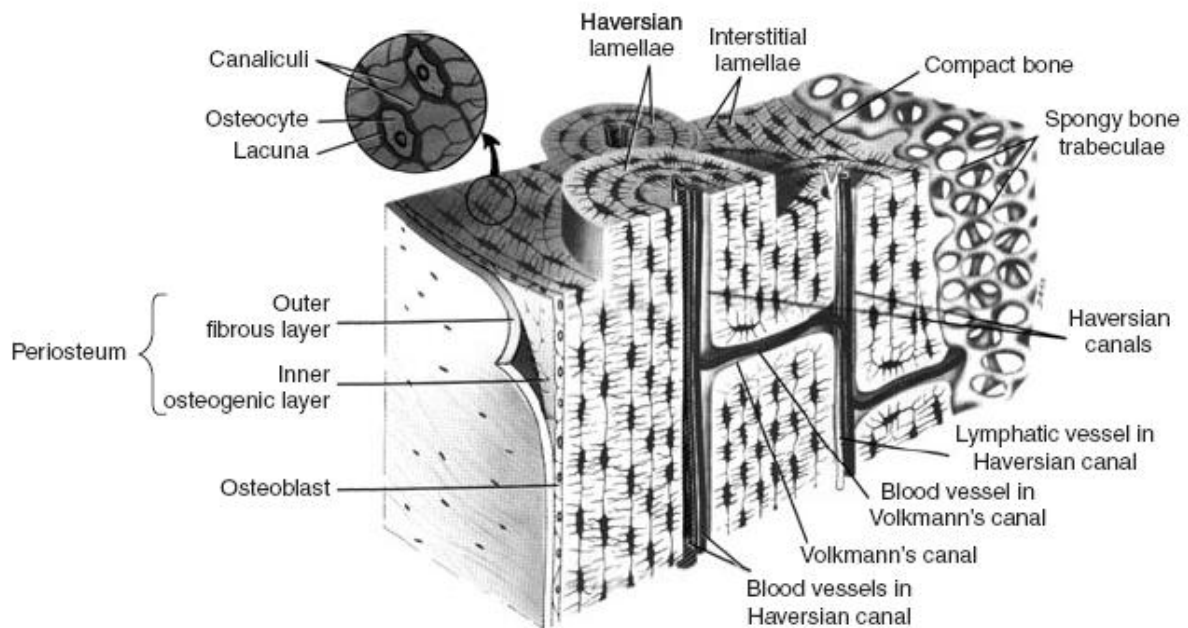


Figure 4. Representative diagram of the bone tissue organization (22).

The cortical bone is a dense and hierarchical organization of cylindrical structural unities, the osteons (trabecular bone also possesses osteons), that surrounds the marrow space. The cortical bone is usually found in the shaft of long bones and forms the outer shell that surrounds the spongy bone at the end of joints and the vertebrae. It is composed by a complex vascular system, with blood vessels and nerves, providing this structure with a high sensibility and regenerative capacity. There are approximately 2.1×10^7 cortical osteons in healthy human adults, with a total cortical area of approximately 3.5 m^2 . The cortical bone porosity ranges about 5 to 10 % while in the trabecular bone it can go from 50 to 90 %. The cortical bone has an outer periosteal surface (periosteum) and an inner endosteal surface (endosteum) (21; 22; 23; 24).

The periosteum is a fibrous connective tissue sheath that surrounds the outer cortical bone, except at joints where bone is lined by articular cartilage. It consists in a dense and irregular connective tissue, which contains blood vessels, nerve fibres and bone cells (osteoblasts and osteoclasts). The periosteum is divided into an outer “fibrous layer” (contains fibroblasts) and in an inner “osteogenic layer” (contains progenitor cells). On the other hand, the endosteum is a soft, thin, membranous structure that lines the inner cavity of long bones. It is in contact with the bone marrow space, blood vessels and trabecular bone (it can also be

found covering the inner surface of this bone). It is a highly vascular system and contains osteoblasts and osteoclasts (23; 24).

The trabecular bone, the lightest, possess lots of spaces where is possible to find bone marrow, which is responsible for the production of the majority of the blood cells. It is composed of plates and rods averaging 50 to 400 mm in thickness and its osteons present a semilunar shape. It is estimated that there are 14×10^6 trabecular osteons in healthy human adults, with a total trabecular area of approximately 7 m^2 . The trabecular bone is usually found in the end of long bones, in vertebrae and in flat bones, like the pelvis. It contributes to about 20% of the total skeletal mass within the body while the cortical bone contributes to the remaining 80% (21; 24).

In a histological level, the bone tissue is composed by three major constituents: osteoblasts, osteoclasts and osteocytes (Figure 5). These are responsible for the extracellular matrix formation (organic and inorganic) and each one of those possesses a particular role in this task (22).

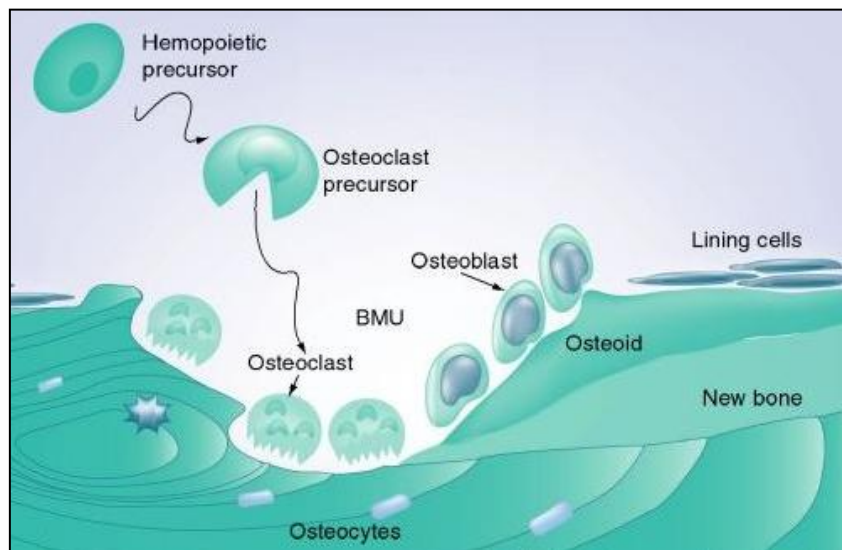


Figure 5. Bone tissue cellular composition: osteoblasts, osteoclasts and osteocytes and lining cells. Totality of cells involved in the bone formation and in the regeneration process (25).

3.2.1 Osteoclasts

Osteoclasts are multinucleated giant cells with a diameter ranging from 20 to over 100 μm . They have acidophilic cytoplasm containing numerous vesicles and vacuoles (lysosomes filled with acid phosphatase) and usually derived from early promonocytes. Under certain

circumstances, however, monocytes and macrophages are also capable of osteoclastic differentiation. Some investigations (26; 27) have demonstrated, although without clear details, that osteoblastic cells are involved in the osteoclastogenesis initiation by inducing the activation of the osteoclastic precursors through the ingrowth of blood vessels. The equilibrium between the osteoclasts and osteoblasts activity defines the velocity of bone regeneration.

Osteoclasts are responsible for the resorption of the bone tissue, which consists in the removing of the mineralized matrix followed by the breaking up of the organic bone. After completing their task they migrate into adjacent marrow space, where they undergo apoptosis. They can live for up to seven weeks (21; 22; 23; 24).

3.2.2 Osteoblasts

The osteoblasts are the bone-forming cells, which make them involved in the entire bone formation process. Typically they are 15-30µm cuboidal-shaped cells, with a large nucleus. The cytoplasm is rich in organelles that assure the biological functionality of the cell and maintain the strong cellular activity.

The osteoblasts arise from osteoprogenitor cells (immature progenitor cells²), located in the deeper layer of the periosteum and in the bone marrow, that differentiate under the influence of growth factors such as bone morphogenetic proteins (BMPs), fibroblast growth factor (FGF), and others.

Active osteoblasts exhibit some functional characteristics which includes, for instance, intensive alkaline phosphatase (ALP) activity and the secretion of type I collagen. They can also synthesize osteocalcin and bone sialoprotein that serve as biomarkers for osteoblastic identification and functional evaluation.

The mineralization phase is considered the second stage of osteoblasts evolution and it is defined by the crescent levels of calcium and phosphate. During the bone matrix (osteoid) formation the osteoblasts are responsible for the synthesis and secretion of the collagen fibres. Some can also differentiate into osteocytes and extend out communication processes with neighbouring osteocytes, osteoblasts surface or lining cells. This last type of cells is also derived from osteoblasts (present on the surface), which are already inactivated.

² Progenitor Cell: biological cell that has a tendency to differentiate into a specific type of cell, a “target” cell (7). In the case of the osteoblasts, the osteoprogenitor cells derived from self-renewing pluripotent stem-cells stimulated under certain environmental conditions (23).

The lining cells (Figure 5) are flat and highly interconnected with each other. They usually form a cellular sheet that covers the entire surface of bone, protecting it and controlling the flux of ions. Besides that, the bone lining cells are very important in the bone remodelling process since they possess hormones and growth factor, both essential for the initiation.

The osteoblasts are also responsible for the secretion of enzymes that lead to the osteoid removal, promoting this way the osteoclasts contact with the mineralized bone surface. Populations of osteoblasts are very heterogeneous, with different osteoblasts having different gene expressions. This may explain the heterogeneity of the trabecular micro-architecture at different skeletal sites, the anatomic site-specific differences in disease states, and the regional variation in the ability of osteoblasts to respond to agents used to treat bone disease (21; 22; 23; 24).

3.2.3 Osteocytes

The osteocytes, star-shaped cells, are the most abundant cell type found in the cortical bone and the only one embedded within the bone matrix. In a mature bone about 95% of the total cells are osteocytes (approximately 20 000 to 30 000 osteocytes per mm² of bone).

They derive from osteoblasts that became trapped inside the osteoid, in small chambers known as *lacunae*, during the bone formation. The process of differentiation into osteocytes requires the loss of the osteoblasts organelles and the cytoplasmic extension into long and slight structures. These slight structures are then encased in tiny channels called *canaliculi*, which interact and communicate with the surrounding cellular substances, producing a network for the exchange of ions, nutrients and extracellular fluid.

Since the osteocytes have reduced synthetic activity, and like osteoblasts are not capable of mitotic division, their physiologic function is not completely defined. Although, thanks to their interactive networks, it is believed that they are responsible for detecting microdamages and for initiating the repair process, which indicates, on its turn, that they are involved in the routine turnover of the bone matrix. They are capable of transducing stress signals from bending and stretching of bone into biologic activity. This function is also responsible for the longevity of the osteocytes that can go to 25 years (average half-life), for the slowest turnover rates (21; 22; 23; 24).

3.3 Biological Dynamics

The bone dynamics involves three main stages: growth, modelling and remodelling. These are the three major mechanisms that modify the bone mass and the structure of the skeletal system for its adaptation to the mechanical and non-mechanical environments. For a patient recovery after a surgical intervention, such as implantation, the remodelling process is the most important one (21). However, to understand completely the human bone nature and its complete development it is essential to introduce all stages.

3.3.1 Growth

The bone formation is initiated in the first weeks of gestation. However, it is only in the end of the adolescence that the definitive composition of all skeletal bones is completed. Bone grows and models under the influence of metabolic, mechanical and gravitational forces, in a very long and complex process.

This stage is divided in two, the longitudinal and the radial growth. The longitudinal is mainly responsible for increasing bone length, while the radial growth is mainly responsible for enlarging bone cross-sectional area (23).

3.3.2 Modelling

Bone modelling is one of the predominant biological mechanisms that governs the enlargement of each individual bone during growth. It is a process in which bones change their overall shape in response to physiologic influences or mechanical forces, leading to a gradual adjustment of the skeletal. On its turn, bone modelling is divided into bone formation drift (osteoblasts action) and bone resorption drift (osteoclasts action). These two occur separately, although they can work together to guarantee the appropriate shape and size of each individual bone.

In adults, bone modelling is less frequent than remodelling, although in certain circumstances, like hypoparathyroidism, the modelling stage can be increased (21; 23).

3.3.3 Remodelling

At a cellular level, the modelling and remodelling processes are not very different. They are both based on the action of the osteoclasts and the osteoblasts.

In the remodelling process the osteoblasts and the osteoclasts closely collaborate in a “Basic Multicellular Unit” or BMU (small packets of cells placed in the cortical and trabecular surface).

During childhood, the remodelling process is responsible for the substitution of immature bone for more bio-mechanically and metabolically competent bone, and during growth it is involved in the bone elongation. In the adulthood, this process is responsible for replacing aged bones (damaged or mechanically unfit) – resorbs old bone and forms new bone to prevent accumulation of microdamage bone –, this way maintaining the skeletal mechanical capacity. This process is impelled by specific hormones that control/regulate the calcium concentration in the blood and can only happen thanks to the high level of plasticity of bone.

The remodelling cycle (Figure 6) is composed of four sequential phases: quiescence phase; resorption phase; reversal phase; and formation phase (21; 23; 28; 29; 30).

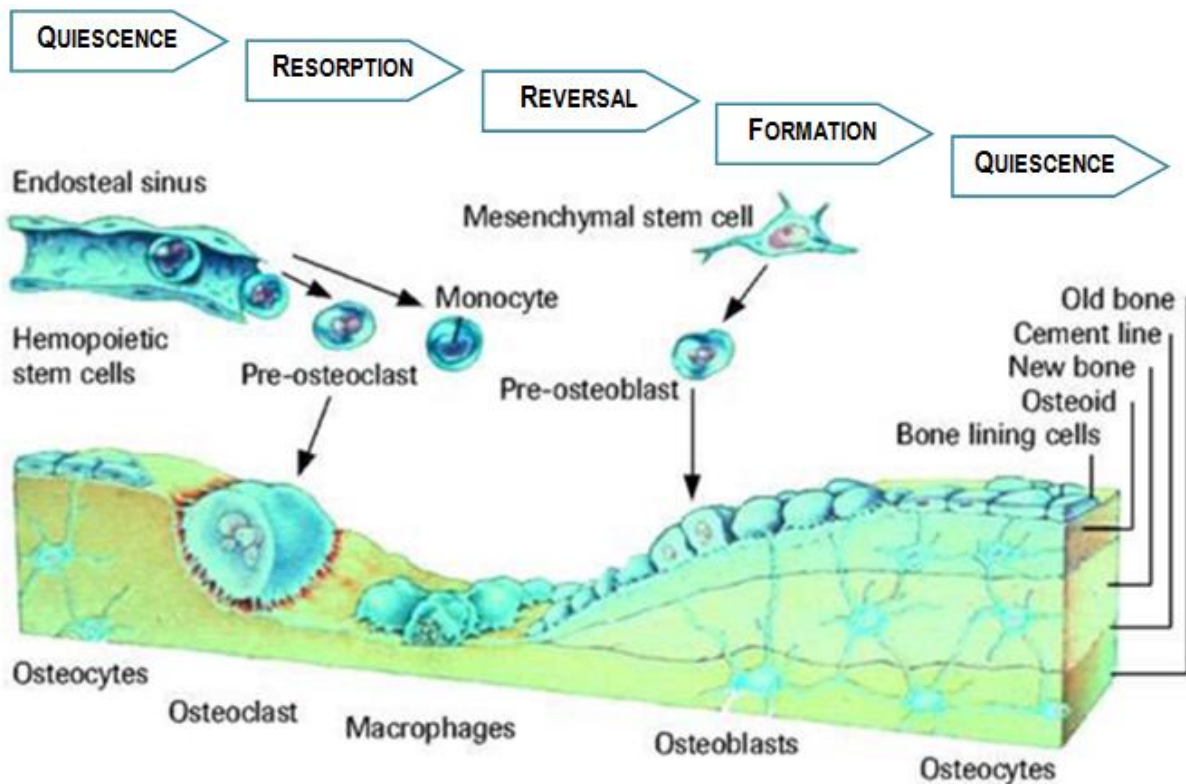


Figure 6. Stages of bone remodelling (adapted from (31)).

- *Quiescence or Activation Phase:* recruitment and activation of osteoclasts (haematopoietic origin) by hormonal stimuli.
- *Resorption Phase:* the osteoclasts adhere to the bone surface and start to erode the mineral structure, which is followed by digestion of the organic matrix. In this phase, small cavities in the surface of the trabecular bone are created by the solubilisation of the mineral structure. This acidifies (pH=4) the surrounding microenvironment inducing the liberation of H⁺ ions against the bone surface. Since osteoclasts have limited life span (≈ 12.5 days) the progression of bone remodelling requires the continual addition of osteoclasts. After completed their task, the osteoclasts die by apoptosis.
- *Reversal Phase:* intermediary between the resorption and the bone formation phases, and the responsible for the transmission of the bone inducing signal. During this phase the osteoclasts disappear and macrophage-like cells are seen on the bone surface. These latter cells can release factors that inhibit the osteoclasts action and stimulate the osteoblasts.
- *Formation Phase:* the bone formation results from a complex cascade of events. It, basically, involves proliferation of primitive mesenchymal cells, differentiation into osteoblasts precursor cells, maturation of osteoblasts that adhere to the previously resorbed surface, formation of the bone matrix, and finally mineralization (28; 29; 32).

3.4 The Healing Process

During dental implantation, the bone tissue that surrounds the area is subjected to tensions and forces. These aggressions can damage the tissue, inducing a healing response.

Usually, the healing process depends majorly on the vascularised system that surrounds the area, which works as an oxygen and nutrients supplier, and on the local stability, which requires the absence of biomechanical actions/forces for a faster recover (33; 34)

Immediately after the surgical intervention, the first healing phase (reactive phase) starts. It involves the formation of a blood clot or hematoma, resultant from the vessels constriction. This hematoma helps stopping the bleeding and at the same time serves as a

building block for the rest of the environment. During this phase, the surrounding region experiences inflammation and the patient suffers pain.

The second phase is the reparative one. This starts few days after implantation, with the fibroblasts and osteoblasts action. The fibroblasts secrete collagen fibres that are arranged into layers, giving origin to a *fibrocartilaginous callus*. Then, the capillaries in the extremities start connecting the tissue and, at the same time, the immune system (macrophages) demolishes the hematoma. On its turn, the osteoblasts produce trabecular bone and soft callus, restoring most of the original local strength.

The third phase, remodelling, consists in the transformation of the callus into bone callus. In other words, it is the process responsible for the substitution of the spongy bone for compact bone, like was defined in the previous section. During that time, the callus is remodelled, re-establishing the original properties and characteristics of the local tissue (35; 36).

4. BONE-IMPLANT INTERACTION

4.1 Biological Mechanisms of Bone Formation in the Interface

The bonding between the implant and the bone tissue is established based on physical and chemical processes induced by three biological mechanisms: osteoinduction, osteoconduction and osteointegration. Each one of those depends on the others and that dependence defines the success or failure of the interaction, at the interface.

4.1.1 Osteoinduction

The osteoinduction is the act or process that induces the osteogenesis. This phenomenon consists in the phenotype conversion of the soft tissue cells into bone tissue precursors, through appropriate stimulation (37). In the 70's, Marshall Urist defined for the first time this stimulus as dependent on the cells presence. Nowadays, after more investigations, it is considered to be determined by the presence of some high molecular weight glycoproteins, like the BMP – among all the available donor areas in the jaw, the cortical bone presents the higher concentration of BMP (38).

This process allows the immature or undifferentiated mesenchymal cells to become a cellular line capable of producing bone, like the pre-osteoblasts. Thanks to this property, some materials (bone grafts, most common) are able to create the conditions necessary to induce the bone tissue formation in places without it, like muscles or ligaments (37; 39; 40).

4.1.2 Osteoconduction

The osteoconduction is a three-dimensional process, observed immediately after the implant contact with the bone tissue. It is characterized as the ability of growing bone in apposition to the existing one or above it.

Contrary to the osteoinduction, where the material possesses elements that stimulate the bone tissue formation, in the osteoconduction the material works as a passive support “waiting” for the tissue response. In this case, the material is defined as a physical structure that favours bone progression by allowing cellular and vascular local invasion. It is expected that the cellular organisms adhere, grow and invade all the material structure. However, for this to happen, the presence of differentiated mesenchymal cells or bone tissue it is obligatory, in other words it depends on the osteoinduction phenomenon.

In implantology, the most common osteoconductive materials are the natural hydroxyapatites and the bioceramics. Since these can be both resorbable (preferred for implants) or non resorbable, depending on the objective of the medical intervention, they are able to adapt (37; 40; 41).

4.1.3 Osteointegration or Osseointegration

There has been much discussion about the meaning of osteointegration, since it was introduced in the 70's. Branemark (1977) was the first one defining this phenomenon. He described it as a “*direct structural and functional connection between the living bone and the surface of a load-carrying implant*” (42). On its turn, the Williams Dictionary of Biomaterials (43) offered a similar description, although a little bit more formal: osteointegration is “*the concept of a clinically asymptomatic attachment of a biomaterial to bone, under conditions of functional loading*”. Neither of these two definitions elucidates the fact that, in some cases, osteointegration can occur when just a physical contact is observed and there is not a real and direct connection between the implant and the bone. However, since the concept has been

generalized, these definitions are still accepted and used by the majority of the specialists in clinical implantology, nowadays (44; 45).

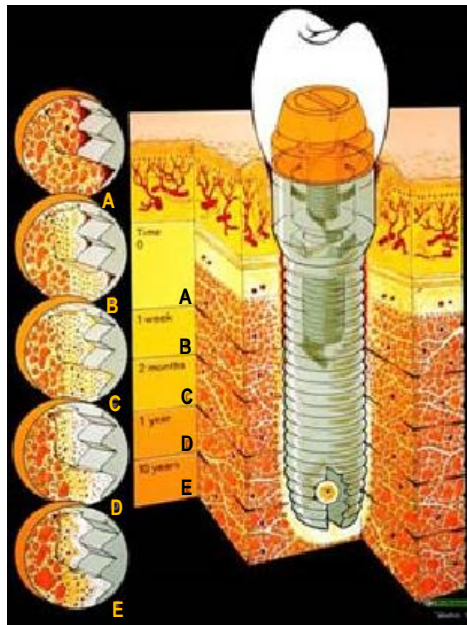


Figure 7. Osteointegration development on dental implants: (A) Time 0; (B) 1 week; (C) 2 months; (D) 1 year; (E) 10 years (46).

Osteointegration has been intensively studied since Branemark. Currently, it is well accepted that an implant is considered osteointegrated when there is no progressive relative movement between the implant and the bone and the anchorage between them is such that can persist under all normal conditions of loading (47). In dentistry, osteointegration can be defined as a biological state where the bone of the mandible or maxilla grows into physiological contact with the implant itself (Figure 7) (48).

The creation and maintenance of osteointegration is dependent on the understanding of the tissue's healing, repair and remodelling capacities, since they are all involved in a later stage of osteointegration – consolidation of the bone at the implant site and maintenance of the normal bone conditions – and since their basic principle is similar. For instance, during the healing process a bond is formed between bone tissues, without intermediate fibrous tissue or fibrocartilage formation. In the case of osteointegration the same thing happen, although instead of attaching two biological structures, the bone tissue is connected to an implant (47; 49).

To achieve a good osteointegration some parameters must be follow: (i) the bone must be viable (should not cause necrosis or inflammation); (ii) the space between the bone and the implant must be small and contain no fibrous tissue; (iii) the material should be properly

choose (biocompatibility is required as well as mechanical stability and resistance similar to the natural bone); and (iv) the bone-implant interface must be able to survive loading by a dental prosthesis. To guarantee a successful implantation, the implant must be allowed to heal for a time without load, after the surgical intervention (4; 42; 48; 50). Vascularisation is, also, essential during osteointegration, as it influences tissue differentiation and ossification.

This phenomenon is an absolute requirement for the successful implant-supported dental prosthesis (51). In humans, the osteointegration of an implant is a slow process that can take up several months.

4.2 Bone Adhesion

To guarantee osteointegration the adhesion of osteoblasts to the biomaterials surface should occur in a very short period of time, during which multiple steps must be complete: focal adhesion (discrete regions in the cell membrane, intimately associated with the substrate); combination between the proteins and the substrate; and cell spreading (52).

Due to the presence of a support matrix or extracellular matrix (ECM) secreted by the cells, the attachment to the material surface is possible. This matrix is composed by a vast group of proteins, proteoglycans and glycoproteins, which will determine the cell shape and ultimately the proliferation, as well as, the proper function and tissue integrity (53; 54). Between those, the fibronectin (high-molecular weight protein and the first one activated by the ECM during bone-biomaterial contact (55)) and the vitronectin are considered the major proteins responsible for cell-substrate adhesion interaction. They have, also, an important paper in the promotion of the osteoblasts proliferation and differentiation (53; 54).

According to Yang et al (2002) (56) the presence of fibronectin on Ti surfaces plays an important role in governing osteoblasts attachment.

In living systems, the blood is the first component to contact with biomaterials and, immediately after, rapid adsorption of plasma proteins occur. When a substrate contacts with a biofluid, a considerable number of events take place, in order to modify the materials state to promote the interaction with the cells. The first step is the material hydration. The water molecules bond to the biomaterial surface originating an ionic layer, which will allow the adsorption of proteins (like fibronectin). Thus, the cells that reach the surface establish contact with the protein-coated substrate and attach to the extracellular matrix of those proteins. For instance, fibronectin proteins can bind to the integrins (membrane-spanning receptor of

proteins) on the osteoblasts and activate signalling pathways that induce cell-cycle progression, gene expression, matrix mineralization and regulates osteoblasts survival. This contact put in evidence that, in reality, this is not a direct attachment between bone and material but a protein intermediate interaction (Figure 8) (52; 53; 55).

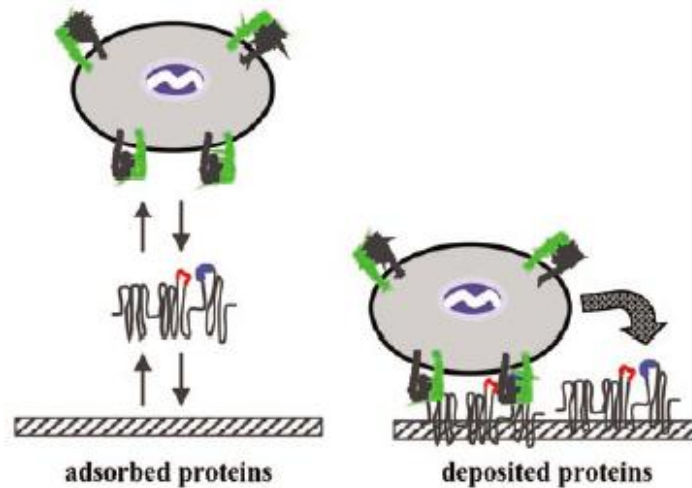


Figure 8. Mechanisms controlling cell adhesion (adapted from (57)).

In the end an effective cell adhesion is completed, allowing a cascade of cellular events to take place, like proliferation and cellular spreading over the surface, in a dynamic environment.

During the previous events (especially protein adsorption) the implant's surface is significantly changed, which occurs both *in vivo* and *in vitro*. Even if the selected material for implantation possesses already a stable oxide film, under these circumstances, it still suffers electrochemical changes. For instance, considering that commercially pure titanium implants possess an oxide from 2 to 6 nm before implantation, after retrieving them from the human body the thickness seems to be two or three times higher (53). That is why the implantable material should respect an entire list of demands before being used in contact with the human body.

5. BIOMATERIALS

Over the years the medical field have suffered astronomic changes. The surgical and medical techniques were improved and the devices used were constantly challenged to achieve higher levels of quality. Those changes led to the emergence of a new range of

materials, the biomaterials. According to the Williams Dictionary of Biomaterials (43), “*a biomaterial is a nonviable material used in a medicine device, intended to interact with biological systems (...) to evaluate, treat, augment or replace any tissue, organ or function of the body*”. Ideally it should be able to sustain a positive interaction with the surround tissues without causing an abnormal response (58; 59).

The idea of preserving the human body integrity and comfort for the longest time possible and restoring lost functions and damaged tissues/organs were the main reasons that motivated the biomaterials development (48; 58).

In medical applications, they are rarely used as isolated materials but are more commonly integrated into devices or implants. Although they are primarily employed in this field, they can also be used in biological investigations, for instance, to grow cells in culture, to assay for blood proteins in the clinical laboratory, in equipments for processing biomolecules for biotechnological applications and others. In both cases, the biomaterials must always be considered in the context of their final fabricated, sterilized form (59; 60).

5.1 Biocompatibility

Although the selection of the best biomaterial for dental applications relies on a substantial range of requirements, there is one that is considered the most important – the biocompatibility (60).

The understanding and measurement of biocompatibility is unique to biomaterials science. It was firstly defined by William (1987) as “*the ability of a material to perform with an appropriate host response in a specific application*” (43; 59). In 2008, considering all the changes and improvements in the biomedical field, William proposes a new definition, “*biocompatibility refers to the ability of a biomaterial to perform its desired functions with respect to a medical therapy, without eliciting any undesirable local or systemic effect in the recipient or beneficiary of the therapy, but generating the most appropriate beneficial cellular or tissue response in that specific situation, and optimizing the clinically relevance of the therapy*” (61). According to these definitions a biocompatible material must not: irritate the surrounding structures, provoke an abnormal inflammatory response, incite allergic or immunologic reaction and cause cancer (58; 59; 60).

Inherent to this, however, was the idea that a single material may not be biologically acceptable in all applications. For example, a material that is satisfactory as a full cast crown

may not be adequate as a dental implant. Also implicit is an expectation for the biological performance of the material. In a bone implant, the expectation is that the material will allow the bone to integrate with the implant. Thus an appropriate biological response for the implant is osteointegration. In a full cast crown, the expectation is that the material will not cause inflammation of pulpal or periodontal tissues, but osseointegration is not. Whether a material is biocompatible or not is therefore dependent on what physical function we ask of and what biological response we require from it (4; 60).

5.2 Classes of Biomaterials

The search for more sophisticated devices to replace and treat damaged body parts have led to a wide range of high quality biomaterials. Although they are usually distinguished in three basic categories – metals, ceramics and polymers –, in this study another one will be taken into consideration, the composites.

5.2.1 Metals

Metals and metallic alloys play a prominent role in dentistry and are used in almost all aspects of dental practice (implants, dental restoration and manipulation instruments). Thanks to their optical, physical, chemical, thermal and electrical properties, these materials can be favourably exploited in dentistry (4; 48; 22). In this category the most distinguished types of metals for medical applications are: titanium, cobalt, stainless steel, nickel, chromium and the noble metals, like gold, tantalum, platinum, palladium, silver, iridium and niobium (59; 62; 63).

5.2.2 Ceramics

The use of ceramics in dentistry was initially based upon the relative biological inertness of ceramic materials. Nowadays, the bioinert and bioactive ceramics, materials that induce normal tissue formation and assure an intimate bond with it, are the preferred choice.

There are lots of ceramics applied in the biomedical field. The most common are the carbon, alumina and zirconia – bioinert ceramics – and the bioactive glasses and glass

ceramics, calcium phosphate ceramics and the combination of the two previous – bioactive ceramics (59; 63; 64).

5.2.3 Polymers

The first polymer used in dentistry was vulcanized rubber for denture bases. Nowadays, other polymers were already introduced in this field: vinyl acrylics, polystyrene, epoxies, polycarbonates, silicones, polyethers, polysulfids and polyacrylic acids. These are used in the construction of prosthetic appliances, artificial teeth, tooth restoratives, implants, temporary crowns, cements, and others (22; 65).

5.2.4 Composites

Although, there is a rich history associated with the development of dental composites and their prominent position in dentistry, it is still evident the discussion around the composite materials definition.

Composite materials have a bulk continuous phase, called *matrix*, and one or more non-continuous phases, called the *reinforcement*, which usually have superior mechanical or thermal properties than the matrix. Although, inorganic materials (titanium, steel, carbon...), thermoplastics (polyesters, polycarbonate...), thermosets (epoxy, silicone...) and resorbable polymers (chitosan, collagen) can be used as matrix, some of them can also be used as reinforcement. The choice is dependent on the material application (59; 63; 66).

5.3 Dental Implants Materials

Dental implants have been manufactured in a wide variety of shapes and materials. According to their design (implant systems), cost and aesthetic purpose, the materials applied to their production can change; however all of them must possess some requirements, like resistance to high intensity mechanical and physical efforts as well as chemical attacks and simultaneously be recognized by the human body as “friendly” substrates (67; 68; 69).

The first implants used were made by precious materials like gold, platinum, palladium or iridium (22). However, the high costs and the resistance deficiencies of those conducted to new categories, such as the ones described in *5.2 Classes of Biomaterials*.

Before choosing the material, it is important to analyse some aspects. As we all know the resistance or strength of a tooth is dependent on their function and position in the oral cavity. For instance, a natural pre-molar (used for breaking the food) should present a fracture toughness of 248 MPa at least, but for a molar the resistance must be higher, at about 305 MPa, since it is used for grinding. That is why the selection of the best material to employ must take into consideration the mechanical and physical properties of the natural tooth, which will be replaced, as well as the conditions and needs of the oral cavity (70; 71).

Nowadays, the category that responds more favourably to these requests is the “metals and their alloys”. Their physical and chemical properties, their good corrosion resistance and biocompatibility are the main points that confer them a grade of excellence for the production of artificial human parts substitutes. For decades, they have been employed successfully in the orthopaedic field and now they are making history in dental applications, as well. Nevertheless, it must be pointed out that not all of this category materials present the same grade of excellence, some like titanium and its alloys have been distinguished, in the last few years, as the best ones (1; 6).

6. TITANIUM AS A BIOMATERIAL

The widespread introduction of titanium implants has revolutionized dental implantology, becoming the most used material (72; 73).

Titanium occupies the 22th position of the periodic table (atomic number), has an atomic mass equal to 47.9 g and a density of 4.51 g/cm³. Its fusion point is approximately 1668 °C and presents two types of crystalline structure: hexagonal close-packed if the temperature is less than 882.5 °C, and body-centered cubic if the temperature is higher than that. It is the fourth more abundant metal in the Earth crust.

The titanium material is classified in two categories, according to American Society for Testing and Materials (ASTM): commercially pure titanium, which is subdivided in four grades according to the content of oxygen (O), iron (Fe), nitrogen (N), carbon (C) and hydrogen (H), from 1 the least ($\approx 0.18\%$) to 4 the most ($\approx 0.4\%$); and titanium alloys, such as Ti6Al4V, the most common, which has in its composition aluminium (Al – $\approx 6\%$) and vanadium (V – $\approx 4\%$). This alloy presents favourable properties for implantation, like less thermal conductivity or higher fatigue resistance compared to CP Ti, although the presence of

vanadium and aluminium in the organism may raise some issues for the patient health security (74).

As it was pointed out in the previous sections, the material should not produce a harmful biological response (local or systemic) and not suffer degradation when in contact with tissue or body fluids, like saliva or blood. Titanium is considered the best material and the one that responds more favourably to these attributes. Moreover, it is resistant to electrochemical degradation and high temperatures; induce a benign biological response; presents low toxicity; has high tensile strength and high durability; has low cost when compared to other biomaterials; is light weight and presents low density (40% of steel density but as strong, which gives it the highest strength-weight ratio of any metal suited to medical use); is non-magnetic; has high ductility; and is easy to work with (75; 76; 77; 78; 79). Besides that, titanium has the ability to react with water and air (oxygen) and produce a very stable, continuous and highly adherent oxide layer (TiO_2 passive film, most common form), with approximately 2 to 10 nm of thickness. This is the basis for its excellent corrosion resistance and exceptional biocompatibility (80; 81).

From a biological perspective, titanium possesses an important characteristic for implantation, which is the ability to osteointegrate. Due to its high dielectric constant, which ranges from 50 to 170, depending on crystal structure, titanium can bind with bone and living tissue, without needing extra adhesives. In consequence, the forces required to break the bond are quite high (the high dielectric constant results in considerably stronger van der Waal's bonds than other oxides) (82).

Another thing that influences the selection of titanium, as the biomaterial for tooth replacement, is the changes introduced by the removal of the periodontal ligament during the substitution/implantation – this ligament is very important, since it is responsible for the attachment and support of the tooth to the alveolar bone and for its protection against heavy or light forces, derived from mechanical contacts. Consequently, to guarantee an uniform distribution of tensions between the bone and the implant, it is essential to take into consideration properties such as elastic modulus or elongation. Table 1 presents an analogy between titanium (commercially pure from grade 1 to 4 and the most common titanium alloy, Ti6Al4V) and cortical bone (most external and hardest part of the bone), based on these properties, in order to prove its viability for dental applications (78; 79).

Table 1. Mechanical properties of commercially pure titanium (grade 1 to 4), titanium alloy Ti6Al4V and cortical bone (78).

Material	Tensile Strength (MPa)	Yield Strength (MPa)	Elongation (%)	Elastic Modulus (GPa)	Density (g/cm ³)
CP Ti Grade 1	240	170	24	102	4.5
CP Ti Grade 2	345	275	20	102	4.5
CP Ti Grade 3	450	380	18	102	4.5
CP Ti Grade 4	550	485	15	104	4.5
Ti6Al4V	930	860	10	113	4.5
Cortical Bone	140	-	1	18	0.7

As it is shown, all the material categories considered are able to substitute the bone. However, since the purity and malleability of the CP Ti decreases from grade 1 to 4, the selection tends to lie on the first two grades as well as on the titanium alloy.

6.1 Passive Film

The oxide layer is formed by the reaction of the oxygen ions, which migrate towards the metal, with the titanium counter-ion at the base of the oxide. This mechanism is unique for titanium and some other elements of valence IV, such as zirconium. Both thickness and chemical composition of the titanium oxide layer play an important role in the adsorption of proteins from biologic fluids and in the attraction of cells to its surface (83; 84). In a natural atmosphere the thermodynamically stable oxide is TiO₂ (titanium dioxide), which can present three crystalline structures: anatase (tetragonal), rutile (tetragonal) and brookite (orthorhombic). It is also possible to find TiO, Ti₂O₃ and Ti₃O₄ depending on the time of exposition to oxygen.

The anatase phase presents unique properties for biomedical applications. Among the three phases, this is the most capable one in the absorption of OH⁻ and PO₄³⁻ ions from the biologic fluids. These are important for the apatite bone deposition, since they can transform the oxide layer in Ti(OH), for instance, which increases the stability of the oxide in contact with tissue (85; 86).

One of the most interesting aspects about the passive film is its ability of repassivation. Even if the film is damaged or mechanically removed, it can be regenerate

In order to achieve an implant system that responds completely to the human body needs, it is necessary to control the characteristics of the outermost layer. Unfortunately the titanium oxide spontaneously formed is not completely ideal for biomedical uses. It usually presents a heterogeneous formation and is very thin, which difficult the implant chemical adhesion to the tissue surrounding (42; 84). Therefore, both CP Ti and its alloys can be submitted to thermal and electrochemical oxidation treatments to produce thicker oxide layers for protection and cell attraction purposes, with a controlled surface morphology, topography and composition. Bioactive components can be added to the oxide to improve osteointegration (81).

According to the Williams Dictionary of Biomaterials (43), a bioactive material is a “*material which has been designed to induce or modulate a specific biological activity*”. In other words, a bioactive fixation is defined as the interfacial bonding of an implant to a tissue by means of formation of a biologically active hydroxyapatite layer on the implant surface. That layer possesses a composition rich in calcium and phosphorus (free ions), which promotes a physical and chemical connection with the tissue (creation of an environment compatible with osteogenesis – bone growth). For implants, the bioactivity will provide a stronger and firmer direct association between it and the tissue surrounding, equal to or greater than bone (91; 92).

In some cases, like titanium dental implants, where the mechanical properties are ideal but the interaction with tissue is not as high as the hydroxyapatite or the calcium phosphates, an oxide layer can be produced with favourable bioactivity. By adding components such as calcium and phosphorus to the electrolyte used, for instance, in the anodic treatment, it is possible to improve the titanium biological properties (93).

7. SURFACE MODIFICATION

The objective of implantology is to design devices that induce controlled, guided and rapid osteointegration (94). In the recent years, lots of scientific investigations have been conducted to achieve these requirements. Ong et al (95) proved that surface modification techniques can affect significantly the outermost layer properties of materials (such as titanium) and, subsequently, induce biological responses and alter the cellular fixation rates.

Surface characteristics are crucial for a successful biological performance of implants. Whereas mechanical properties such as Young’s modulus and fatigue resistance are mainly

determined by the bulk of the material, chemical and biological interactions between the material and the host tissue are closely associated with the surface properties. These interactions include early events, such as binding of water molecules, ions and biomolecules, as well as mineralization at the implant surface, which will provide the conditions to an eventual cell interaction (81; 96; 97).

Macroscopic and especially microscopic properties of implant surfaces play a major role in the osseous healing of dental implants. Several studies have demonstrated that surface morphology or topography as influence in the cell response, leading to extraordinary and unexpected results (1; 98; 99). Even during both healing and remodelling phases, biological processes at the interface can affect the properties of the native surface oxide. Studies have shown that the thickness of the oxide layer increases with time and that ions (Ca, P) from the physiological environment can be incorporated into the growing oxide (80; 100).

In recent years, these modifications have received an especial attention and many investigations have been conducted. Surface modifications methods such as blasting, anodic oxidation, thermal spraying, sol-gel, ion implantation, etc. were already examined and it was proved that those treatments are able to change not only the topography but also the chemistry of the implantable surface, in order to improve biological, chemical and mechanical properties. These studies also underline the fact that an intentional change in surface roughness often leads to changes (sometimes non-intentional) in the surface composition and in the oxide thickness (53; 101).

7.1 The Anodic Treatment

Over the years, different treatments and techniques have been employed to modify the chemistry and tribology of implantable materials surface to enhance its biocompatibility (1; 102). Between the available alternatives, anodization has been recently reported as the preferred one to form rough, porous and thick oxide films on titanium surfaces (3), using simple and cheap approaches. It consists in an electrochemical method that combines physical and chemical processes for increasing oxide thickness and improving resistance against ions release (98; 102). The general principle relies on the application of an electrical charge to the specimen embedded in an electrolyte solution.

This treatment uses a titanium anode and a palatine, silver or stainless steel cathode for the production of a stable and biocompatible oxide layer, on the substrate surface. All the

reaction takes place in an electrochemical cell (Figure 10) composed by these two electrodes, the anode (oxidation reaction) and the cathode (reduction reaction), an electrolyte solution (the composition can change according to the application specifications) and a power generator.

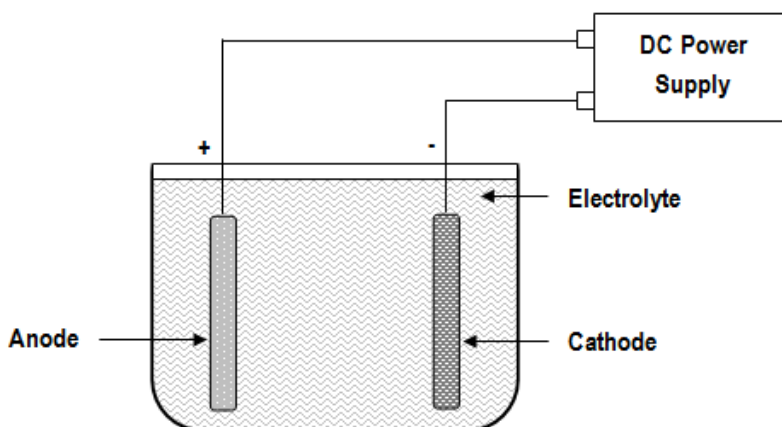


Figure 10. Simple schematic representation of an electrochemical cell (adapted from (103)).

In the titanium anodization, the oxide layer grows thanks to the adsorption of the anions from the electrolyte and the nature of the oxide formed is defined not only by the reactions that take place and the titanium properties but also by the electrolyte composition. Depending on the anodizing conditions, especially voltage, current intensity and electrolyte concentration, it is possible to achieve different types of surfaces (104). For instance, with determined electrolyte concentration, temperature, agitation speed, surface area ratios of cathode and anode and others, the oxide thickness can vary and consequently the surface coloration (4). In consequence to these alterations the tissue reactions change and the biological responses are affected.

The anodic process allows the formation of oxide porous layers favourable to a good biological response. Another advantage of this method is the possibility of incorporation of calcium and phosphate ions into the surface. In this case the control of the electrolyte composition and concentration is the decisive factor (104).

7.2 Titanium Surface Modifications: Characterization

A substantial number of studies have been conducted to examine the osteoblasts behaviour in contact with different surfaces. *In vitro* and *in vivo* studies demonstrated that the

surface composition, topography, wettability and free energy can significantly affect the osteoblasts attachment and development on titanium implants (98).

7.2.1 Chemical Composition

The alteration of the titanium surface composition that contacts with the bone cells, for regenerative purposes, is not new. Over the years, investigations have been conducted to alter the physical-chemical properties of implantable materials, in order to enhance their osteointegration capacity, and different characterization techniques developed to test the viability of those changes. In this case, the characterization techniques must evaluate the purity level of the metal as well as the presence of contaminants that can affect the success of the implantation.

Titanium and its alloys are well-established biomaterials. However due to the generally rather biopassive properties of titanium, the healing process is slower compared to other implant materials with bioactive properties, such as bioglass or hydroxyapatite. On the other hand, CaP-based ceramics have poor mechanical properties, which prevent their use as bulk materials for load-carrying implants, in bone applications. Several strategies based on coating titanium with bioactive CaP-based materials have been developed, in order to combine the favourable mechanical properties of titanium with the outstanding biological properties of CaP-based ceramics (105).

Zhu et al (106) tested the incorporation of Ca and P into anodic oxide films and realized that the osteoconductivity properties of the materials in contact with physiological fluids were improved. For that, they used X-Ray Diffraction (XRD) to characterize the anodic oxide structure, an Electron Probe Micro Analyzer (EPMA) to evaluate the oxide composition and a Scanning Electron Microscope (SEM) to examine the adherence of the cells to the anodic surfaces. Conducting a similar investigation Feng et al (104) proved that theory, demonstrating that increasing levels of protein adsorption can be obtained by the presence of Ca and P ions and, consequently, bioadhesion. In this case, the surface characterization, focusing on the surface chemistry, was carried out using X-Ray Photoelectron Spectroscopy (XPS).

Cui et al (107) showed, through XRD surface analysis and Field-Emission Scanning Electron Microscopy (FE-SEM), that an apatite layer covering the totality of the titanium

surface is able to enhance the bonding strength between living tissue and implant. An anodic film was formed on each titanium surface using different electrolytes and under various electrochemical conditions. It was demonstrated that anodic oxidation is an effective method for preparing bioactive titanium surfaces for artificial bone substitution even under load-bearing conditions.

On his turn, Li et al (108) proved the biocompatibility of bioactive Ti oxides, produced by anodic oxide treatments. In this study they used two types of samples, one with a simple oxide (TiO_2) and other with calcium and phosphate incorporated, and the surfaces were observed and analysed by SEM, XRD and Transmission Electron Microscopy (TEM). Samples were incubated with fibroblasts growth factors mixed with PBS solution, for 24h. After that time, thanks to the CaP presence, a new apatite layer was formed and the growth factors were immobilized into it. With this once again the biocompatibility of bioactive surfaces was proved as well as the applicability of the anodic treatments. This investigation also showed the possible synergic effects on osteointegration, *in vivo*.

Kim et al (72) demonstrated, by SEM and XRD analysis, that using anodic oxidation it is possible to obtain desired roughness, porosity and chemical composition of the oxide. Thanks to the ability of this technique to incorporate new compounds, like calcium and phosphate, into the surface of an implant, it is possible to alter its structure and chemistry. With this, Kim and his collaborators proved the higher surface energy and greater biological activity of bioactive titanium surfaces.

7.2.2 Roughness

There are numerous reports that demonstrate that the surface roughness of titanium implants affects the rate of bone tissue integration and biomechanical fixation. Several *in vitro* and *in vivo* studies have shown that modified surfaces have a higher early level of cell attachment than the untreated Ti surfaces, especially when the roughness is the variable. This property has also been pointed out as the main factor for cell adhesion, migration and differentiation promotion (109; 110), as well as a stimulant factor in the creation of a favourable microenvironment for bone formation (111).

Surface roughness can be divided into three levels, depending on the scale of the features: macro-, micro- and nano- sized topologies, which, consequently, induce different bone reactions. Depending on the size of the topologies, the characterization techniques must be adjusted, although the aim remains the same: evaluate the topography and morphology of the surface (porosity, roughness...).

Larsson et al (112) showed that increasing the roughness of titanium surfaces and the thickness of the oxide layer it is possible to achieve higher levels of bone formation. In this investigation, the totality of the surfaces suffered an electropolish treatment, which was followed, for half of them, by anodization. The surface elemental composition was analysed by Scanning Auger Electron Spectroscopy, whereas the surface roughness and topography was evaluated by SEM and Atomic Force Microscopy (AFM). It was demonstrated that the anodic treatment promoted bone formation around the implant region. Schneider et al (113), in a very similar research, also showed that osteoblasts attachment to titanium is directly related to the surface roughness. On his turn, Bren et al (114) proved that surfaces with nano-scale roughness have greater influence on osteoblasts differentiation than micro-scale roughness, and suggested that high levels of differentiation can be achieved with high surface free energy. In this case, cells' morphology, proliferation and differentiation were examined by Optical Microscopy, SEM and Kinetic ELISAs (for alkaline phosphatase activity); the roughness by AFM and Light Profilometry; the chemical composition of the oxide layer through Auger Electron Spectroscopy; and the surface free energy was determined through contact angle measurements.

Anselme et al (115), conducting an original experiment, evaluated the long term evolution (till 14 days) of the osteoblasts adhesion on CP Ti surfaces with different morphologies. To achieve that, the surfaces topography was extensively analysed using a Tactile Profilometer and the roughness parameters were correlated with the adhesion power (new adhesion parameter) to determine the surface with the highest influence on the cell adhesion. Using SEM, they observed that the human osteoblasts spread more intimately on surfaces with lower roughness amplitude. In contrast, the roughest surfaces exhibited the highest adhesion power. Besides that, with this experiment they confirmed that the human osteoblasts are more sensitive to the organization and morphology of roughness than to its amplitude.

Studies like this one are not that common since most of the investigations focus on the early stages of osteoblasts adhesion and not on the long term evolution.

Gabbi et al (3) demonstrated that titanium surface modifications, in particular surface micro-roughness, can considerably affect the osseointegration process, *in vivo*. The aim of this study was to compare the response of bone tissue to different treated titanium implants: chemically-treated rough titanium achieved by a double step acid etching; bioactive titanium obtained by Bio-Spark; and untreated machined titanium. In the end it was observed, through Stereomicroscopy (characterization technique used for histological analysis) and Fluorescent Microscopy, that these surface modifications improve and speed up the osseointegration process, with an especial attention to the early stages of cells development promoted by the double acid attacked titanium. Roughness is considered by Gabbi et al as a key factor for osteoblasts adhesion and colonization during neo-deposition around the implant.

Das et al (116) conducted an experiment where a bioactive TiO₂ layer was produced on CP Ti samples using three different electrolytes. The resulting surfaces were characterised by a surface Profilometer and exhibited different morphologies with distinct properties. The behaviour of the human osteoblasts from the cell line OPC1 was evaluated for three different periods of time and in the end the results demonstrated that high levels of roughness, high surface free energy and low contact angles (contact angles and surface free energy determined by the Sessile Drop Method), promoted cell materials interaction, which included an improvement of the cells attachment, proliferation and differentiation.

Later, Chiang et al (117) using a simple and fast electrochemical anodic treatment created a structured nano-network layer of TiO₂ on a Ti surface for dental implantation, in order to test its ability to improve cell growth, more specifically the human bone marrow mesenchymal stem cells (hMSCs) growth. To characterize the anodic treatment XRD and FE-SEM analysis were made. This study was conducted both *in vitro* and *in vivo* and in both cases the results were favourable, proving *in vivo* the points of the previous investigations. With a TiO₂ multilayer nano-network the cells growth was enhanced and, in *in vivo* conditions, signals of differentiation toward osteogenic lineage was also observed.

The majority of the studies involving bone cells adhesion to modified metallic surfaces revealed a great improvement on the cells activity with the increasing roughness of the surface. However, there are also some that admit a negative effect.

Stanford et al (118), using a dental implant model (*in vitro*), studied the effect of the CP Ti oxide roughness and chemistry on the osteoblast-like cells phenotype expression. The samples were, firstly, polished through a series of silicon carbide papers and after the sand blast technique was employed. This procedure was followed by sterilization processes, which culminated in the production of three different clinically relevant surfaces. After those, the osteoblasts culture on the samples unities was initiated and lasted for twelve days. The results showed that the bone-specific protein markers, osteocalcin and alkaline phosphatase activity, presented lower levels on rougher surfaces, which contradicts the previous investigations.

Lange et al (119) analysed the cell adhesion dynamics on modified CP Ti surfaces (polished, machined, blasted and vacuum plasma sprayed) and the influence of its structural organization. To evaluate the physical-chemical surface properties they used SEM, surface profiling and Electrochemical Impedance Spectroscopy (EIS). The results revealed that the structural and functional properties of the cell adhesion components were determined by the surface topography. They also concluded that, despite the similar cells morphology on the different surfaces, the spreading, which is an active process and involves integrines, was reduced on more rough surfaces.

7.2.3 Contact Angle and Free Energy

The composition and roughness of the implant surface play an important role in the definition of the interaction between it and the biological environment. However, these properties are not the only ones. Studies have shown that the wettability and the surface energy are both very important in the protein adsorption and additionally in the cell attachment to titanium oxide. Kasemo (120) even reveal that the surface wettability is the real instigator of the osseointegration phenomenon. He pointed out that the water molecules are the first ones to arrive and establish an interaction with the biomaterials surface and just later the proteins, other molecules and cells do the same thing. Macak et al (121) also suggested that the osseointegration mechanism starts when the implant gets in contact with the body

fluids, such as blood: in the hydrophobic surfaces, the signs of the antibodies reduce cell adsorption, while in the hydrophilic surfaces, the signs of the trombines and prontotrombines are predominant and the adsorption is stimulated.

The contact angle is defined as the angle formed between a liquid and a solid, and its value depends on the relation between the liquid and solid adhesive forces and the liquid cohesive forces (Figure 11). If the adhesive forces are higher than the cohesive forces, the liquid wets the surface and the angle formed is less than 50° - the surface is hydrophilic. On the other hand, if the adhesive forces are superior, the liquid does not wet the surface and the angle formed between the liquid and the solid is higher than 50° - the surface is hydrophobic. The same surface can present different behaviours if in contact with different liquids.

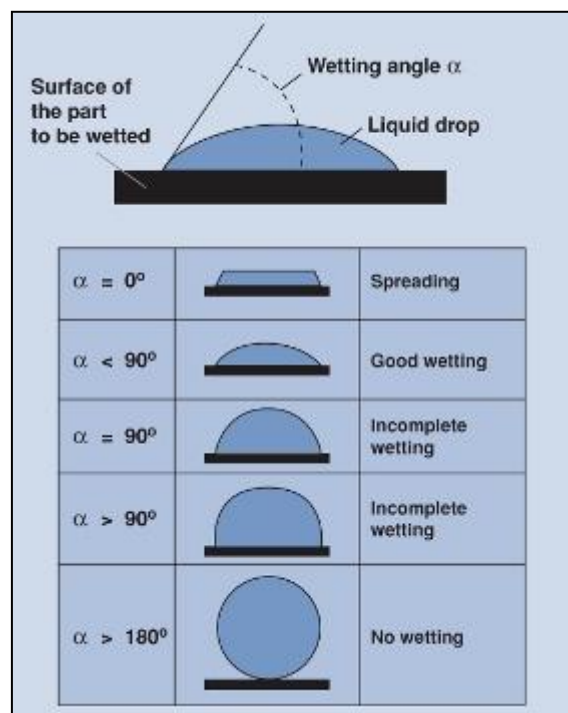


Figure 11. Possible classification for contact angles (122).

The surface free energy can also be determined by the contact angle. Thus, if a surface presents higher levels of energy that means it exhibits a hydrophilic behaviour. On the contrary, if the surface energy is lower the hydrophobic behaviour prevails.

Feng et al (104) conducted an experiment where the titanium oxide films were submitted to different heat-treatments and their surfaces were characterized through XRD and XPS. With this they intended to see the influences of the oxide films and their surface

chemistry on the osteoblasts adhesion and culture. They observed that, besides the surface characteristics, the number of hydroxyl groups on the titanium surface had influence in the behaviour of the osteoblasts that were in contact. They also concluded that the greater the roughness, the larger the surface energy (contact angles measure by Sessile Drop Method and the surface free energy calculated using the Owens-Wendt-Kaeble's equation) and the higher the number of hydroxyl groups, the greater the number of adhered osteoblasts and cell activity.

Rupp et al (123) showed that the surface wettability and energy have a great influence in the protein adsorption and the osteoblasts adhesion to the implants surface. On his experiment, he evaluated the wettability and the fibronectine interactions in specific surface topographies using a Dynamic Contact Angle analysis (DCA, a very sensitive method to detect time-dependent interfacial changes at biomaterial-biosystem interfaces). As a result he was able to identify the relationship between the roughness and wettability of a surface: micro-structured surfaces have great wettability, which may improve the initial biological response at the interface. They demonstrated that these two properties can work together to improve osseointegration.

Zhao et al (124) studied the MG63 osteoblast-like cells growth on modified titanium surfaces. Through sand blasting and acid etched techniques, they created a micro-scale and submicroscale structured surface, similar to the osteoclasts resorption pits on bone wafers. To test the wettability of the resulting surface a DCA analyser was used, and a XPS approach was employed to evaluate the surface composition. The results demonstrated that the surface energy and hydrophilicity allowed an intense osteoblast differentiation by increasing the alkaline phosphatase activity of the cell layer and created an osteogenic microenvironment by enhancing local factors such as PGE and TGF- β 1 levels.

8. SUMMARY

Dental implants are an important tool in dentistry to replace damaged or lost natural teeth. The successful rate of dental implantation is higher, although, sometimes, failure happens. To avoid that, numerous factors must be controlled and understood. Between all, the bone biology and the implantable material are the critical ones.

The human bone is a dynamic system that involves lots of mechanisms working together to maintain its viability and functionality. Osteoblasts, osteoclasts, osteocytes, proteins and others, play an important role in the implant integration, interacting with the materials surface to create a strong bond that should prevail the longest possible period of time in a patient life.

On its turn, the implantable material should respond favourably to the human body demands. It should be:

- Resistant to high intensity mechanical and physical efforts as well as chemical attacks;
- Biocompatible, to guarantee a favourable biological response;
- Present physical and chemical properties similar to the replaced natural bone structure, to avoid biological disorders and physical stresses.

According to the literature review, the best material for dental implantation and the one that responds more favourably to the previous requirements is the titanium. It presents a protective oxide layer that facilitates the titanium integration. Since the oxide natural form does not guarantee the complete success and sustainability of the implantation, to help in this task, surface treatments can be applied.

Over the years different techniques have been used to modify the chemistry and tribology of dental implant materials. Between the alternatives, anodization has been recently reported as the preferred one. With this technique is possible to change the composition, roughness, hydrophilicity/hydrophobicity and free energy of the titanium surface, to alter the cells behaviour and subsequently enhance the biocompatibility.

This theoretical research allowed an overview of all the subjects involve in dental implantation and the main parameters that this process depends on. Based on this information, it was developed an experiment that intends to analyse in detail the interaction between the human osteoblasts from the cell line MG63 and the commercially pure titanium surfaces, modified by anodic treatment. Since the surface chemistry and topography interferes with the bone cells performance, the plan for this work is to evaluate that behaviour on the anodic surfaces and follow the cellular evolution.

CHAPTER 3:

MATERIALS AND METHODS

1. SAMPLES PREPARATION

Commercially pure titanium (CP Ti) samples with 20 mm of edge (square form – Figure 12) and 2 mm of thickness were used in this study and were all cut from the same original plate (CP Ti grade 2, Goodfellow Cambridge Limited, England). These Ti samples were firstly cleaned in an ultrasonic bath with acetone for 3 min and then submitted to an etched treatment in Kroll's reagent (2 ml HF and 10 ml HNO₃ in 88 ml H₂O) for 10 min.

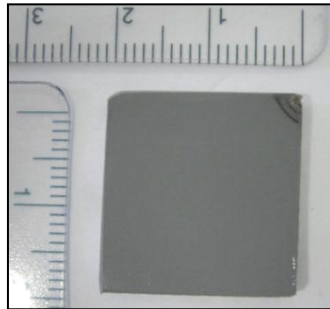


Figure 12. Aspect of a CP Ti sample, after anodic treatment application.

For half of the samples, the etched treatment was followed by anodization. The electrolyte used was composed of 0.7 mol/l of calcium acetate (*Sigma*) and 0.04 mol/l of β -glycerophosphate (*Sigma*), which offers the conditions necessary to create a bioactive coating. The procedure was applied for 1 min, at room temperature, and used 300 V DC (GPR-30H10D) of power. In this case the anode was the CP Ti sample and the cathode a platinum leaf. After anodized, the samples were cleaned in an ultrasonic bath in propanol for 10 min and then in distilled water for 5 min.

2. SURFACE CHARACTERIZATION

The knowledge of the surface properties is essential for a complete evaluation of the biological performance of an implant. The surface morphology, chemical composition, topography, contact angle and surface free energy were the main analysis performed, to test the viability and the influence of the material surface on the biological environment.

2.1 Surface Morphology and Chemical Composition

The morphology of the etched and anodized surfaces was analysed by Scanning Electron Microscopy (SEM) (JEOL JSM – T220A Scanning Microscope). This technique allows the observation of materials in macro and submicron ranges (large depth field and resolution) by generating three-dimensional images, useful for understanding the surface structure of a sample.

This instrument uses a high-energy beam of electrons in a raster scan pattern to scan the samples in observation. The base of this technique consists in the interaction of the electrons from the beam with the atoms at or near the samples' surface, producing signals full of information. For conventional imaging in the SEM, the specimens must be electrically conductive, at least the surface, and electrically grounded to prevent the accumulation of electrostatic charge. Metal objects, such as the titanium samples used in this investigation, require little special preparation for SEM, since they are already conductive. Only cleaning and correct size to fit over the samples holders is necessary (125; 126; 127).

Before SEM observation, all samples were washed in an ultrasonic water bath (60°C) for 10 min and left to dry in a laminar flux chamber for one night. A new sample holder (cylindrical tube) was produced for the observation of those, since their dimension exceeded the common holders, prepared for smaller sizes. After inserting the samples in the SEM chamber, the vacuum was activated to remove all air inside, the intensity of the electron beam was defined to interact with the surface, and the magnification and contrast were adjusted to achieve an image with good resolution.

The previous technique only provides the morphological analysis. To identify the different elements present in the specimen, another application was used: an Energy Dispersive X-Ray Spectrometer (EDS) (EDS INCA model 5785, Oxford Systems). This is an analytical technique that uses the x-rays emitted by the sample in response to the SEM bombardment with a high-energy electron beam. EDS measures the number of emitted x-rays versus their energy, which is characteristic of the element from which the x-ray was emitted. In other words, its principle is based on the unique atomic structure of each element, which, on its turn, provides a unique identification. This is a qualitative and quantitative evaluation (126; 127).

The surface characterization, morphology and chemical composition, was followed in three samples of each type. For each sample, three evaluations were conducted – this includes morphologic and chemical analysis.

2.2 Surface Topography

The surface topographic analysis was entirely developed by a Biomedical Engineering student, Luís Castanheira, at *École Centrale de Paris*, France.

The first technique used was the Microtopography, which allows a complete evaluation of the surface roughness through two distinct ways: contact and non-contact methods. Like the name suggests, in the first case, a stylus tip, connected to a sensor that reads the surface anomalies, contacts directly with the material. However, as a consequence, the surface can be damaged or modified during the test, which explains why this approach is being replaced, nowadays. In the second type, non-contact method, a Confocal Chromatic Technology is usually employed, since only light travels above the surface. This is the approach used in this investigation.

This technique is based on the confocal microscopy principle. The microtopographer (Micromesure STIL, model CHR150-N, France) uses a light source and an objective that focus the light beam in a specific point on the surface. Due to the presence of a displacement table in the X and Y axis, the sample can be moved and the light can traverse the entire surface. When the white light contacts with the samples surface it is reflected and the specific wavelength (of the point) detected by a set of chromatic lens coupled to the equipment. Through this, it is possible to determine the specific position of the light in the measuring field and, subsequently, delineate the profile (2D evaluation) or the surface area (3D evaluation) of the sample (128; 129). Thus, the information is compiled in 3D models and 2D graphics providing the surface microarchitecture and, consequently, its distinctive roughness. This procedure was applied to six samples of each type.

To confirm the validity of the results a second technique was also used, the White Light Interferometry (New-View 6300, Zygo Corp., Middlefield, CT). This is an extreme powerful tool that has been used for many years as a reliable non-contact optical profiling system for measuring step heights (till 0.1 nm) and surface roughness (lateral resolution equal to 2.72 μm , and objective working distance of 9,3 mm). It combines old white light interferometry techniques, with modern electronics, computers and software. The

interferometry principle of operation is based on the presence of a pattern of bright and dark lines resultant from an optical path difference between a reference and a sample beam. The interferometer incoming light is divided, one beam going to an internal reference surface and the other to the sample. After reflection, the beams recombine leading to the production of the bright and dark pattern, which is then converted into a 3D interferogram that will be transformed by frequency domains into a quantitative 3D image of the surface structure. This image will allow the topographic analysis (130; 131; 132). Usually the samples do not need any type of preparation, although in some cases it might need layer deposition to increase reflection or diffuse scattering (133). In this case such was required for the anodic film, since it does not reflect light. This procedure was applied to two samples of each type.

2.3 Contact Angle and Surface Free Energy

The contact angle evaluation was performed at *Universidade do Minho*, Portugal, using a Goniometer as the instrument.

The contact angle is specific for any given system and is determined by the interactions across the three interfaces that composes the system: solid-liquid (γ_{sl}), liquid-vapour³ (γ_{lv}) and solid-vapour (γ_{sv}). The most common method consists of measuring the angle between a small liquid drop (in equilibrium or stable) and a solid surface, as suggested in Figure 13.

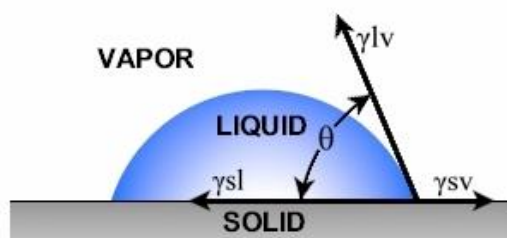


Figure 13. Schematic representation of a contact angle between a liquid and a solid surface. θ = contact angle; γ_{sl} = solid-liquid interface free energy; γ_{lv} = liquid free energy; γ_{sv} = solid free energy (134).

To analyse the hydrophilicity/hydrophobicity of the anodic and etched surfaces, three distinct liquids were used and afterwards the results compared: pure water (polar liquid); formamide (polar liquid); and bromonaphtalene (apolar liquid). Drops of 2 μL of each liquid were gently deposited on the samples surface by a syringe controlled by computer software. After achieving the equilibrium above the surface, an image of the system was taken and the

³ The vapour in this case refers to the atmosphere that surrounds the system.

angle between the drop and the sample measured with the help of the same software. It was used a *Laplacian* approach to determine the angle of contact. This procedure was repeated 7 times with each one of the previous liquids on each type of sample.

To determine the surface free energy a sequence of mathematic formulations were followed. Considering the drop on Figure 13 in equilibrium, we have:

$$\gamma_S = \gamma_{SV} + \gamma_{LV} \cos \theta, (2.1)$$

more commonly known as the Young equation.

On its turn, the adhesion work, Wa , between a solid and a liquid can be expressed by Dupré equation:

$$Wa = \gamma_{LV} + \gamma_S - \gamma_{SL}, (2.2)$$

Thus, combining the previous two equations, it is achieved the Young-Dupré formulation:

$$Wa = \gamma_{LV}(\cos \theta + 1), (2.3)$$

With this, it is possible to relate the contact angle (θ) and the surface free energy of the liquid (γ_{LV}) easily and with high levels of precision.

Fowkes suggested that the totality of the surface free energy was the result from the contribution of different intermolecular forces:

$$\gamma = \gamma^d + \gamma^p, (2.4)$$

γ^d = dispersive forces, such as London interactions;

γ^p = polar interactions, which are mainly interactions between dipoles or hydrogen donors or receivers.

Fowkes considered that only the dispersive forces were important through the interface and for the adhesion work. So he proposed,

$$Wa = 2(\gamma_S^d \gamma_{LV}^d)^{\frac{1}{2}}, (2.5)$$

The Young-Dupré equation can now be re-written as:

$$\gamma_{LV} (1 + \cos \theta) = 2(\gamma_S^d \gamma_{LV}^d)^{\frac{1}{2}}, (2.6)$$

It gives the value of γ_S^d using only one contact angle measure, if just dispersive forces act on the liquid.

Owens, Wendt and Kaelble adjusted the Fowkes equation to a more general form:

$$Wa = 2(\gamma_S^d \gamma_{LV}^d)^{\frac{1}{2}} + 2(\gamma_S^p \gamma_{LV}^p)^{\frac{1}{2}}, (2.7)$$

which combined with 2.6 gives,

$$\gamma_{LV}(1 + \cos \theta) = 2(\gamma_S^d \gamma_{LV}^d)^{\frac{1}{2}} + 2(\gamma_S^p \gamma_{LV}^p)^{\frac{1}{2}}, \quad (2.8)$$

where the exponent d represents the dispersive components and p the polar components, including all solid and liquid interactions.

The equation 2.9 gives an estimation of the surface free energy of a solid, using two liquids with γ_{LV}^d and γ_{LV}^p known and the contact angle measures (134; 135). After knowing the contact angles between the three considered liquids (water, formamide and bromonaphthalene) and the solid surface, using the previous equation, the surface free energy was determined.

3. STERILIZATION

Before cell culture, samples were sterilized in two different steps. The first one was applied in order to achieve the physiologic pH (pH = 7.4) and to eliminate the surfaces impurities produced during the manipulation. To accomplish that, samples were immersed in a 1.5 M NaCl (Sodium Chloride, *Fisher*) solution for 4 h and then, for another 4 h, in a 0.15 M NaCl solution. After, they were left, overnight, in 500 ml of PBS (Phosphate Buffered Saline, *Gibco*) solution, and finally, each side of the sample, was sterilized with ultra-violet (UV) radiation (30 W) for 15 min.

In the second phase, the goal was to assure the ionic and proteic equilibrium required for the cellular contact. For this, samples were left in a non-complete medium of Dulbecco's Modified Eagle Medium (DMEM, *Gibco*) for 24 h at 37°C and 5% of CO₂, and overnight in a complete medium with DMEM and 10% of Fetal Bovine Serum (FBS, *PAMTM*) (Table 2), in the same conditions.

Table 2. Composition of the mediums used in the sterilization process.

NON-COMPLETE MEDIUM	COMPLETE MEDIUM
98% DMEM + L-Glutamin, <i>Gibco</i>	88% DMEM + L-Glutamin, <i>Gibco</i>
1% Penicillin-Streptomycin, <i>Gibco</i>	1% Penicillin-Streptomycin, <i>Gibco</i>
1% Fungizone, <i>Gibco</i>	1% Fungizone, <i>Gibco</i>
-	10% Fetal Bovine Serum, <i>PAMTM</i>

DMEM is a basal medium consisting of 4.5 g/l of glucose, 0.6 g/l of L-glutamine, vitamins, salts and a pH indicator. It contains no proteins or growth factors, which explains the addition of the antibiotics and the FBS to complete it.

4. OSTEOBLASTS CULTURE

The MG63 osteoblast-like cell line derived from the human osteosarcome (from American Type Culture Collection) were used in this study. This cell line is a well established model for studying the effects of surface morphology/topography on osteoblast-like cells and represents a less differentiated stage of osteoblastic maturation (124). The MG63 are also capable of preserving their cellular characteristics for a long period of time without the risk of losing phenotype expression. Thanks to this property, up to fifty culture passages can be accomplished using the same original criovial.

4.1 Culture Expansion

The osteoblasts were cultured in a complete medium of DMEM (Table 2). Since the cells were already used in previous investigations and crio-preserved in the passage five (P₅), the expansion started in the passage six (P₆). After unfrozen the criovial cellular content, in a 37°C water bath, it was quickly mixed with 10 ml of medium, to avoid DMSO (Dimethyl Sulfoxide) contamination, and seeded in a T₇₅ (75 cm² of area, *Falcon*) polystyrene culture flask (Figure 14). To maintain the viability of the cells and to promote their proliferation, the flask was kept in the incubator at 37°C with a 95% humidified atmosphere and 5% CO₂ in air. The osteoblasts culture was monitored every 24 h and the medium changed at least twice a week.

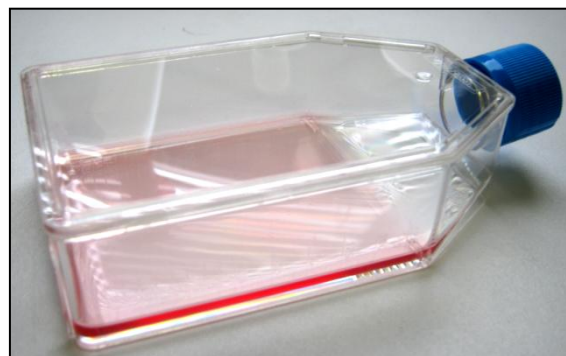


Figure 14. Osteoblasts culture in a polystyrene culture flask (T₇₅) (CANON A480).

At 80% of confluence the medium was removed, the flask washed three times with PBS (10 ml) and the cells were finally detached using trypsin-EDTA (*Gibco*) (5 min). The

cellular content was then passed for three new flasks (10 ml for each flask) and this procedure was followed until cells are needed to the assays.

Subsequently to the obligatory passages, the cells were seeded onto the CP Ti samples surface. In this case, to inactivate the trypsin action, only 4.5 ml of medium were required. Cells were then counted and viability tests applied (the procedure followed is described in the next section). The initial concentration of 2×10^4 cell/ml, prepared in complete medium, was used in each assay, due to the osteoblasts rapid proliferation.

A total of 2 ml of cellular suspension was inserted in each well, which means 4×10^4 cells per well. The six well plates (Figure 15) were left in the incubator, at 37°C and 5% of CO₂, for the respective period of time, with constant monitorization.

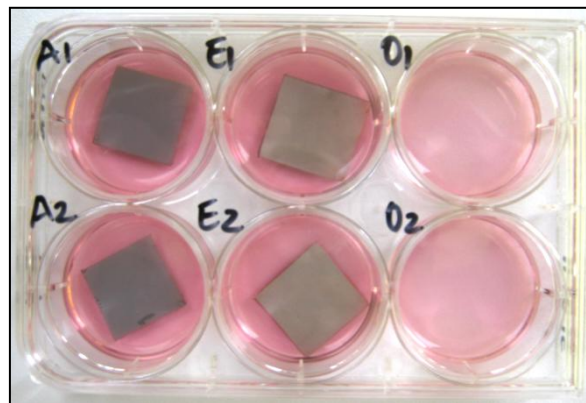


Figure 15. Six wells plate prepared for culture. A1 and A2 – Anodized samples; E1 and E2 – Etched samples; and O1 and O2 – Control (without sample). To each well, 2 ml of medium with a total of 4×10^4 osteoblasts was added.

4.2 Adhesion

To quantify the osteoblasts cell attachment onto the titanium surface and to study their interaction in the first moments of contact, adhesion was assessed. Four samples, 2 anodized and 2 etched, were used for each period of time: 0.5, 2 and 4 h. Besides that, two wells without sample were, also, filled with the cellular suspension creating the culture controls.

The osteoblasts adhesion and spreading were evaluated through the assessment of their viability and the number of cells attached to the samples.

After each time point, the medium was removed, the samples were washed three times with PBS and then placed into new plates. For each sample 2 ml of trypsin-EDTA were added and left in action, at 37°C and 5% of CO₂, for 10 to 15 min, in order to detach the totality of the cells. Subsequently, the trypsin was inactivated with 2 ml of medium.

The cellular content achieved was then divided for posterior evaluations: viability and number of cells. In the first case, trypan blue was the reagent applied. It was used in a reason of 25/25 μl of cellular content and viability was assessed using a *Malassez Cell (PolyLab)* by counting the live (only cytoplasm coloured but not the nucleus) and death (coloured nucleus) cells, following the equation:

$$\frac{\text{Nr cells with coloured cytoplasm}}{\text{Nr Malassez large squares}} \times 10^5 = \text{Total nr of cells alive}$$

This test was performed as fastest as possible to guarantee the accuracy of the results. In the second case, to count the number of cells in each place (medium, plate and sample, Figure 16), 1 ml of the suspension was combined with 9 ml of isotope (*IsoFlowTM*) and the evaluation preformed by an Automatic Cell Counter (Z2, Beckman Coulter).

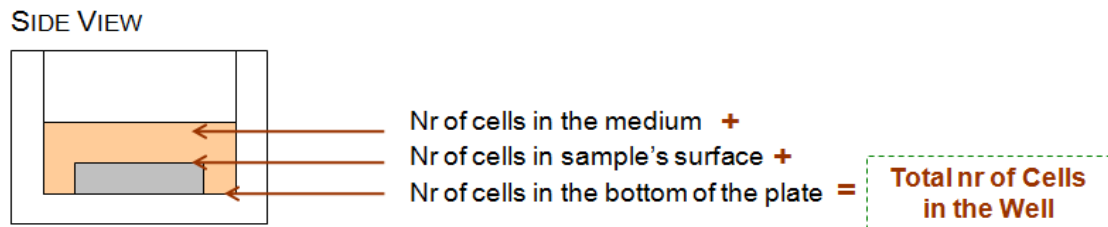


Figure 16. Side view, schematic representation of a plate well with culture medium and sample, showing the three main parts from where the cells are removed and afterwards counted.

In the end, to verify the absence of cells on the surface, samples were fixed with formaldehyde (*Sigma*). Firstly they were washed 2 times with PBS, then 2 ml of medium were introduced with 100 μl of formaldehyde and after 45 min morphology was evaluated as described in section 4.3.

4.3 Spreading and Morphology

The morphology tests allowed the observation of the cells connection to the samples surface, their organization, shape and size. For that, 2 samples of each type were required, for each control time: 0.5, 2.0 and 4.0 h.

After each time, samples were washed 3 times with 2 ml of PBS and passed to a new plate. Then, the osteoblasts MG63 were fixated with 100 μl of formaldehyde (37°C) combined with 2 ml of medium and left for 45 min at 4°C. Later than, they were washed again 2 times with PBS (5 min) and then another 2 times with a PBS and BSA (Bovine Serum

Albumin, *SAFC*) solution, in a concentration of 0.4 g/l, for 5 min. To achieve the cells membrane permeabilization, 2 ml of Triton X100 (*Labosi*) in a 0.1% v/v of PBS, at room temperature (5 min), were added.

A new PBS and BSA solution (30 g/l) was then prepared and inserted in each one of the wells (it should cover completely the sample). It was left there for 30 min, at room temperature. This step allowed the blocking of the non specific cells connections. Succeeding that, 3 new washes were done with PBS and BSA in a concentration of 0.4 g/l. Afterwards a *Bodipy Phalloidin (FluoProbesTM)* solution was added, to stain actin fibers on the cells' cytoskeleton (main constituents of the cells architecture) in a quantity of 2 ml/well (this means 50 µl of methanolic solution for 2 ml of final PBS) and left there for 4 h. In the end, the surfaces were washed 4 times with sterile PBS and left to dry at room temperature. A total of 6 pictures per sample were taken using a fluorescent microscope (ZEISS Axioplan, Germany) coupled with a photographic camera (Olympus C-5050).

The images were analysed using a specific software, the Quantity One: 1D Analysis Software, which allowed the scaling in size of each cell from each picture. Thanks to this, a statistical analysis of the average size of the cells attached to the anodic and etched samples was possible.

4.4 Proliferation

In this assay the number of cells was the most important factor to retain. Therefore, 2 samples of each type were again required for each considered day: 1, 3, 7, 10 and 14 days. To conduct a complete evaluation of the number of cells (Automatic Cell Counter), three spaces were considered: medium, plate and sample – the total number was acquired by the sum of these three parts (see Figure 16).

Before starting any procedure the medium was removed and the wells (which include the samples) were washed three times with PBS. In this case, the control was again the cellular culture directly onto the plate.

The procedure followed was the same described in 4.2 *Adhesion and Spreading*.

4.5 Alkaline Phosphatase Activity

The alkaline phosphatase (ALP) activity test is used to reveal the presence of this enzyme, which is responsible for the liberation of phosphate into the extracellular matrix during the transformation of the p-nitrophenylphosphate substrate into p-nitrophenol.

The ALP activity was followed for 7, 14, 21 and 28 days. Since the osteoblasts do not possess the ability to produce calcium and phosphate by themselves, in *in vitro* cultures the composition of the DMEM complete medium was changed to induce this production. Besides the known constituents, ascorbic acid (*Sigma*) and β -glycerophosphate (*Sigma*) were included in a reason of 0.00805 g and 1.08 g in 500 ml of DMEM, respectively. This change promotes the osteoblasts MG63 maturation stage of evolution.

In the beginning of this test, the culture medium was removed, the samples were washed 3 times with PBS and placed in a new plate. Subsequently, 2 ml of Tris Buffered Saline (TBS)-Triton X100 solution (0.4844 g Trizma Base (*Sigma*), 1.6 g NaCl, 2 ml Triton and 198 ml distilled H₂O), at 37°C, was added to each well (the ones with samples and the two considered as controls) and the plates left there for 1 h. All the content was then removed to tubes and strongly mixed for 5 min, followed by three cycles of freezing at -80°C and unfreezing at 37°C. Between each cycle, the cellular suspension was submitted to a strong agitation for 5 min.

The next steps aimed to measure the enzymatic activity. For that, it was used a spectrofluorimeter (Safas Xenius) which measures the solutions' absorbance.

Firstly 500 μ l of cellular material were mixed with 500 μ l of p-nitrophenylphosphate substrate (*Acros*) in a concentration of 20 mM (buffer solution AMP, at pH = 10.2 composed by 0.742 g p-Nitrophenylphosphate (20 mM, *Acros*), 0.0407 g MgCl₂ (2 mM, *Merck*), 0.0891 g 2-Amino-2-Methyl-Propanol (10 mM, *Acros*) and 100 ml of distilled H₂O) and left in the incubator for 30 min at 37°C. The quantity of p-nitrophenol produced was measured by optic density at 405 nm of absorbance against a p-nitrophenol (*Acros*) range of concentrations (Table 3) in the buffer AMP.

Table 3. p-Nitrophenol (p-NP) range of concentrations in the buffer AMP⁴.

[p-NP] (μmol/ml)	0	0.05	0.1	0.15	0.2	0.25	0.3	0.4
Solution p-NP (μl)	0	5	10	15	20	25	30	40
Buffer AMP (μl)	1000	995	990	985	980	975	970	960

The ALP activity results were, in the end, normalised in order to consider the totality of proteins contained in the cellular suspension. This quantity was detected using a commercial kit, BioRad (*Bio-Rad Laboratories*). For that, 25 μl of cellular suspension were combined with 125 μl of a reactive A' (reactive A' = 10 μl of reactive S + 500 μl of reactive A) and 1 ml of reactive B, well mixed and left in repose for 15 min before quantification. The results were measured by optic density at 750 nm of absorbance against a BSA range of concentrations in TBS-Triton (Table 4).

Table 4. BSA range of concentrations in TBS-Triton.

BSA (μg/ml)	0	0.05	0.1	0.2	0.3	0.4	0.6	0.8
BSA 1 mg/ml (μl)	0	5	10	20	30	40	60	80
Tampon TBS-Triton (μl)	100	95	90	80	70	60	40	20

4.6 Mineralization

The mineralization starts with the calcium and phosphate precipitation induced by the ALP activity. Thus, the results should show an advanced stage of the bone mineralization as well as the osteoblasts evolution into osteocytes. Although, as happened in the previous test, the culture medium composition was altered and enhanced with ascorbic acid and β-glycerophosphate (in the same quantities), to induce the osteoblasts maturation.

For this assay, 4 culture periods of time analysed: 7, 14, 21 and 28 days. Like the previous trials, the medium was initially removed, the samples washed three times with PBS and placed in a new plate. After that 2 ml of trichloroacetic acid (TCA, *Sigma*) at 15% in ultra pure water were added and let there for 1 h.

Since this trial consists in the analysis of the calcium and phosphate levels, it was divided in two parts. The first one, related to the calcium detection, was initiated 1 h after the

⁴ The range of concentrations in this table (Table 3) and in the next ones (Table 4, Table 5 and Table 6) gives the calibration curves used to compare the absorbance results from each correspondent trial and, consequently, allows the change of unities, from optic density to concentration in μg/ml.

TCA exposure. Later that time, 300 μl of solution were removed to a new container and the rest of the suspension remained in contact with the samples and wells for 48 more hours – posterior phosphate detection. From that 300 μl , 10 μl were combined with 1 ml of Arsenazo III (*Sigma*) at 0.2 mM in PBS (1X), well mixed and left for 15 min before quantification. The quantity of calcium produced was measured by optic density, using a spectrofluorimeter, at 650 nm of absorbance against a calcium chloride (CaCl_2) and TCA range of concentrations in Arsenazo III (Table 5).

Table 5. Calcium range of concentrations in TCA (15% (m/v)).

Ca^{2+} ($\mu\text{g/ml}$)	0	50	100	200	500	600	800	1000
CaCl_2 10 mg/ml in TCA	0	5	10	20	40	60	80	100
TCA 15%	1000	995	990	980	960	940	920	900

For the phosphate detection, after 48 h, 100 μl of the suspension were combined with 800 μl of AAM (2 volumes of acetone (*Carlo-Erbra*), 1 volume of 2.5 mol/l of sulphuric acid in distilled H_2O (*Acros*) and 1 volume of 10 mM of ammonium molybdate in distilled H_2O) solution and strongly agitated. After that, 80 μl of citric acid (*Sigma*) at 1 mol/l in ultra pure water were joined and, again, strongly mixed. Before measuring the phosphate quantity extracted, the solution was let for 30 min without agitation. The quantity of phosphate produced was measured by optic density at 355 nm of absorbance, in a spectrofluorimeter, and compared to a (di) sodium hydrogenophosphate (Na_2HPO_4) and TCA range of concentrations in AAM solution (Table 6).

Table 6. Phosphate range of concentrations in TCA (15% (m/v)).

PO_4^{2-} ($\mu\text{g/ml}$)	0	10	20	40	100	120	160	200
Na_2HPO_4 0.2 mg/ml TCA	0	50	100	200	500	600	800	1000
TCA 15%	1000	950	900	800	500	400	200	0

5. OSTEOBLASTS RESPONSE TO TRIBOLOGICALLY MODIFIED SURFACES

The samples used in this experiment were prepared at the *École Centrale de Paris* by a Biomedical Engineering student, Luís Castanheira. The cellular culture was conducted for 4 h, 3 and 7 days.

These samples suffered tribological alterations induced by unidirectional sliding tests, which were produced by an unidirectional *pin-on-disc* tribometer (Multispecimen-tester, FALEX-TETRA) stationed on a stabilizer table (Vibration Isolation System with Stabilizer™ Technology, BenchTop™, Newport), in order to avoid interferences to the test. The pin-on-disc approach can be better understood if we consider the next figure (Figure 17 A):

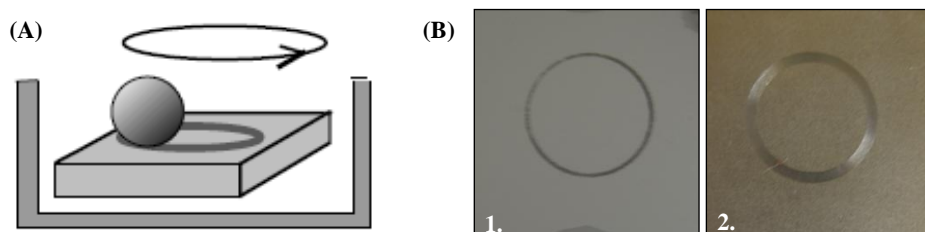


Figure 17. (A) Unidirectional *pin-on-disc* approach on the samples surface (136). (B) 1. Anodized sample, 0.8 N; 2. Etched sample, 0.8 N.

As a result, from this frictional rotative movement executed by the pin against the stationary sample (136), embedded in artificial saliva (pH = 5.5), a wear track is formed in the centre of the sample, like Figure 17 B shows. To achieve that, 7200 rotational cycles were applied with a velocity equal to 100 rpm and load 0.8 N, in each sample.

Before cell culture, all samples were cleaned in an ultrasonic pure water bath (60°C), for 10 min, and then sterilized in an Autoclave (SANO Clay, WOLF) at 120°C, for 30 min. Contrary to the previous trials that followed a specific pathway of sterilization, in this case, since toxic material was applied during the tribocorrosion test to isolate the sample and the electrolyte from the equipment electronic mechanisms, a more aggressive sterilization process was necessary. The same amount of osteoblasts MG63 were seeded into the CP Ti samples (2×10^4 cells/ml).

The results were observed using a Scanning Electron Microscope (SEM, JEOL JSM – T220A Scanning Microscope). Although, before visualization, all cells on the samples were fixated using a solution of DMEM and 4% of formaldehyde; then the samples were

dehydrated in a range of ethanol concentrations (50%, 70%, 90% and 100% in pure H₂O – 20 min each immersion), in order to achieve a better quality of image; and in the end coated with a gold pander to guarantee the electrical conductivity of the samples. A significant number of images from the osteoblasts MG63 on the normal surface and on the wear track were taken.

6. STATISTICAL ANALYSIS

Each trial, including surface characterization, was repeated between three and six times, always following the same conditions. In the adhesion, morphology, proliferation, ALP activity and mineralization assays two samples were tested in simultaneous, during each repetition. However, for the last trial, *5.Osteoblast response to surface chemical and mechanical modifications*, since the samples production took more time and the cleaning and sterilization was more difficult to apply; only three repetitions were conducted using just one sample at the time.

The statistical analysis was conducted using the software GraphPad Prism following the Anova parameters. Differences between the results were only considered significant if the percentage was up to 95% and $p < 0.05$.

CHAPTER 4:

RESULTS AND DISCUSSION

As referred the main goals of this research are the study of the osteoblasts MG63 response to anodized CP Ti and the evaluation of the differences between the anodized and etched surfaces. Besides that, the influence of the anodic surface bioactivity on the osteoblasts maturation was also a highlight point of the study.

Firstly the materials surface characterization will be examined and then the results from the osteoblasts culture will be discussed. An analogy between these two parts will provide a better understanding of the osteoblasts MG63 behaviour on the two types of surfaces.

1. SURFACE CHARACTERIZATION

1.1 Surface Morphology and Chemical Composition

The morphology of the anodized and etched surfaces was observed by Scanning Electron Microscopy (SEM). The images from Figure 18 are representative of the surface aspect before any cell culture.

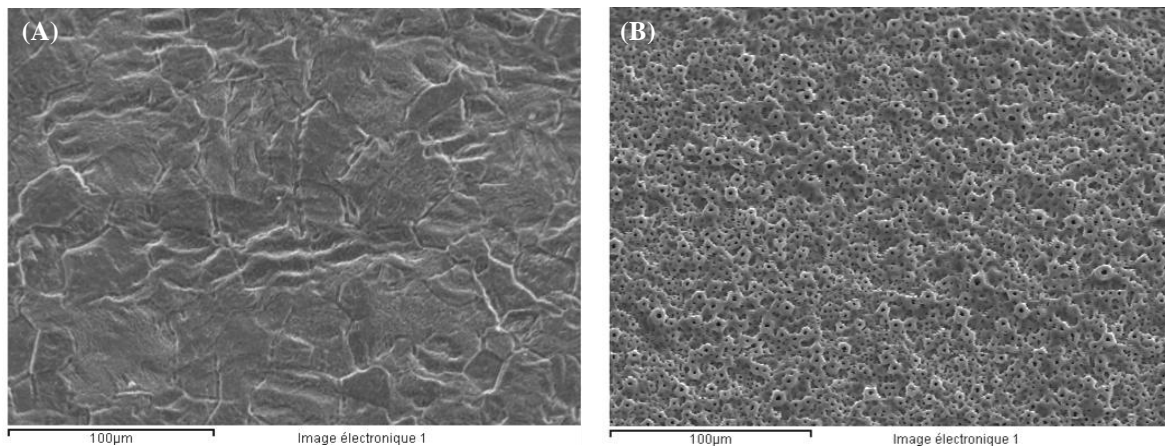


Figure 18. SEM micrographies of the (A) etched and (B) anodized surface morphology. Magnification of 500X.

The differences observed between the two surfaces are mainly determined by the treatment applied. In the first case, etched samples (Figure 18A), the Kroll's reagent was used to clean and remove all impurities from the surface. However, since this reagent is an acid solution, its application resulted in a rough and crimped surface, which is evident by the range of grey colours in the picture (darker for lower and brighter for higher elevations). In the

second case, anodized samples (Figure 18B), a very porous film with a wide and heterogeneous range of porous size is exhibit – the porosity is a result of the electrical discharges characteristics of the anodic treatment (dielectric breakdown) (1; 3; 80). It is also evident a discrepancy in the surface elevation, translated by the difference in the porous size – higher and more discernible porous at the top (probably derived from interconnections of some other pores) and smaller and harder to distinguish at the bottom – and by the grade of coloration, like happened in the etched surface. These differences can be explained by the fact that all samples were firstly submitted to etched treatment and just then the anodization was applied. Thus, the undulation detected in the first treatment was then “printed” in the anodic film, during its production – the oxide film formed followed the original surface topography, as expected (80).

In relation to the chemical composition, the analyses were conducted by Energy Dispersion X-Ray Spectroscopy (EDS), a tool associated with the SEM evaluations. The spectra (Figure 19) resulted from the analysis of a specific point from each image of Figure 18 – these results are representative of various evaluations performed (standard deviation on the percentage values) in three samples of each type.

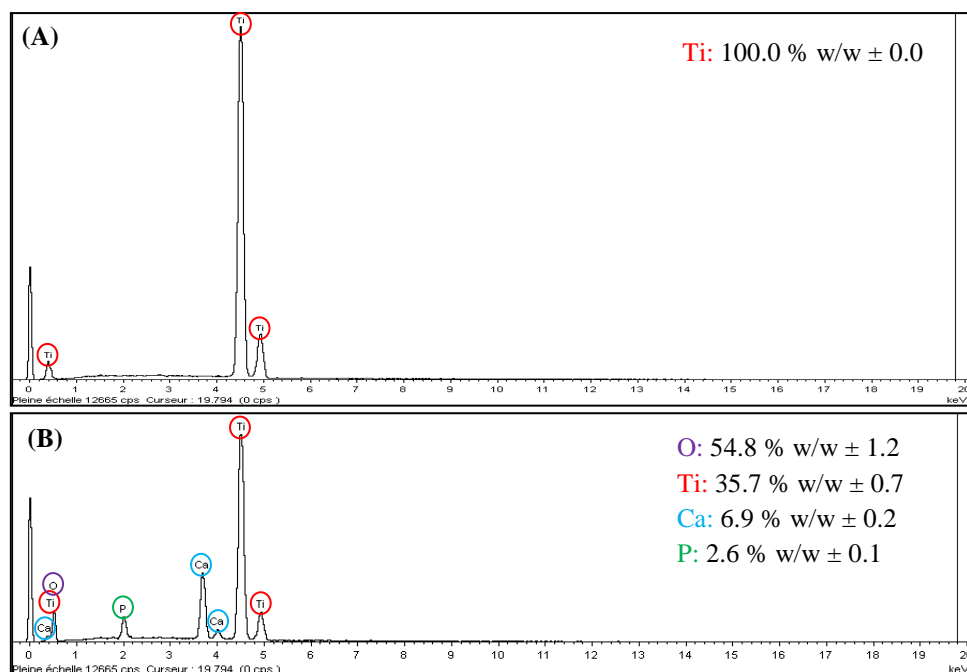


Figure 19. Spectra representative of the (A) etched and (B) anodic surface chemical composition – EDS analysis.

The chemical analysis of the etched surfaces revealed only one element, titanium (100 %). It proves the applicability of the etched treatment as a cleaner and an impurities remover and its capacity of maintaining the surfaces original composition, pure titanium (grade 2).

On the contrary, the anodized surface exhibits more elements, aside from titanium, like oxygen, calcium and phosphorus. These elements are all inherent to the anodic treatment. As was referred in the third chapter of this thesis, the electrolyte used to produce the protective film was composed of calcium acetate and β -glycerophosphate. During the treatment, these elements were attracted to the surface due to a chain of oxidation and reduction reactions induced by electrical discharges (1), which explains the presence of calcium and phosphorus on the surface. Through this, it was possible to determinate the Ca/P ratio as equal to 2.65, much higher than the standard stoichiometric ratio of 1.67 (100; 106). A considerable difference is also evident comparing this value with the one from the initial electrolyte composition – 1.75. The only possible explanation for this may rely on the anodic treatment conditions. Any small change in the parameters associated with the production of a bioactive layer (pH of the reaction, time of control, temperature, matter stoichiometry...) can lead to huge changes in the oxide conformation (1).

On the other hand, the oxygen presence is explained by the titanium oxide formation. According to Kuromoto et al (80), when the anodic voltage is high (near to 300 V) the oxide film formation occurs due to the migration of O^{2-} ions from the electrolyte into the metal/film interface and migration of the Ti^{4+} ions from metallic Ti to the film/electrolyte interface. During the treatment, lots of reactions participate in the film growth, although the most relevant ones are those that give rise to O_2 and TiO_2 (titanium dioxide most common form: $Ti^{2+} + O^-$ ions), which clarifies about the higher quantity of oxygen ions (54.8 % \pm 1.2) on the surface. This high rate of O_2 is also related to the particular morphology of the anodic surface, observed in Figure 18. Under high anodic voltages, the electrolyte becomes unstable and the O_2 formed lead to an enhancement of the system pressure, damaging the film and giving rise to the formation of pores (80).

Another important aspect about these results is the accomplishing of a bioactive surface. The incorporation of calcium and phosphorus ions on the materials surface has the ability of improving the osteointegration, which guides to a better connection and relationship between the bone cells and the implantable structure (100; 104).

1.2 Surface Topography

Over the years, many studies have reported the influence of the implantable surface topography (in this case roughness) on the cells behaviour and in the implant success. In order to conduct a consistent analysis on the osteoblasts MG63 development on the etched and anodized surfaces, it was indispensable to consider a roughness analysis. As was described in Chapter 3, two techniques were used to measure this property: Microtopography, through Confocal Chromatic Microscopy, and White Light Interferometry (by doing this, it is possible to confirm the data obtained). Both evaluations were conducted in 2D and 3D, and the results presented in the form of Ra (average roughness) and Rz (single roughness depth), and Sa and Sz (analogous to the previous), respectively.

Table 7 gives the average values of roughness of the etched and anodized samples, followed by the respective standard deviations.

Table 7. 2D and 3D topographic (roughness) evaluations of etched and anodized titanium surfaces using Microtopography and Interferometry as techniques.

Method	Sample	2D Analysis		3D Analysis	
		Ra (μm)	Rz (μm)	Sa (μm)	Sz (μm)
Microtopography	Etched	0.88 (± 0.08)	7.62 (± 1.16)	1.08 (± 0.01)	12.97 (± 0.30)
	Anodized	0.83 (± 0.08)	6.30 (± 0.66)	1.03 (± 0.05)	10.85 (± 1.20)
Interferometry	Etched	0.98 (± 0.04)	6.01 (± 0.41)	0.98 (± 0.00)	10.71 (± 0.42)
	Anodized	1.00 (± 0.02)	6.63 (± 0.32)	1.02 (± 0.03)	10.52 (± 0.74)

Comparing the results obtained by the two techniques (Table 7), it is possible to observe that there are no significant differences between the etched and anodized treated samples, only minor changes can be observed ($p > 0.05$). However, considering the standard deviation associated to each result, those minor changes can be neglected and, once again, the similarity of the values, between each category, confirmed.

Exploring the results from both techniques, it is possible to detect that 3D analysis (surface) have a small tendency to exhibit higher values than 2D analysis (profiles). This could be a reflection of the amount of material evaluated, since 3D analysis consider more extensive surfaces and, by the Rz and Sz correlation, better perception of the vertical distance between the highest peak to the deepest valley.

The images from the surface morphology (Figure 18) showed a complete transformation of the samples surface after anodization – a porous heterogeneous layer was

formed. Through a visual analysis, it was expected that the average roughness and even the single roughness depth changed too. Although, both evaluations (microtopography and interferometry) proved it wrong. Ehrenfest et al (137) have already explained this event by testing different types of surfaces. They concluded that the presence of different morphologies do not always mean different topographical properties.

Rodriguez et al (102), conducting a similar investigation showed a great difference on the Ra parameter between the titanium samples cleaned by etched treatment (HF and HNO₃ ratio of 1:3, instead of 1:5 as it was used) and the anodized surfaces prepared with calcium-glycerophosphate (Ca-GP, 0.02 M) and calcium acetate (CA, 0.15 M) at 350 V (following analogous conditions to our treatment). The results obtained were $0.34 \pm 0.01 \mu\text{m}$ and $0.73 \pm 0.02 \mu\text{m}$ for the etched and anodized surfaces, respectively. Despite the proximity between the anodic Ra from their research and this work (Table 7), the etched value presented a large discrepancy. This can possibly be explained by potential irregularities on the CP Ti material used on this study. However, this speculation can only be attested through a considerable number of meticulous tests on the material surface, which is left as a suggestion for future research projects.

To prove the existence of possible inconsistencies on results obtained by following the exactly same procedure, it can be proposed an analogy between Rodriguez et al (102) and Zhu X. et al (106) anodic CP Ti surfaces production and topographic characterization. The conditions followed by both studies were equal: etching with HF and HNO₃ in a ratio of 1:3 (same cleaning and procedure time); electrolyte prepared with 0.02 M Ca-GP and 0.15 M CA; voltage equal to 350 V; and constant current mode at 70 A/m^2 . As was shown before, the Ra obtained in the former study, was near to $0.73 \mu\text{m}$. On the other hand, on the latter, the Ra value was $0.98 \mu\text{m}$. Through this, it is confirmed the validity of the results of the present study (Table 7).

Since only a microroughness analysis was conducted, no argument will be made on the possible presence of nanoroughness on the anodized surface. However, this possibility might be real and can affect the osteoblasts MG63 development.

1.3 Contact Angles and Surface Free Energy

The contact angle and surface free energy are both very important in the protein absorption and, additionally, in the cells attachment to titanium surfaces. In this study to

measure the contact angles three liquids were used: pure water (polar), formamide (polar) and bromonaphtalene (apolar liquid). The results from the contact angle measurements are presented in Table 8.

Table 8. Contact angles of water (θ_w), formamide (θ_f) and bromonaphtalene (θ_b) of the etched and the anodized surfaces, measured using a Goniometre, and determination of the total surface free energy (ΔG).

Sample	θ_w (°)	θ_f (°)	θ_b (°)	ΔG (mJ/m ²)
Etched	92.24 ± 2.98	93.34 ± 1.26	29.87 ± 4.21	-26.81
Anodized	98.74 ± 3.19	94.08 ± 2.02	53.27 ± 1.10	-44.58

Comparing the results from the etched and the anodized samples, it is possible to conclude that, although without significant differences on water contact angles, regarding the free energy, the anodized sample is more hydrophobic than etched sample, since it has the lowest surface energy. According to these, it is expected that the osteoblasts interaction with the etched surfaces to be stronger than with the anodized (138; 139).

As presented before, both surfaces presented high levels of roughness (Table 7). Lim et al (140), conducting an investigation on the contact angles of different titanium surfaces for dental implantations, discovered that there is an intimate relationship between the resulting contact angles and this property. They found that the contact angle increases linearly with the average roughness, when the angles were higher than 45 degrees. Thus, given that there were no significant differences between the etched and anodized surfaces and both presented high levels of roughness, this can justify their hydrophobicity and the negative surface free energy.

Kasemo et al (141) have proved that in hydrophilic surfaces the protein interactions are intermediated by a water layer and there is no direct contact. On the other hand, in hydrophobic surfaces, a direct bond with the proteins is created, leading to conformational changes. It is believed that hydrophilic surfaces induce a more rapid progression in the osteoblasts fixation and expansion (142). Given that, it is expected a slower progression in both surfaces compared to previous similar investigations and a slight improvement in the MG63 cells expansion for the etched surface, thanks to its higher hydrophilicity.

2. OSTEOBLASTS CULTURE

The main practical application of this study is dental implants. During implantation, the bone tissue is surrounded by bone forming cells (osteoblasts), which will form the bond

with the implantable material, if all the required conditions are reunited, and stimulate the osteointegration. This is the key reason for the osteoblasts MG63 cell line selection. Since the osteoblasts from this line are in a less differentiate stage of maturation, it provides the conditions necessary to analyse the progressive evolution of the contact between them and the material, from the early stages of development. The osteoblasts MG63 behaviour was studied on anodized and etched surfaces.

2.1 Adhesion

The first moments of contact between cells and material are crucial for a successful implantation. A suitable surface for osteointegration should first promote cell attachment and then sustain proliferation, maintain cell differentiation and improve extracellular matrix secretion. Therefore, all these subsequent stages of cells development depend on the first one, cells attachment. This is a very specific parameter that describes the relative adherence of a cell to its substrate, generally at an early stage of culture (143; 144).

The MG63 osteoblast-like cells adhesion was tested for three periods of time: 0.5, 2 and 4 h, and in the three situations the viability was between 87 and 90%, based on Trypan blue exclusion. The results from Figure 20 are in the form of percentage, in which the 100% represents the totality of cells on each well (medium, plate and sample), at each time point.

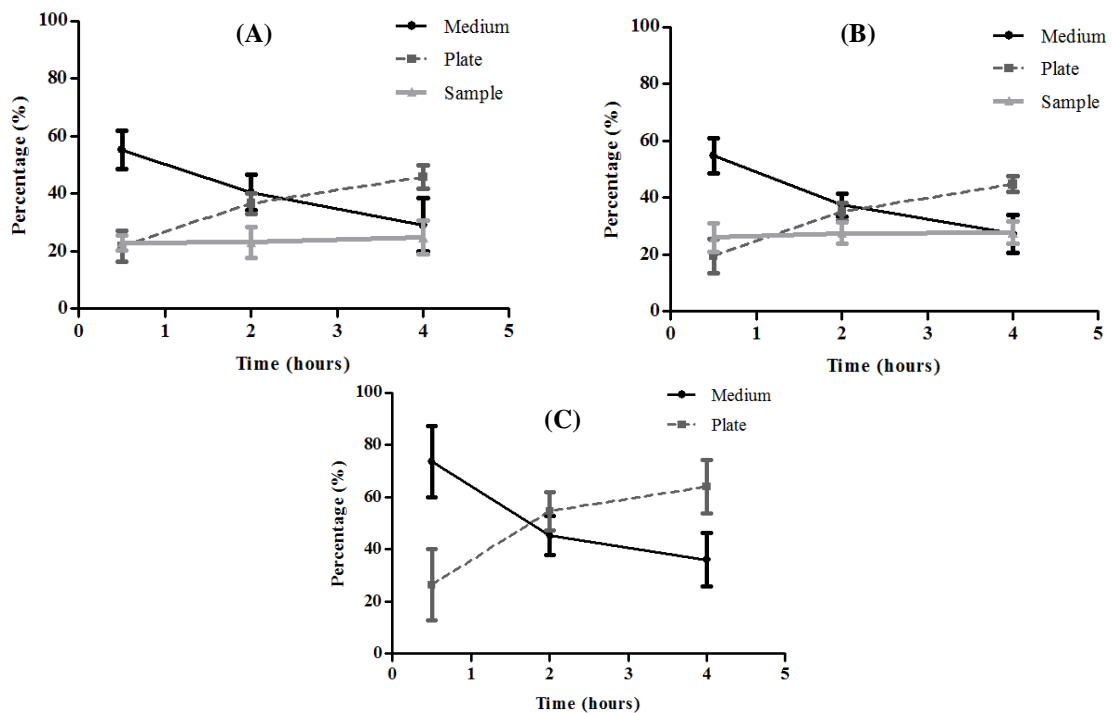


Figure 20. Evolution of the osteoblasts MG63 adhesion to (A) etched and (B) anodized surfaces from 0.5, 2 and 4 h of culture. (C) Control results obtained by the direct culture on the well (without any sample).

The graphic representations (Figure 20) showed that, even after 30 min of contact, there is already a significant percentage of osteoblasts (near to 40%) attached to the surfaces available (sample and plate). There is not a significant difference between the osteoblasts MG63 affinity to etched or anodic samples, although it seems that the anodic treatment possess a slight advantage, reaching about 27% against 22% from the etched cultures. As it was expected and demonstrated by the control results (Figure 20 C), the highest percentage of cells is still embedded in the culture medium.

With the passage of time, a change of events occur. After 2 h of incubation, the percentage of cells in the medium decreases, from approximately 60% to less than 40%, indicating that the majority of cells are now adhered to the available surfaces. This event became much more consistent at the end of the trial, 4 h of incubation, with a total increasing of 30% of the cells attachment. Another interesting aspect in Figure 20 A and B is the more apparent affinity of the osteoblasts MG63 to the plate surface than to the samples itself. This fact can be easily explained by the nature of the culture plates, which are produced in polystyrene (submitted to surface treatment to induce tissue culture, followed by intensive sterilization) and are negatively charged. Usually these characteristics tend to induce cells attachment (145; 146). Since the size of the well exceeds largely the samples' size, there are numerals gaps to where cells prefer to attach.

From 30 min to 4 h of culture, a minor increase in the percentage of cells associated to the etched and anodized surfaces was detected. However, this was not significant to establish a difference between those two, especially since they were kept apart only for $5\% \pm 1.0$, at all time. For a more accurate analysis, the totality of cells on each well (Table 9) must be evaluated, as well as the actual number of cells fixated onto the samples' surface (Figure 21).

Table 9. Total number of cells presents on each well, considering medium (M), surface of the plate (P) and sample (S), according to the trial duration (0.5, 2 and 4 h).

Time (hours)	Total number of cells on each well (M+P+S)		
	Anodized	Etched	Plate (Control)
0.50	7.42E+04	7.22E+04	6.28 E+04
2.00	7.46E+04	7.32E+04	6.33 E+04
4.00	7.48E+04	7.44E+04	6.39 E+04

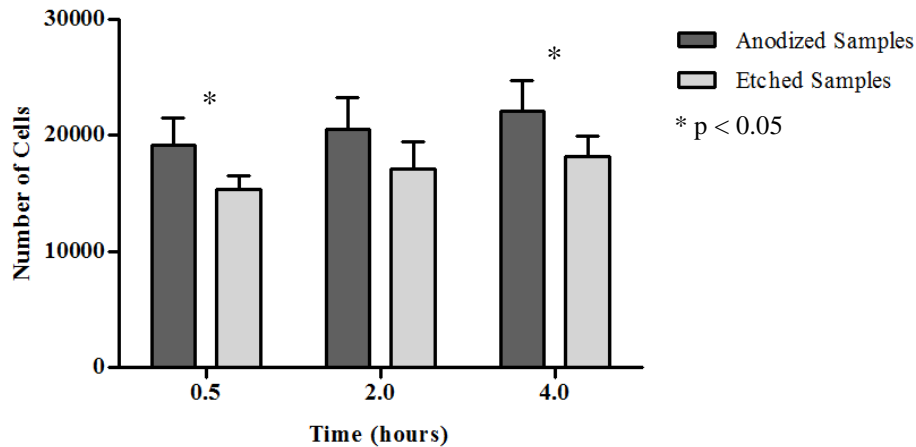


Figure 21. Evolution of the number of osteoblasts MG63 adhered to the anodized and etched surfaces with time. Trial followed from 0.5 to 4 h of incubation at 37°C and 5% CO₂ in air ($p < 0.05$ for 0.5 and 4 h).

The first thing to consider about the previous results (Table 9) is the total number of cells, which increased significantly with time (almost double), compared to the originally plated number, 2×10^4 cells/ml. In the etched and anodized wells this value is almost the same. It seems cells started to proliferate more rapidly on the anodized culture wells but the progression rate, with time, was superior for the etched culture. On the other hand the number on the control culture was slightly smaller. This difference can be explained by the smaller surface area available and the treatments applied. The progression with time was also noticed in the samples surface, where the amount of cells was near to 2×10^4 after 30 min and continued to increase till 4 h of incubation (Figure 21). As happened in previous investigations, using the same type of cells and same culture conditions (98; 147), these indicate that all specimens (medium, plate and sample) offered a biologically favourable environment for osteoblasts MG63 development and progression.

During the three periods of culture, the quantity of MG63 cells attached to the anodized and etched surfaces differed. An improvement was clearly evident for the anodic treated samples, especially at 0.5 and 4 h ($p < 0.05$). This fact is in agreement with Lee et al (148) results, who showed that in the first moments of contact the anodized surfaces detain more cellular affinity than others.

As was extensively discussed in the second chapter, the surface topography plays a major role in the biological response. Multiple researches defend that higher levels of surface roughness affect positively the cells behaviour, in early stages of development (3; 112; 114). Thus, considering the topographic results and the lack of significant differences between both surfaces, it is logical the similarity of the cells attachment levels. However, as was already pointed, there was a smaller, but significative, improvement introduced by the anodized

surfaces. A possible explanation for this fact may rely on the sharp angularity of the etched surface extremes (R_z , vaguely higher than anodized), which may hindered the anchorage of cells on adjacent regions and thus slowed down the process of attachment (149). Another possibility is the probable presence of nanoporosity on the anodized surfaces. By the morphologic analysis it was possible to observe an oxide film with various ranges of pores. According to multiple investigations (100; 150; 151) nanoporosity can enhance the connection between cells and material and by this, if the environment conditions are favourable, increase the cell adhesion and proliferation rates. Besides the previous reasons, the limitations associated with the method used to detach and count the cells could also be in the origin of such differences. It is probable that cells on rougher surfaces are more strongly adhered; therefore some of the cells on the etched surface might remained there after trypsin action.

According to Zhu J. et al (67) and Feng et al (104) other explanation could be in the origin of the highest number of cells in the anodized samples. They defend that the presence of Ca and P on the oxide surface can favour greatly the cells attachment, since these free ions possess the ability of promoting a physical and chemical bond with tissue and, thanks to this, an environment compatible with osteogenesis. A bioactive oxide layer on titanium implants can induce a specific biological activity, capable of attracting the osteoblasts from the surrounding medium and promoting its adhesion.

On the other hand, contradicting Feng et al (104) research are the results from the wettability. On their investigation, they concluded that higher hydrophilicity induced cell attachment. Here the opposite happened: anodized surfaces possessed the lower hydrophilicity but the higher number of cells attached. This might be explained by the probable interfacial energies overshadow by the surface topography (especially at a nano scale) and/or composition, which were previously pointed as having great influence on the cells interaction with the biomaterials surface.

2.2 Spreading and Morphology

To attest the results from the adhesion assay, cells' morphological analyses were performed, for the same periods of time (0.5, 2 and 4 h). The results (Figure 22) were observed by Fluorescent Microscopy using *Phalloidin* as a marker, which allows the

coloration of the actin fibres, the main components of the bone forming cells, and by this providing a general observation of the cells' cytoskeletal organization.

The interaction between cells and surface is a complex process that involves numerous proteins from the extracellular matrix (ECM) and multiple steps that must be complete in short periods of time: focal adhesion, combination between proteins and substrate and cell spreading (52). The ECM is responsible for such connection and determines the cell geometry and conformation and, ultimately, the integrity and development of the tissue. Thus, it is intended to understand how osteoblasts interact with the titanium surfaces by means of geometry and surface spreading.

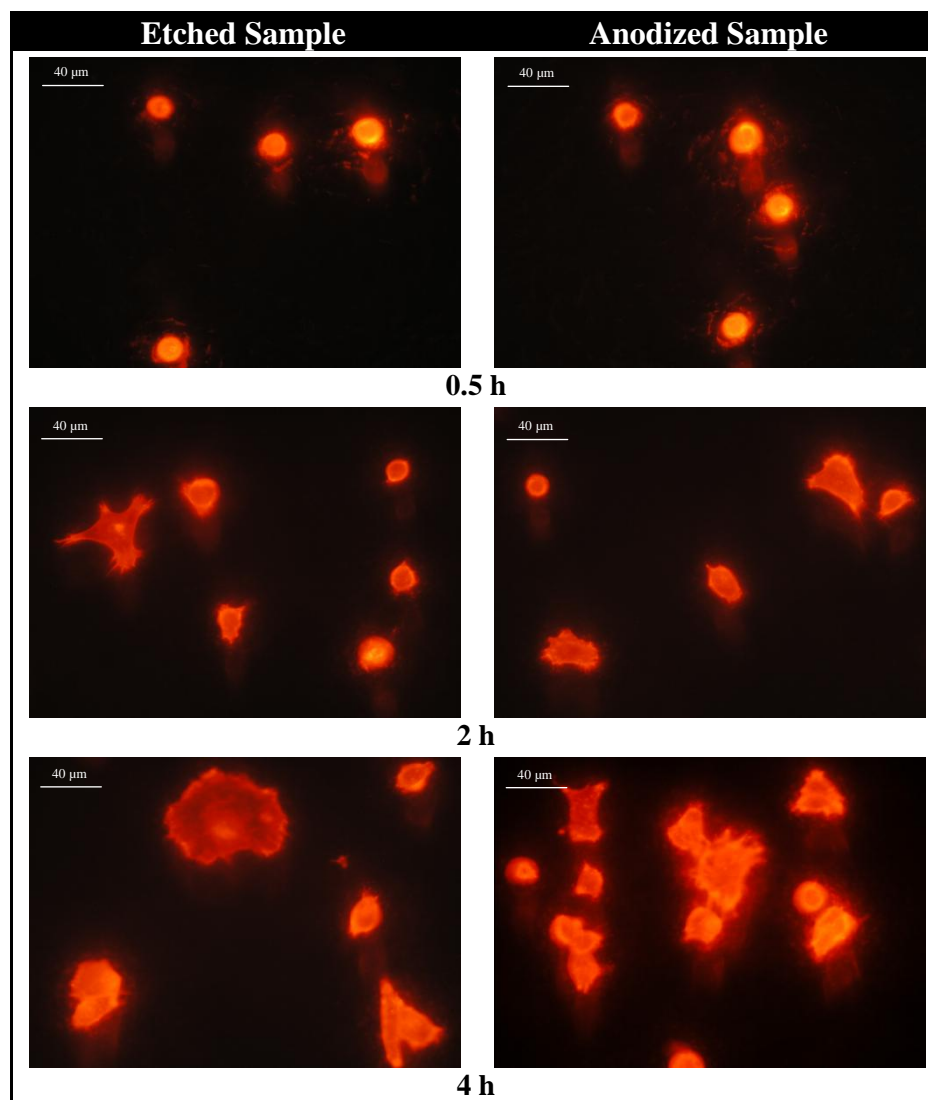


Figure 22. Osteoblasts MG63 morphology and geometry after adhesion on etched and anodized samples after 0.5, 2 and 4 h of culture. The images were obtained by fluorescent microscopy using *Phalloidin* to colour the actin fibres (resolution of 40X and scale = 40 µm).

From 0.5 to 4 h of culture, there was a significant change on the osteoblasts conformation and spreading above the etched and anodized surfaces. However, no visual significant changes were evident between the two surfaces.

As the images showed (Figure 22), the cells evolved, with the passage of time, from a round shape to a more stretch and elongated aspect. After 30 min of contact, the majority of cells still presented a more spherical profile. Since the time was not yet sufficient for the development of a strong connection and for the evolution of the cells into the Ti surfaces, no prolongations of the cells cytoplasm were evidenced, in both samples. Feng et al (104) defends that, at this point, cell adhesion should be only based on chemical interactions rather than physical ones, which explains the osteoblasts conformation. They also supported that bioactive surfaces should present much stronger interactions given that both calcium and phosphate ions are capable of adsorbing proteins as cell ligands and through this stimulate adsorption of proteins and osteoblasts adhesion. However, since adhesive force assays were not conducted on this investigation such statement cannot be confirmed.

After 2 h of culture the heterogeneity of the cells attached to the surfaces is much more evident: some are already elongated, others presented a polygonal shape and some are still round. Few spherical shaped cells exhibit already small extensions of the cytoplasm. This indicates that they are starting the first phase of physical contact, finding strong points of interaction with the surface to support their evolution (104).

After 4 h of culture, almost 80% of the osteoblasts, in both surfaces, exhibited, already, an elongated or polygonal shape representative of the typical morphology of the osteoblasts. According to Angelis et al (144) this typical conformation consists in a central spherical body with the cytoplasm extending away from the central area in all directions and adhering to the titanium surfaces with filamentous protrusions. Using fluorescent microscopy such aspect is difficult to assess, and therefore, SEM analysis was used to elucidate it (Figure 23). Due to the irregularity of the surface, at this moment, the orientation of the osteoblasts is not yet well defined. They spread in all directions without concerning for posterior occupations.

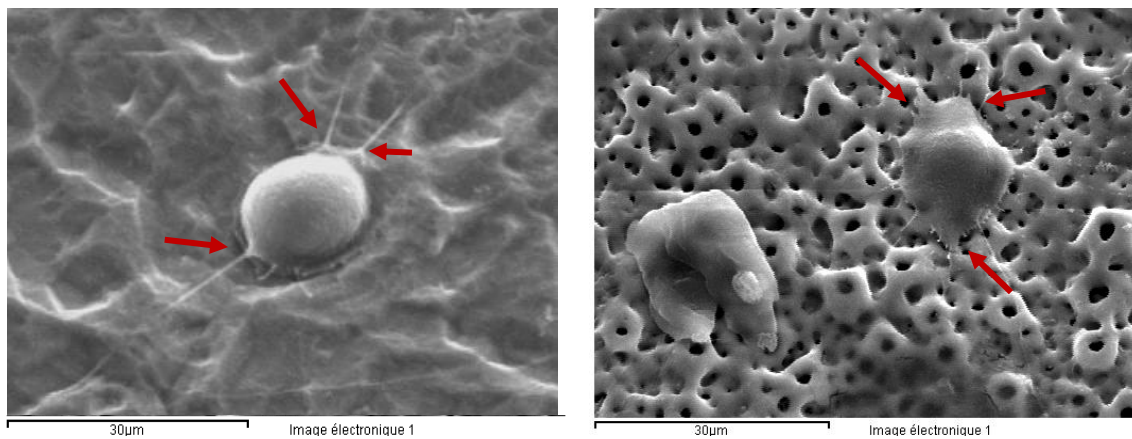


Figure 23. SEM micrographies of osteoblasts MG63 on (A) etched and (B) anodized samples with 2000x of magnification. These are representative of the osteoblasts dispersion above the samples' surface after 4 h of culture.

To confirm the previous evaluations on the extension and shape of the osteoblasts, a correlation between those and the Zhu X. et al (81) attached cells division was preformed (Table 10).

Table 10. Analogy between the osteoblasts aspect after 0.5, 2 and 4 h of culture and the cell division introduced by Zhu X. et al (81).

Division	Significance of Zhu et al Division	Correspondence*
Not Spread	Cells were still spherical in appearance, protrusions or lamellipodia were not yet produced.	0.5 and 2 h
Partially Spread	Cells began to spread laterally at one or more sides, but the extensions of plasma membrane were not completely confluent.	2 and 4 h
Fully Spread	Extension of plasma membrane to all sides, combined with distinctly larger surface area than the previous stages and obvious flattening of the cell.	Mostly 4 h

* The correspondence relates to the results from the present Master Thesis research.

Besides the visual analysis, it was also conducted a dimensional investigation (osteoblasts size). Each cell from each group of cells present in the captured images (Fluorescent Microscopy observation) of both surfaces was analysed individually. Using a specific software, the shape of the cells was delineated and the size analysed, like Figure 24 suggests.

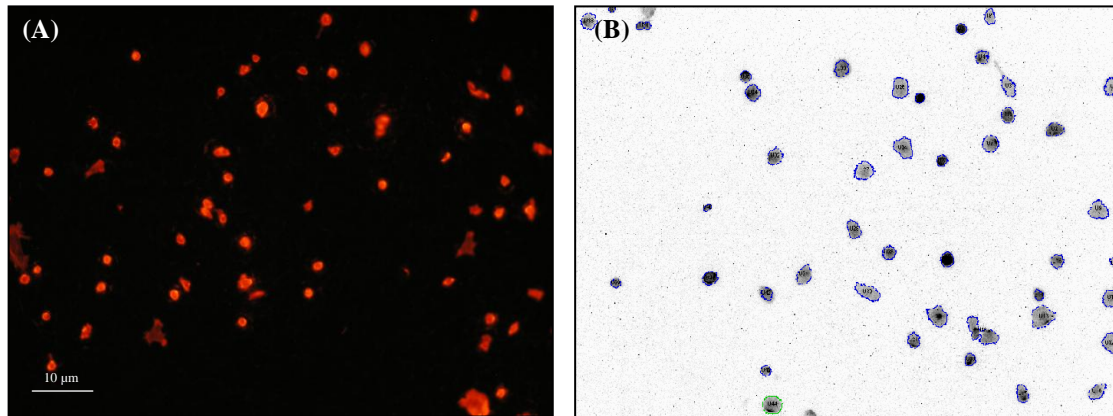


Figure 24. (A) Osteoblasts conformation and spreading after 4 h of culture above an anodized surface. Image taken using Fluorescent Microscopy and Phalloidin as marker (resolution of 10X and scale = 10 μm). (B) Conversion of the image B to format *.tif* for shape and size analysis.

As a result from this analysis, three graphic representations were obtained, indicating the average size of the cells according to the total number of cells found in each picture and the time of contact with the materials surface (Figure 25).

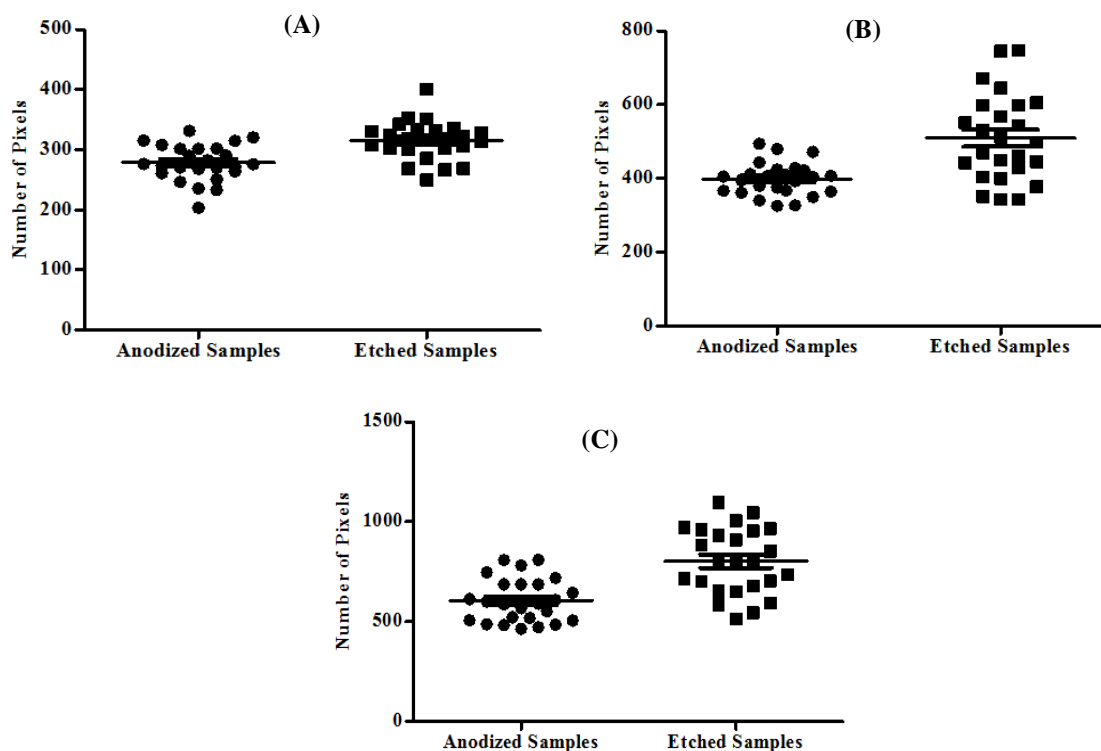


Figure 25. Osteoblasts dimension after (A) 0.5 h, (B) 2 h and (C) 4 h of incubation onto anodized and etched Ti surfaces.

During adhesion and spreading, special structures are formed between cell and substrate, and the cellular skeleton is reorganized to adapt and maintain their viability (152). These facts are corroborated by the results showed on Figure 25. With the passage of time and

the evolution of the cell adhesion, the aspect of the cells changed and, at the same time, its size increased – extensions on the cytoplasm skeletal of the cellular organisms were observed on Figure 23. From 30 min to 4 h, cells started to expand above the anodized and etched surfaces exhibiting a distinctly larger surface area than the previous stages and a more obvious flattening of the cells. These results are in agreement with Hélyary et al (153) investigation which concluded that after 4 h of culture, the MG63 cells are already spread and exhibit a large surface area, with evident protrusions in connection with the titanium surfaces.

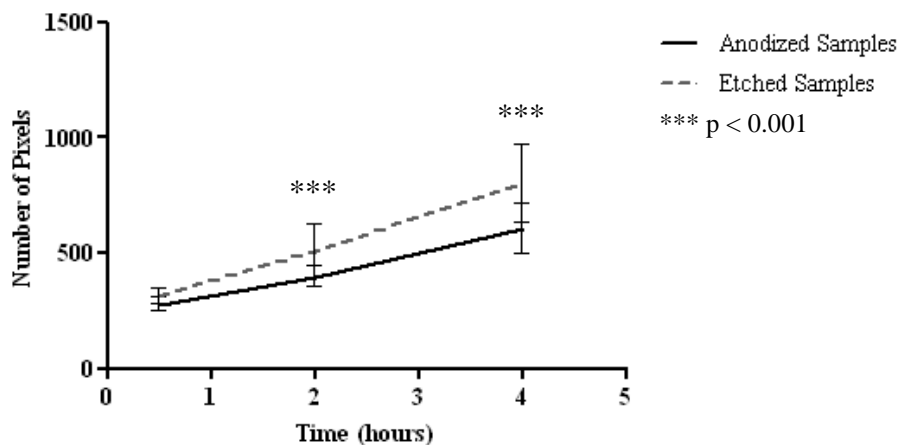


Figure 26. Evolution of the osteoblasts MG63 dimension on the anodized and etched samples, with time.

Comparing the results from the etched and anodized samples, it is clear the faster evolution of the cells size on the etched surface, for all periods of time (Figure 26). Even at 30 min a small difference is detected, although not significant. This distinction becomes more consistent at 2 and 4 h ($p < 0.001$), having the average of the cells size approximately 100 and 200 pixels superior to the anodized numbers, respectively. One possible hypothesis for this phenomenon, knowing that there are no significant differences on the surface roughness between the two types of surfaces, may be set up on the presence of small size pore geometry formed during the anodic treatment. This irregular porosity could be in the origin of stronger forces between cells and the material surface, inducing, this way, an intense resistance to the cells spreading tendency. Because of the uneven distribution of pores and peaks, the surface may exert different amounts of resistance against the spreading of the cells. The same thing was verified by Zhu X. et al (154) on the bone cells response to micro- and submicron-scale porous titanium surfaces. Another possibility for these results could be related to the higher hydrophilicity of the etched samples. Lots of investigations have shown that this property is intrinsically related to the attachment of cells and their posterior spreading, shape and

orientation above the surfaces (138; 139; 155). It is reported that surfaces with more hydrophilicity develop more focal points of contact with cells by protein binding and this way incite more intensively their spreading above the surfaces.

2.3 Proliferation

The osteoblasts MG63 proliferation was evaluated quantitatively from 1 to 14 days of culture, as well as their viability.

After each incubation time, the percentage of cells adhered to the surface was determined. The MG63 cells presents on the sample, on the plate and in the medium of each well were counted – the quantitative evaluation was performed using an Automatic Cell Counter – and the viability evaluated. The graphic representations (Figure 27) relate the disposition of the cells (percentage) in the culture and the incubation periods of time. The viability was determined as between to 91 and 97%, for the three cultures (etched, anodized and control), during the entire trial.

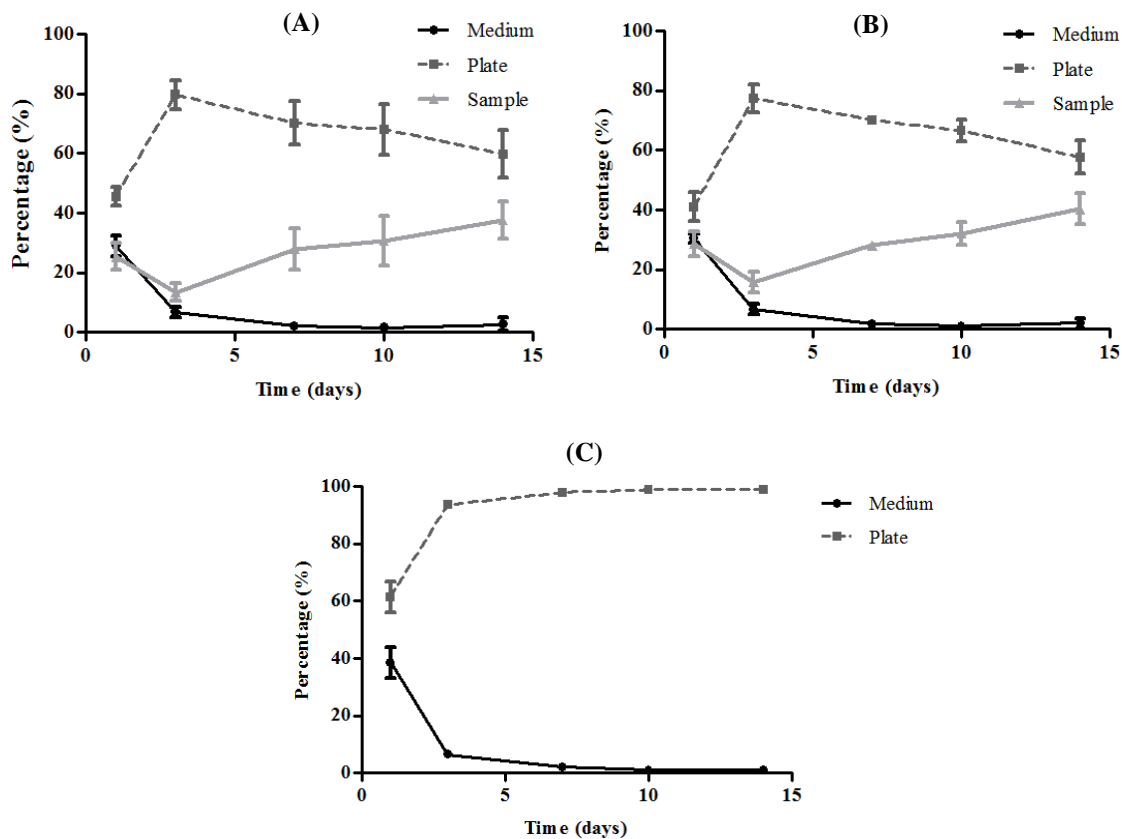


Figure 27. Evolution of the osteoblasts MG63 proliferation on (A) etched and (B) anodized surfaces from 1 to 14 days of culture (5 periods of time). (C) Control results obtained by the direct culture on the plate (without any sample), for the same periods of time.

The same cellular evolution pattern is observed in both etched and anodized surfaces. After 1 day of incubation, the majority of cells is connected to the surfaces ($\approx 70\%$), but mostly to the plate (42-47%). At the 3rd day, the percentage of MG63 cells on the medium decreases intensively (achieving less than 10%) leading to an extraordinary enhancement of the percentage of cells on the plate. This means that the proliferation rate is much more intense in the plate during the first moments of cellular evolution than in the samples, probably due to its properties (surface treatment, sterilization process or charge), which may induce this type of behaviour. From the 3rd day to the 14th, for both anodized and etched surfaces, an improvement is observed on the surfaces cellular proliferation ($\approx 40\%$, at day 14 for both cases) leading to a reduction in the percentage of cells on the plate. Through this, it was possible to notice that osteoblasts MG63 on etched and anodized surfaces experiment the highest evolution rates after the 3rd day.

All these results are consistent to the control (Figure 27C). As it was pointed before, initially the cells are still divided between the medium and the surfaces. However, with the evolution in time, especially after 3 days of incubation, an enhancement in the cells interaction with the plate is observed, reaching almost 100% (99.9%). This means that from 1 to 14 days the entire cellular development (proliferation, in this case) takes place on the samples or plate surface. For a more accurate analysis, the totality of cells on each well (Table 11) must be evaluated as well as the actual number of cells fixated onto the samples' surface (Figure 28).

Table 11. Total number of cells presents on each well, considering medium (M), surface of the plate (P) and sample (S), according to the trial duration (1 to 14 days).

Time (days)	Total number of cells on each well (M+P+S)		
	Anodized	Etched	Plate (Control)
1	5.52E+04	5.58E+04	5.53E+04
3	2.34E+05	2.35E+05	2.36E+05
7	7.22E+05	6.31E+05	7.40E+05
10	1.06E+06	9.98E+05	1.36E+06
14	1.42E+06	1.39E+06	1.98E+06

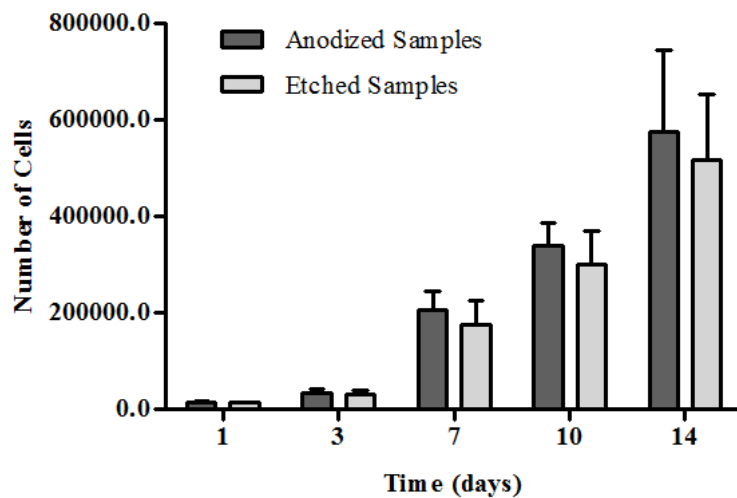


Figure 28. Evolution of the number of osteoblasts MG63 on the anodized and etched surfaces, with time. Trial followed from 1 to 14 days of incubation at 37°C and 5% CO₂ in air (no significant differences $p > 0.05$).

The total number of cells (Table 11) increased significantly with time, more than 35 times, compared to the originally plated number (4×10^4 cells/well). The cellular growth in the anodized and etched cultures was very similar for the entire assay. On the other hand, the control exhibited a small improvement, which became more evident for the last days of culture. This variation can be explained (theoretically) by the adhesion strength between the osteoblasts and the samples. The culture plates present a very smooth surface, thus the probability of detaching the totality of cells, after trypsinization is near to 100%. In contrast, the etched and anodized surfaces are very rough, so it is possible that some of the osteoblasts remained attached to the surfaces even after 20 min of trypsin action (maximum time applied for the 14th day of culture).

Once again, these results proved the viability of the environment (medium, plate and sample) for osteoblasts MG63 development and progression (98; 147).

Comparing the results from Figure 28, it is clear, especially from the 7th day till the end of the assay, a slight improvement on the anodic proliferation numbers, but, as before, no significant differences were detected ($p > 0.05$). This lack of significance was also confirmed visually by the cells confluence above the etched and the anodized surfaces, after 7 and 14 days of culture (Figure 29).

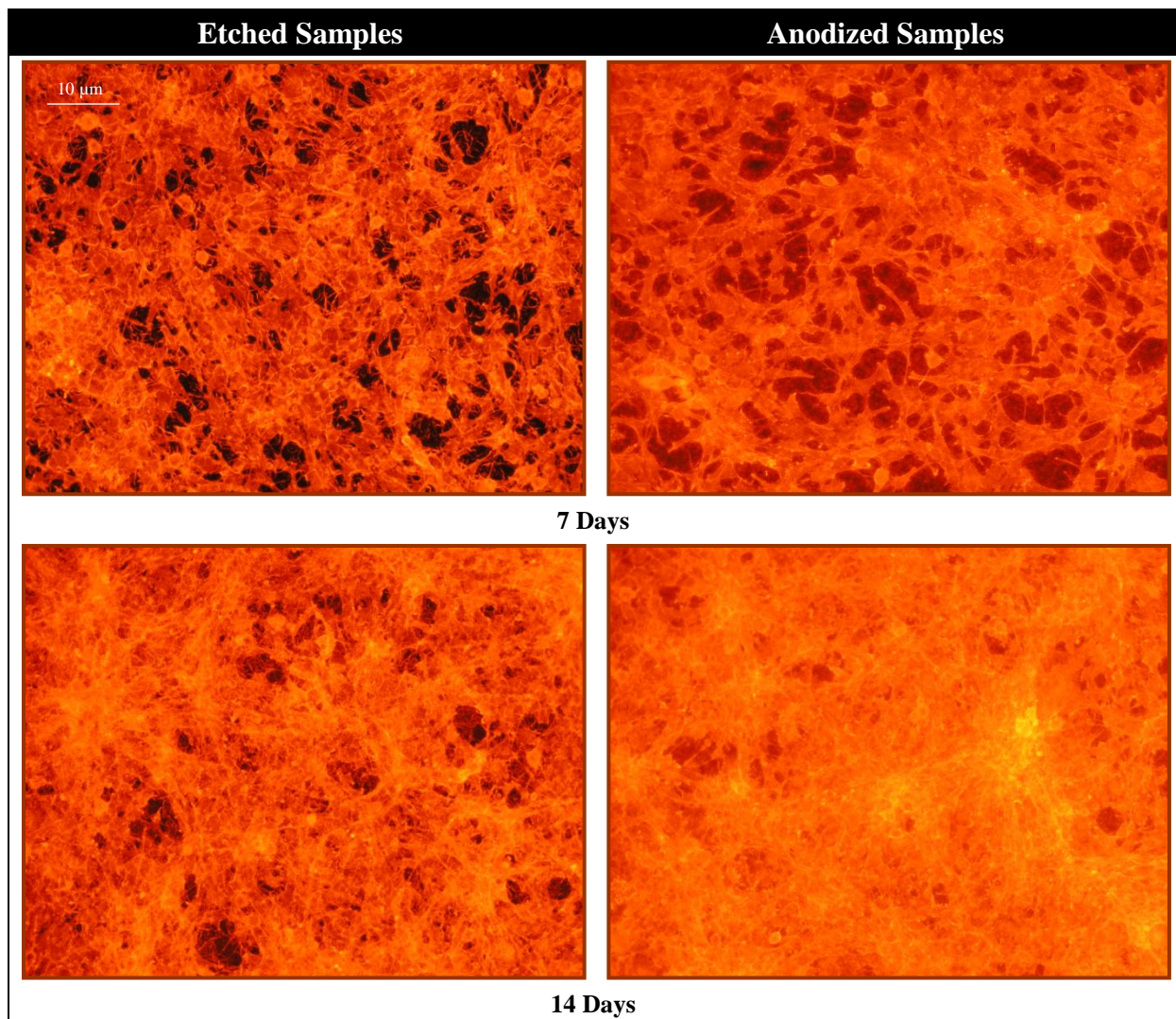


Figure 29. Osteoblasts MG63 confluence on etched and anodized samples after 7 and 14 days of culture. The images were obtained by fluorescent microscopy using *Phalloidin*, to colour the actin fibres (resolution of 10X and scale = 10 μm).

Establishing a line of evolution, that starts on the adhesion assay and finishes on the 14th day of proliferation, it is possible to see that, even after 4h of culture, the number of cells attached to the anodic surface was slightly superior. Thus, based on this, it is natural that if there were more cells in the beginning, and considering the viability similar for both samples, more cells should also be noticed in the end (the initial number is multiplied during time thanks to the environment/culture conditions) (144; 148). Besides, the presence of calcium and phosphorus on the anodic surface could also work as an instigator for the osteoblasts evolution. Another possible explanation could be related to the higher hydrophilicity of the etched surface, which may induced higher immediate cellular adhesion strength, inhibiting this way the cells proliferation on this surface (104).

2.4 Alkaline Phosphatase (ALP) Activity

The osteoblasts MG63 differentiation was followed from 7 to 28 days of culture (4 periods). It was evaluated by the cells enzymatic activity, more precisely through the alkaline phosphatase activity, which is an indicative of the osteoblastic functional evolution and, usually, its presence is coincident with the bone formation.

The ALP is an enzyme present in the cellular membrane, capable of liberating phosphate to the ECM. This, on its turn, will induce a second phase (marker) of bone evolution, the mineralization (precipitation of calcium phosphate) (156).

The following graphic representation (Figure 30) shows the ALP concentration progress with time.

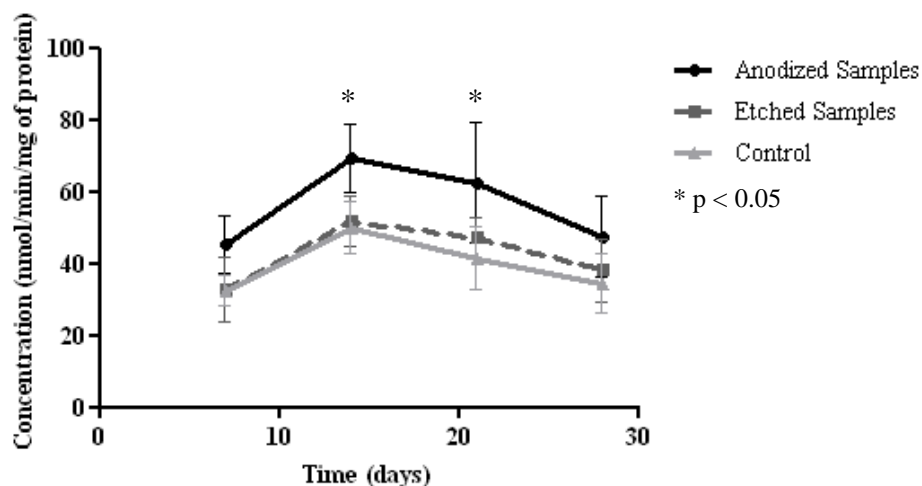


Figure 30. Evolution of the ALP activity with time (from 7 to 28 days of culture; control = culture directly on the plate surface, without sample) – significant results were detected for 14 and 21 days of culture, $p < 0.05$.

These results are in agreement with previous investigations (153) that illustrated the higher level of ALP activity in the 14th day of the osteoblasts culture. It is also consistent with the highest point of metabolic activity, indicating, this way, the initial phase of the extracellular matrix formation. As was expected, the ALP values from the beginning of the trial (day 7) were the lowest ones, in all cases. This happened because in the beginning of the osteoblasts MG63 evolution, the proliferation is the dominant phase (157). After the 14th day, a decrease in the ALP concentration is evident, for the three specimens, which can be explained by the beginning of the second phase of the osteoblasts differentiation, the mineralization (maturation of the ECM).

According to Kim et al (147) generally the surface roughness affects negatively the cells proliferation rate, but increases the ALP activity. In this case, the exact opposite happened for both samples: the proliferation rates were significantly improved with time (more than 35 times) but the ALP results were lower (even for the anodized samples), comparing with previous researches (153). The only result that agrees with Kim et al studies is the control and this happens due to the smoothness of the plate surface. A possible reason for this may rely on the surface wettability. Zhao et al (124) studied the MG63 osteoblast-like cells growth on modified titanium surfaces and concluded that the hydrophilicity of the surfaces allow an intense osteoblast differentiation by increasing the ALP activity. Since both surfaces are hydrophobic it could explain the decrease in the ALP levels, for both samples.

The anodized samples presented a superior ALP concentration relatively to the etched samples, for the entire trial (especially at 14 and 21 days of culture, $p < 0.05$). The fact behind these results is related to the difference in the surface composition. While the etched samples only possessed titanium on the surface, the anodized had calcium, phosphorus and oxygen besides titanium. Studies have shown (72; 106) that the presence of calcium and phosphorus can induce cell differentiation and therefore the enhancement of the ALP concentrations, especially in the presence of a complete medium (ascorbic acid and β -glycerophosphate favours this development). That happens thanks to the similarity of these components to the inorganic phase of bone (60%), which is translated by bone affinity.

2.5 Mineralization

The second phase (or marker) of the bone differentiation, mineralization, was followed for 4 periods of time: 7, 14, 21 and 28 days of culture. To induce this stage of development two components were added to the culture medium, ascorbic acid and β -glycerophosphate.

The mineralization phase corresponds to the ECM maturation, which is the last stage of the bone formation. During the ALP activity, the phosphate liberated interacts with the calcium present on the medium and induces the formation of the inorganic phase of bone.

The graphic representations below show the calcium (Figure 31A) and phosphate (Figure 31B) concentrations evolution with time.

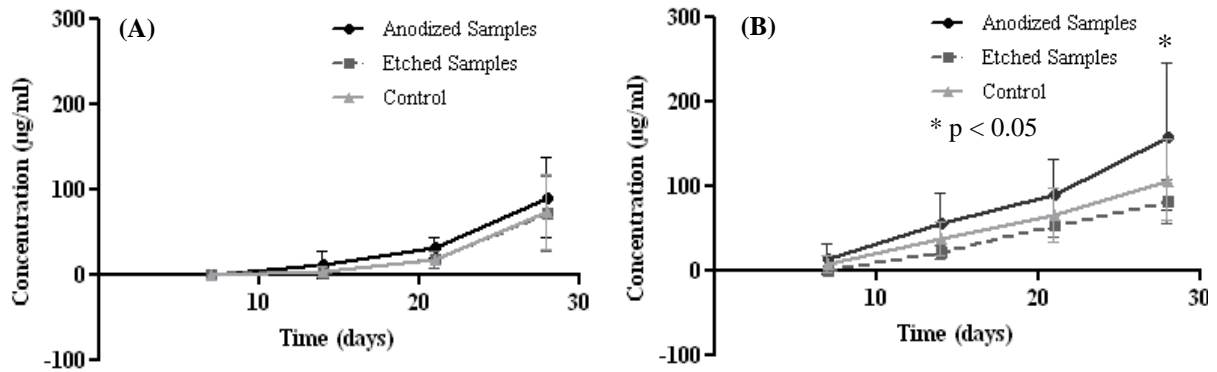


Figure 31. Evolution of the (A) calcium and (B) phosphate levels with time (from 7 to 28 days of culture).

Analysing both representations it is possible to see that there are no significant differences between the three specimens (anodized, etched and control). However, once again, a small improvement is noticed for the anodic samples, both on the calcium and phosphate levels (no significant differences ($p > 0.05$), except for the 28th day on the anodized phosphate levels, $p < 0.05$). The reason behind this improvement is on the samples composition. As it was pointed before, for the ALP results, the presence of calcium and phosphorus on the biomaterials surface has a crucial role on the induction of the osteoblast like-cells differentiation. These components mimic the constitution of the primary inorganic phase of bone, favouring, this way, the affinity between cells and biomaterial. This standpoint is supported by many authors (106; 116; 153). However, on their researches, the difference between bioactive surfaces and the other types was significant, for both calcium and phosphate levels. The explanation for this is related to the type of bioactive surface produced. In this case, only free ions of calcium and phosphorus were identified on the titanium surfaces (previous analysis conducted by the PhD student from the same research group, Alexandra Alves), while the other investigations showed calcium phosphate groups. Since those favour considerably more the interaction and posterior development of MG63 osteoblasts, it could be the motive behind that discrepancy.

Based on the previous knowledge that pointed the importance and influence of the calcium and phosphorus ions on the anodic surface, it was expected that the stoichiometric ratio of calcium phosphate (Ca/P) was equal to 1.67, the standard (100; 106). Instead, it was 0.67, which is translated by higher production of phosphate than calcium, and the same pattern was followed by the other surfaces (etched equal to 0.69 and control equal to 0.67). A possible explanation for such results could be related to the medium composition. Ascorbic acid ($C_3H_7O_6PN_{a_2}.xH_2O$) and β -glycerophosphate ($C_6H_6Na_3O_9P.xH_2O$) were added to the

medium culture to induce the differentiation of the osteoblasts and subsequently mineralization. Their chemical composition does not include calcium, but phosphorus and oxygen ions (present in the phosphate: PO_4^{2-}) are in abundance. Thus, the combination of those with other free ions of phosphorus and oxygen on the system might lead to an improvement of phosphate and consequently to this ratio. Another probable explanation could be the possible liberation of free ions from the samples surface (especially from the anodic sample), which may have conducted to interferences on the absorbance measurements and consequently to these results. Besides a possible conjugation between the available calcium ions with other components could also be in the basis of such grades. Unfortunately, since no XPS analyses were conducted these expostulations cannot be proved.

Another interesting aspect on the results is the similarity between the MG63 cells behaviour on the control plate and the etched surface. According to previous analysis, it was expected that the etched surface presented a more intense production of calcium and phosphorus than the control, especially since the surface roughness is completely different. Many studies have shown that rougher surfaces can favour the ECM maturation (112; 114). However, considering the plate treatment (to induce cells interaction and development) and the proliferation rates on the two surfaces, which showed a much higher quantity of cells attached to the plate than to the etched surface (correlation between the results from Figure 27 and Table 11), it is possible to justify the improvement of the calcium and phosphate production on the plate and, through this, the resemblance of both results.

3. OSTEOBLASTS RESPONSE TO TRIBOLOGICALLY MODIFIED SURFACES

The MG63 cells morphology and spreading above the normal and the tribologically changed surfaces was investigated for three periods of time: 4 h, 3 and 7 days. Given that, with the passage of time, the analysis of the individual cells morphology becomes harder, on this study, that evaluation was just performed for 4h. For the 3 and 7 days, instead of an individual analysis a global one was conducted, which included cells morphology, spreading and confluence.

The following SEM micrographies show the individual aspect of the osteoblasts MG63 on the etched (Figure 32) and anodized (Figure 33) normal and tribologically changed (TRIBO, 0.8 N of load) surfaces.

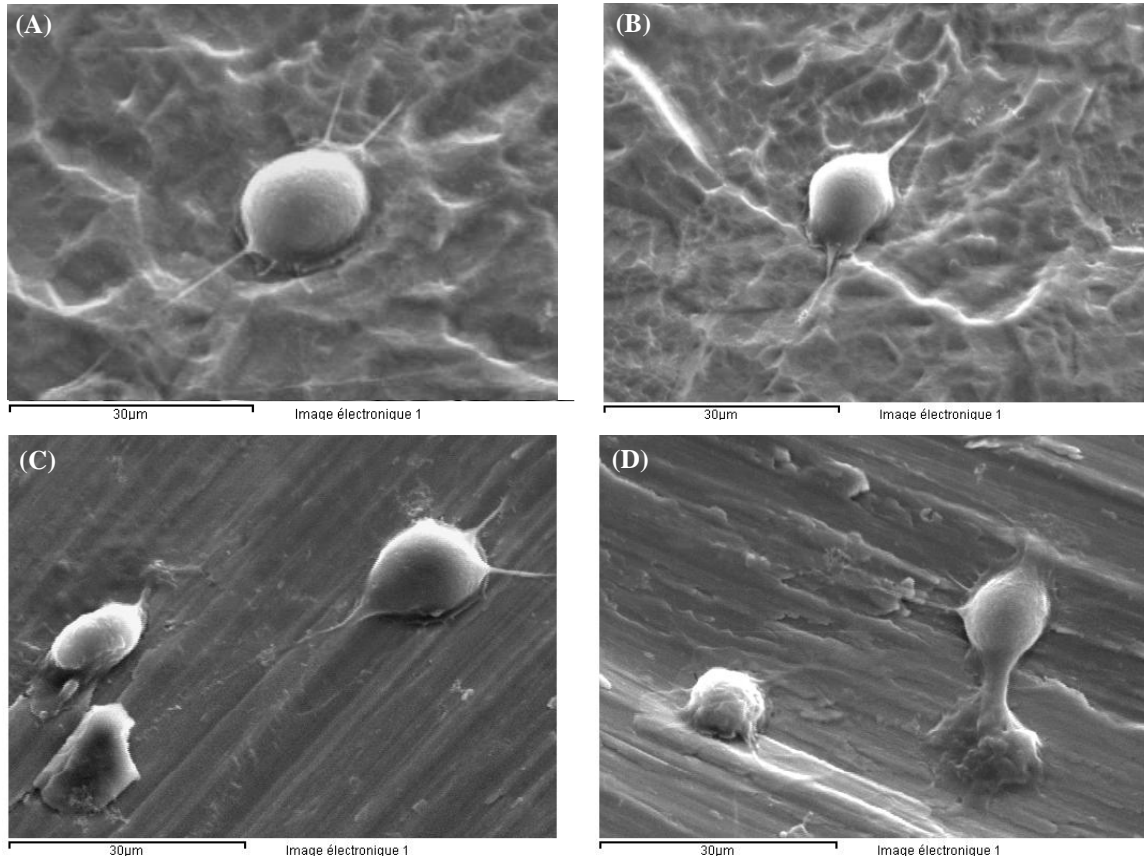


Figure 32. SEM micrographies representative of osteoblasts MG63 dispersion on the etched samples after 4 hours of culture (2000x of magnification). (A) and (B) images on the normal surface, and the (C) and (D) on the wear track (centre of the samples).

The pin-on-disc approach used during the tribocorrosion assays induced the formation of a wear track on the centre of the etched and anodized samples. Through a macroscopic visualization of the etched samples, the only difference detected between the wear track and the rest of the surface was the brightness of the central ring. Usually, this brightness is associated with smoother surfaces. This conclusion was proven to be correct by the surface morphology correlation of A and B (rougher) with C and D (smoother) images from Figure 32.

Many studies have shown that osteoblasts express a higher tendency to spread and interact with rougher surfaces (3; 112; 114). From Figure 32 results, such information is difficult to attest with 100% of conviction. However, considering these images as representatives of the entire surface and doing an analogy between the groups of cells present on each image, differences on the behaviour (according to the type of surface) can be noticed. The osteoblasts MG63 from Figure 32 A and B exhibited a very similar conformation: central spherical body, with the cytoplasm extending away from the central area in all directions (144), forming different points of interaction with the etched surface. On the contrary, Figure

32 C and D revealed osteoblasts with irregular shapes and sizes (heterogeneous behaviour): some cells presented a polygonal form, others exhibited already extensions of the cytoplasm and a more elongated/flattened profile, but there were some that still displaying a spherical shape as if the physical interaction with the surface was not yet complete. Another interesting aspect about the osteoblasts conformation, on the TRIBO surface, is the tendency of the protrusions to be connected with rougher regions present on the ring area. This might indicate that MG63 cells need these points of contact to maintain the consistence and cohesion of the interface.

Regarding the anodized samples (Figure 33), a very similar observation can be made.

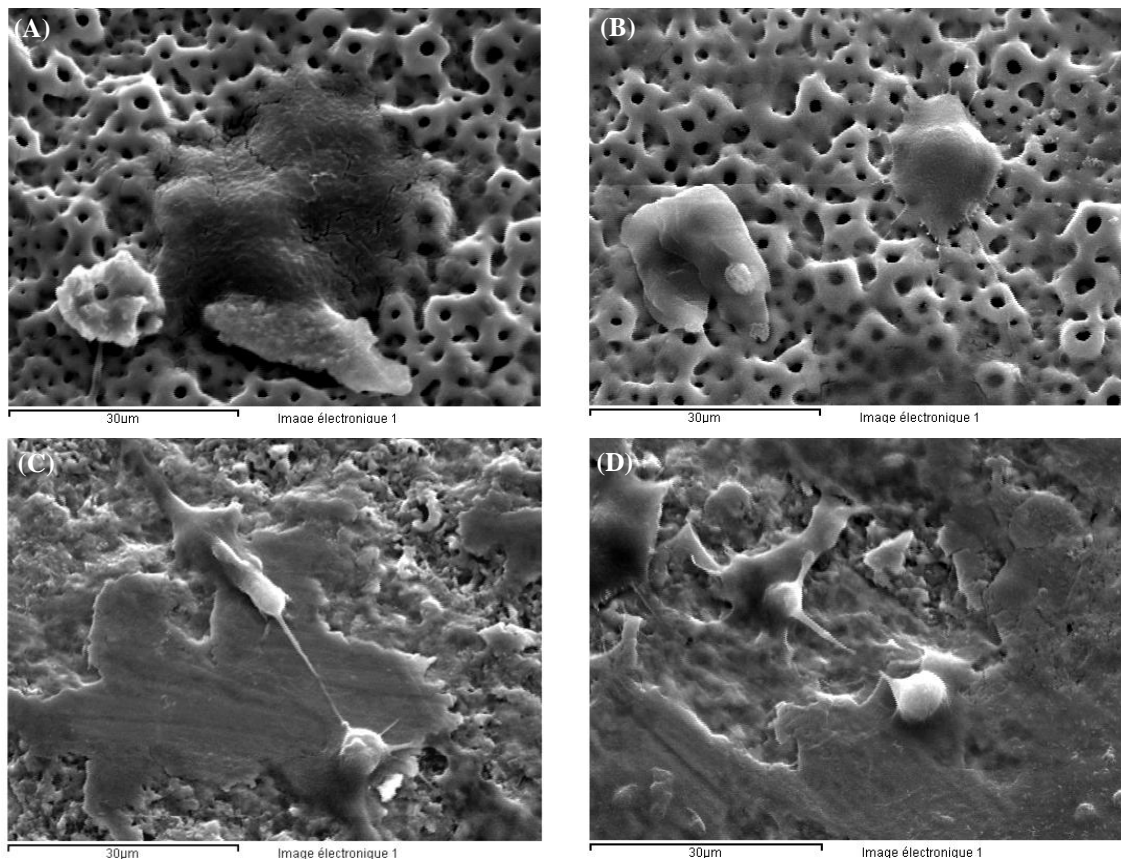


Figure 33. SEM micrographies representative of osteoblasts MG63 dispersion on the anodized samples after 4 hours of culture (2000x of magnification). (A) and (B) images on the normal surface, and the (C) and (D) on the wear track (centre of the samples).

The macroscopic observation of the anodized wear track was a bit different from the etched. In this case, the central ring formed was smaller and, instead of brighter, it was darker, putting in evidence the pure titanium surface. By the SEM micrographies (Figure 33), it was evident that the pin-on-disc approach was not as effective as it was on the etched surface, where a complete and well defined wear track was formed. Here, only disperse smooth

regions were found. The explanation behind this result is based on the resistance of the anodic oxide layer, which is superior compared to the resistance of the etched treatment (3; 102).

As happened for the etched surface, the MG63 cells exhibited a more evident tendency to interact with the rougher regions (normal surface). In Figure 33 A and B is possible to see that the majority of cells are already well spread above the surface, presenting cytoplasm extensions in all directions. Besides, Figure 33 A, put in evidence an advanced stage of interaction, where the cells are completely integrated with the surface (in the etched samples this is much difficult to identify since the cells and the surface present similar coloration). In Figure 33 C and D, the osteoblasts MG63 exhibited two types of physical morphology: mainly spherical in the areas that contact directly with the smooth regions and flatted and well spread in the frontier between this and the normal surface. Once again, it is evident the strategic distribution and dispersion of the osteoblasts, in order to be in contact with the anodic surface (normal). It is well known that the presence of a bioactive oxide layer can increase the interaction between the titanium and the biological environment (106), thus, it is not a surprise that the cells preferred to interact with the anodic (presence of Ca and P and rougher) surface instead of the wear track (smoother).

One of the objectives of this assay was to attest the capacity of osteoblasts to interact with tribologically altered surfaces. The results pointed a slower integration process, since the majority of the cells for both etched and anodized samples revealed a more round shape, although this does not invalidate their ability of interacting and establishing a strong connection. Through this, it is possible to extrapolate (theoretically) a probable response for *in vivo* implantations – during and after implantation the material is submitted to forces and to biological fluids action that can damage or altered the original conformation of the surface, although according to the previous results the cells may still be able to interact.

In Figure 34 the results from the osteoblasts MG63 expansion and spreading above the etched and anodized surface, after 3 and 7 days of culture, are presented. These results confirm the previous conclusion, indicating a slower but possible interaction between MG63 cells and TRIBO surfaces (tribologically altered).

In both cases, etched and anodized, after 3 days of culture, the cellular behaviour changed completely. The cells covered almost the entire material surface and became much more difficult to distinguish individual cells; however it was still clear the prevalence of polygonal shaped cells with many adhesion points at the surface and with a more fattened

morphology. The cellular conformation and progression followed the surface topography and morphology. At 7 days of culture, well defined cellular tissues covering larger areas on the etched and anodized samples, preferentially on the normal surfaces, were observed – some regions were not yet completely filled with cells. According to Angelis et al (144), a complete and confluent monolayer is only accomplished between 14 and 28 days of culture.

Comparing the TRIBO with the normal surfaces, it was evident the cells preference for the normal surface, in both etched and anodized cultures. After 7 days of incubation, there were still observed lots of “depopulated” regions on the wear track and this remark was much more obvious at the etched samples due to the larger TRIBO surface area. On the anodized samples, parts of the wear track were by now (7 days) completely covered with cells, but, in some empty regions, the cells orientation seemed to prevail from the anodic to the TRIBO surface, as it was observed for the 4 h trial.

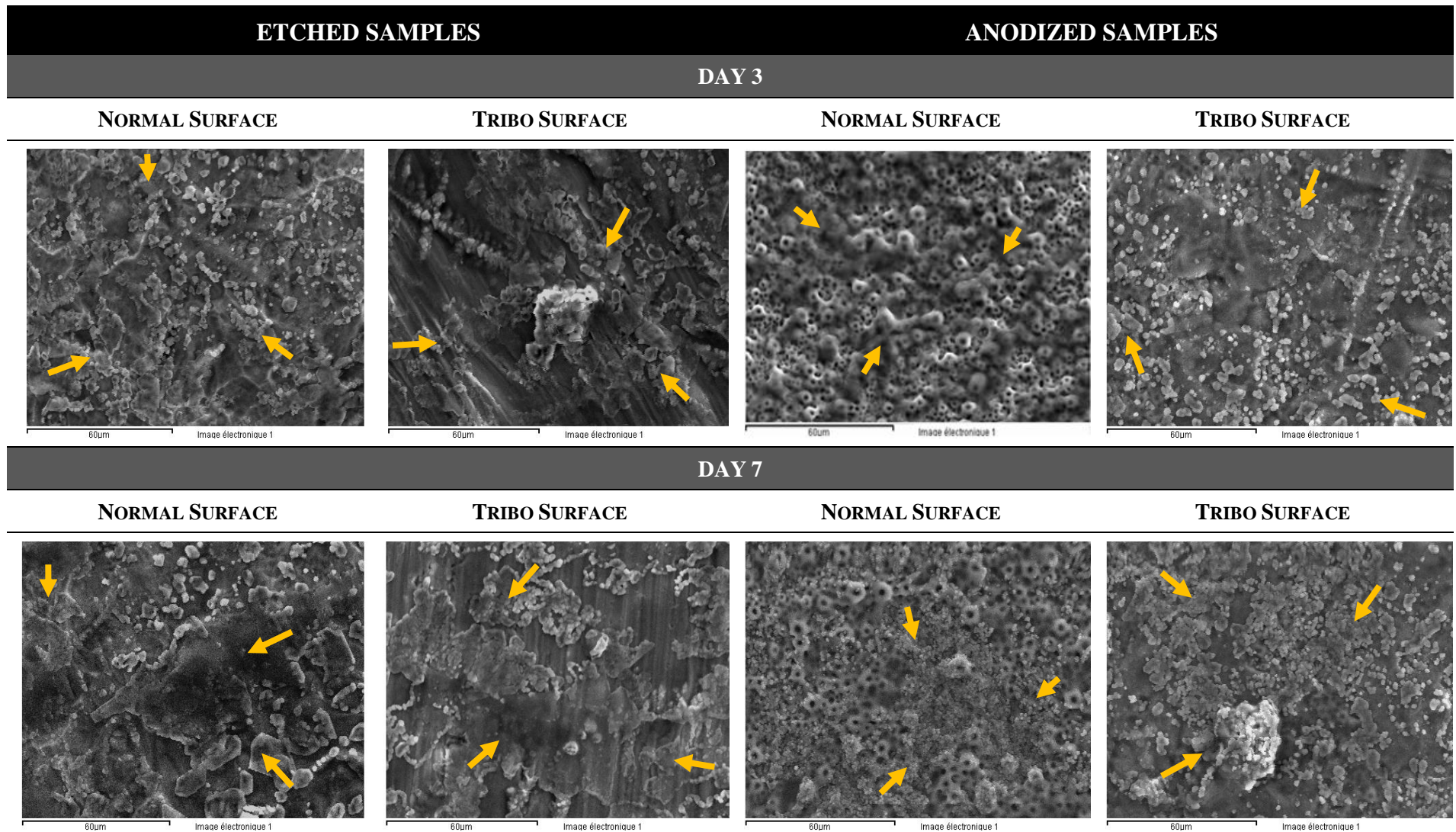


Figure 34. SEM micrographies of osteoblasts MG63 cultured on etched and anodized surfaces, for 3 and 7 days (magnification 1000 X). The designation “TRIBO Surface” indicates the visualization on the wear track (→ assembly of osteoblasts).

CHAPTER 5:

**CONCLUSIONS AND
FUTURE PERSPECTIVES**

CONCLUSIONS

The main objective behind this work was to prove the viability of anodic surfaces for future applications in dental implants. To get there multiple analyses were conducted:

- The morphology, composition, topography and wettability of the surface, before any culture, were tested;
- Biological assays, including adhesion, morphology, proliferation, differentiation and mineralization, using MG63 osteoblast-like cells were conducted to assess the surface viability;
- MG63 cells culture on tribologically altered titanium surfaces were performed to attest the ability of osteoblasts to interact with them.

Regarding the first evaluations on the anodized and etched surfaces, it was possible to observe a significant change on the morphology and surface composition. The etched samples exhibited a rough and crimped surface only composed by titanium. On the other hand, the anodized, also very rough and with a similar undulation as the previous, presented a heterogeneous (size) porous layer, composed by titanium, oxygen, calcium and phosphorus – the last two derived from the anodic treatment electrolyte. Through the topographic measurements, the roughness of the surfaces was determined, although without the differences expected. The surface roughness was similar in both cases (only microtopographic evaluations were conducted; there was no nanotopographic analyses). The same happened with the contact angle analyses, concluding that the anodized and etched samples were hydrophobic – presented negative values of surface free energy. A slightly lower value, although, was noticed for the etched samples regarding the surface energy.

The biological assays were followed from few moments of contact to several days and weeks. The adhesion results showed a great facility of MG63 cells to interact with the samples surface even after 30 min of contact. A small, but significant ($p < 0.05$ for 0.5 and 4 h of culture), improvement in those numbers was noticed in the anodized samples during the entire test, probably thanks to the porosity or the presence of Ca and P on the surface. These elements are known to be great instigators of the osteoblasts biological response, since they mimic the natural composition of bone. Through the morphological evaluation, for the exact same periods of time, the spreading and size of the cells was followed. As a result, it was seen that MG63 cells spread quicker on the etched samples ($p < 0.001$) than on the anodized, but in

both cultures extensions of the cytoplasm, after 4 h of incubation, were already evident. In this case, the explanation behind the etched improvement could be related to the surface wettability. It is reported that surfaces with higher hydrophilicity develop more focal points of contact by protein binding and, this way, incite more intensively their spreading above the surfaces.

According to the proliferation results, MG63 osteoblast-like cells were able to continue the progression on the two surfaces, achieving approximately 35 times more cells (total number – sample + plate + medium) than the original plated number, after 14 days of incubation. As was observed in the adhesion results, a slight enhancement of the anodic samples was evident, although not significant. Thus, it is natural that if there were more cells in the beginning, and considering the viability similar for both samples, more cells in the end should also be noticed for the anodic samples. Besides, the presence of Ca and P on the anodic surface could also work as an instigator for the osteoblasts evolution.

The MG63 differentiation was followed by the enzymatic activity of the alkaline phosphatase from 7 to 28 days of culture. It was observed that the highest levels of ALP were obtained at the 14th day, in agreement with previous researches. This was also consistent with the highest point of metabolic activity, which indicates the initial phase of the extracellular matrix formation. However, once again, the surface composition played an important role and the presence of Ca and P on the anodic samples conducted to a significant improvement on the ALP levels ($p < 0.05$) – these two elements have a great influence in the osteoblasts maturation process. The same happened for the second phase of ECM maturation, mineralization, however the improvement was not significant. In the course of the previous results, it was possible to identify a complete and well defined line of evolution for the osteoblasts, with the highest differentiation rates at 14 days and the maturation of the ECM matrix after that.

Through the TRIBO assays, followed from 4h, 3 and 7 days, it was possible to attest the resistance of the anodic surface treatment, given that only dispersed regions on the central ring were really affected and became smother – the etched exhibited a well defined and complete wear track. Regarding the osteoblasts development, it was confirmed the MG63 cells preference for rough surfaces, in both etched and anodized samples, indicated by a more advanced morphological aspect of cells (more spread, elongated, flattened and expanded cells) on the normal surfaces in analogy to the TRIBO. One interesting phenomenon observed was the strategic cells distribution and dispersion on the wear track. It was evident that cells

on these smooth regions presented a more spherical body but the cytoplasm extensions were preferentially connected to rougher areas, which probably would offer more cohesive points of interaction (sustain the interface). Besides, it was also noticed a slower cells progression on the TRIBO surface in analogy to the normal, in both cases. However, this did not invalidate their ability to interact and establish strong connections.

Therefore, it can be concluded that no significant differences were found between the etched and the anodized samples, pointing this way the validity and positive performance of the etched treatment, which could not be overpassed by the anodic.

FUTURE PERSPECTIVES

Previous researches have shown the improvements introduced by the anodic bioactive treatment on the interaction between cells and biomaterial. In this case, however, such improvement was not that obvious. Thus, one important thing to do, before following to the next step of this research, is to verify all the components and conditions related to the samples preparation and even if possible change the layer composition for phosphate ions instead of phosphorus.

Another thing that is necessary to analyze carefully is the titanium surface used: more topographic and morphologic assays should be done, especially at a nanoscale size; the chemical composition should also be followed using both EDS and XPS analysis to identify possible chemical groups that could influence the cellular response, such as mineralization; and contact angle analysis should be repeated a considerable number of times, to assure the reproducibility of the results. Besides, the cellular adhesion strength should also be considered as an important point to test the osteoblasts interaction to these surfaces as well as the identification and quantification of the focal points between them.

To achieve more accurate results and to establish a much closer line between this *in-vitro* study and the actual results on the human being, the cellular line used could be changed for a primary line, also derived from the human osteosarcome.

BIBLIOGRAPHY

1. **Guéhenec, L. L., et al.** Surface treatments of titanium dental implants for rapid osseointegration. *Dental Materials*. 2007, Vol. 23, pp. 844–854.
2. **Ho, C. and Spry, C.** *Specifications of Endosseous Dental Implants: A Review of the Advantages, Disadvantages, and Success Rates*. Canada : Health Technology Inquiry Service, 2009 .
3. **Gabbi, C., et al.** Osteogenesis and bone integration: the effect of new titanium surface treatments. *Ann. Fac. Medic. Vet. di Parma*. 2005, Vol. 25, pp. 307-318.
4. **Craig, R.G. and Powers, J.M.** *Restorative Dental Materials*. Eleventh edition. USA : Mosby, Inc., 2002.
5. **Ratner, B.D., Hoffman, A.S. and Schoen, F.J. and Lemons, J.E.** *Biomaterials Science: An introduction to materials in medicine*. First Edition. USA : Elsevier Academic Press, 1996.
6. **ADA, American Dental Association.** Titanium applications in dentistry. *JADA*. 2003, Vol. 134, pp. 347-349.
7. **EA, Encarta Association.** *Encarta*. [Online] 2008. http://encarta.msn.com/dictionary_561538208/alloplastic.html.
8. **Iacono, V. J.** Dental Implants in Periodontal Therapy. *Journal Periodontol*. 2000, Vol. 71, 12, pp. 1934-1942.
9. **Knight, J.** Types of dental implants. *Fitzgerald Dental Implant Center*. 2007.
10. **Radford.** Implant Parts. *Radford*. [Online] 2005. <http://www.radfordheath.com>.
11. **Pye, A. D., et al.** A review of dental implants and infection. *Journal of Hospital Infection*. 2009, Vol. 72, pp. 104-110.
12. **Misch, C.E., Poitras, Y. and Dietsch-Misch, F.** Endosteal Implants in the Edentulous Posterior Maxilla. *Oral Health*. 2000, pp. 7-16.
13. **Brunski, J.B.** Biomaterials and Biomechanics in Dental Implant Design. *Journal Oral Maxillofac Implants*. 1998, Vol. 3, pp. 85-97.
14. **Quirynen, M., Soete, De and Van Steenberghe, D.** Infectious risks for oral implants: a review of the literature. *Clinic Oral Implant Restoration*. 2000, Vol. 13, pp. 1-19.
15. **Al-Johany, S., et al.** Dental patients' awareness and knowledge in using dental implants as an option in replacing missing teeth: A survey in Riyadh, Saudi Arabia. *The Saudi Dental Journal*. 2010, Vol. 22, pp. 183–188.
16. **Brånemark, R., et al.** Osseointegration in skeletal reconstruction and rehabilitation: A Review. *Journal of Rehabilitation Research and Development*. 2001, Vol. 38, 2, pp. 175–181.

17. **Misch, C.E. et al.** Implant Success, Survival, and Failure. *Implant Dentistry*. 2008, Vol. 7, 1, pp. 5-15.
18. **Adya, N., et al.** Corrosion in titanium dental implants: literature review. *The Journal of Indian Prosthodontic Society*. 2005, Vol. 5, 3, pp. 126-131.
19. **Kieswetter, K., et al.** Surface roughness modulates the local production of growth factors and cytokines by osteoblast-like MG63 cells. *Journal of Biomedical Materials Research*. 1996, Vol. 32, pp. 55-63.
20. **Lee, C. K., Karl, M. and Kelly, J. R.** Evaluation of test protocol variables for dental implant fatigue research. *Dental Materials*. 2009, Vol. 25, pp. 1419–1425.
21. **Deng, H., et al.** *Current Topics in Bone Biology*. London : World Scientific Publishing, 2005.
22. **Kutz, M.** *Biomedical Engineering and Design Handbook*. Second Edition. USA : MacGraw Hill, 2009. Vol. 1.
23. **Clarke, B.** Normal Bone Anatomy and Physiology. *Clinical Journal of the American Society of Nephrology*. 2008, pp. 131-139.
24. **Afonso, A. S.** *Interação entre Biomateriais e Tecido Ósseo*. Faculdade de Medicina Dentária da Universidade do Porto. Porto : s.n., 1998.
25. **Gogakos, A.I., et al.** Bone Signaling Pathways and Treatment of Osteoporosis: Bone Cell Biology. *Expert Rev Endocrinol Metab*. 2009, Vol. 4, 6, pp. 639-650.
26. **Bosetti, M.** Regulation of Osteoblast and Osteoclast Functions by FGF-6. *Journal of Cellular Physiology*. 2010, pp. 466-471.
27. **Stains, J.P. and Civitelli, R.** Cell-Cell Interactions in Regulating Osteogenesis and Osteoblast Function. *Birth Defects Research (Part C)*. 2005, Vol. 75, pp. 72-80.
28. **Hill, P.A.** Bone Remodelling. *British Journal of Orthodontics*. 1998, Vol. 25, 2, pp. 101-107.
29. **Mandalunis, P.M.** Remodelación Óssea. *Actualiz Osteología*. 2006, Vol. 2, 1, pp. 16-18.
30. *Bone Remodelling Model of a Basic Multicellular Unit*. **Wendling-Mansuy, S., et al.** France : ISB XXth Congress - ASB 29th Annual Meeting, 2004. p. 107.
31. **Roche, F.H.L.** Disturbed balance in bone remodelling. *Roche*. [Online] 2011. <http://www.roche.com/pages/facets/11/ostedefe.htm>.
32. **Lilly, E.** *The Bone Remodelling Process*. s.l. : Eli Lilly and Company, 2001.
33. **Winet, H.** The role of microvasculature in normal and perturbed bone healing as revealed by intravital microscopy. *Bone*. 1996, Vol. 19, 1, pp. 39S-57S.

34. **Hijazy, A. et al.** Quantitative monitoring of bone healing process using ultrasound. *Journal of the Franklin Institute*. 2006, Vol. 343, pp. 495–500.
35. **Kalfas, I.H.** Principles of bone healing. *Neurosurg Focus*. 2001, Vol. 10, 4, pp. 1-4.
36. **Shih, A.T. and Zainalabidin, Z.** *Bone Healing*. USA : American College of Foot and Ankle Surgeons, Health Care PLC: Advanced Eye and Foot Care, 2008.
37. **Gutierrez, M., et al.** Substitutos Ósseos: Conceitos Gerais e Estado Actual. *Arquivos de Medicina*. 2006, Vol. 19, 4, pp. 153-162.
38. **Kretlow, J.D. and Mikos, A.G.** Tissue Engineering: A Historical Perspective. Chapter1. *TISSUE ENGINEERING FOR THE HAND - Research Advances and Clinical Applications*. [Online] <http://www.worldscibooks.com/lifesci/7808.html>.
39. **Cheng, L., et al.** Osteoinduction of hydroxyapatite/b-tricalcium phosphate bioceramics in mice with a fractured fibula. *Acta Biomaterialia*. 2010, Vol. 6, pp. 1569–1574.
40. Biomateriaux en perodontie: Classification & Bases Biologiques de L'Osteo Integration. 2003, 5, pp. 57-67.
41. **Manso, M.C. and Lang, R.D.** *Enxerto ósseo retro-molar "onlay" para restauração ideal do contorno do rebordo alveolar*. Brasil : s.n., 2000.
42. **Branemark, P.-I.** Introduction to Osseointegration. [book auth.] P.-I. Branemark, G.A. Zarb and T. Albrektsson. *Tissue-Integrated Prostheses: Osseointegration in Clinical Dentistry*. Sweden : Quintessence Publishing Co., Inc., 1985, 1, pp. 11-76.
43. **Williams, D. F.** *The Williams Dictionary of Biomaterials*. Liverpool : Liverpool University Pree, 1999.
44. **Albrektsson, T.** Bone Tissue Response. [book auth.] P.-I. Branemark, G.A. Zarb and T. Albrektsson. *Tissue-Integrated Prostheses*. Sweden : Quintessence Publishing Co., Inc., 1985, 6, pp. 129-143.
45. **Sul, Y.-T.** The significance of the surface properties of oxidized titanium to the bone response: special emphasis on potential biochemical bonding of oxidized titanium implant. *Biomaterials*. 2003, Vol. 24, pp. 3893–3907.
46. **Brånemark, B.K.** Schematic drawing of the principles of osseointegration. *The Brånemark Osseointegration Center (BOC)*. [Online] 2010. <http://www.branemark.se/Osseointegration.html>.
47. **Dimitriou, R. and Babis, G.C.** Biomaterial osseointegration - Enhancement with biophysical stimulation. *J Musculoskelet Neuronal Interact*. 2007, Vol. 7, 3, pp. 253-265.
48. **McCabe, J. F. and Walls, A. W. G.** *Applied Dental Materials*. Ninth Edition. Newcastle : BlackWell Publishing, 2008.

49. **Schenk, R.K. and Buser, D.** Osseointegration: a reality. *Periodontology 2000*. 1998, Vol. 17, pp. 22-35.
50. **Jokstad, A.** *Osseointegration and Dental Implants*. First. Canada : John Wiley & Sons, 2008. ISBN: 978-0-813-81341-7.
51. **Ravanetti, F., et al.** In vitro cellular response and in vivo primary osteointegration of electrochemically modified titanium. *Acta Biomaterialia*. 2010, Vol. 6, pp. 1014–1024.
52. **Baxter, L. C., et al.** Fibroblast and Osteoblast Adhesion and Morphology on Calcium Phosphate Surfaces. *European Cells and Materials*. 2002, Vol. 4, pp. 1-17.
53. **Haj, A.J.E., et al.** Controlling cell biomechanics in orthopaedic tissue engineering and repair. *Pathologie Biologie*. 2005, Vol. 53, pp. 581–589.
54. **Mosher, D.F., et al.** Assembly of extracellular matrix. *Current Opinion in Cell Biology*. 1992, Vol. 4, pp. 810-818.
55. **Jimbo, R., et al.** Protein Adsorption to Surface Chemistry and Crystal Structure Modification of Titanium Surfaces. *J Oral Maxillofac Res*. 2010, Vol. 1, 3, pp. 1-9.
56. **Yang, Y., Cavin, R. and Ong, J.L.** Protein adsorption on titanium surfaces and their effect on osteoblasts attachment. *J Biomed Mater Res*. 2003, Vol. 67, A, pp. 344-349.
57. **García, A.J. and Reyes, C.D.** Bio-adhesive Surfaces to Promote Osteoblast Differentiation and Bone Formation. *Journal of Dental Research*. 2005, Vol. 84, 5, pp. 407-413.
58. **Curtis, R. V. and Watson, T. F.** *Dental Biomaterials*. Cambridge : Woodhead Publishing Limited, 2008.
59. **Ratner, B.D., Hoffman, A.S. and Schoen, F.J. and Lemons, J.E.** *Biomaterials Science: An introduction to materials in medicine*. Second Edition. USA : Elsevier Academic Press, 2004.
60. **Schmalz, G. and Arenholt-Bindslev, D.** *Biocompatibility of Dental Materials*. Germany : Springer, 2009.
61. **Williams, D. F.** On the mechanisms of biocompatibility. *Biomaterials*. 2008, Vol. 29, pp. 2941–2953.
62. **Oshida, Y. et al.** Corrosion of dental metallic materials by dental treatment agents. *Materials Science and Engineering C*. 2005, Vol. 25, pp. 343-348.
63. **Cordas, C.M.** Biomateriais: utilização e controlo em meios fisiológicos. *Faculdade de Ciências da Universidade de Lisboa*. Vol. s.n., pp. 1-18.
64. **Sevilla, P. et al.** Evaluating mechanical properties and degradation of YTZP dental implants. *Materials Science and*. 2010, Vol. 30, pp. 14-19.

65. **Shalaby, S. W. and Salz, U.** *Polymers for dental and orthopedic applications*. New York : CRC Press, 2007.
66. **Daguano, J. K. M. F. et al.** The ZrO₂-Al₂O₃ composite for dental materials. *Revista Matéria*. 2006, Vol. 11, 4, pp. 455 – 462.
67. **Zhu, J., Yang, D. and Ma, F.** Investigation of a new design for zirconia dental implants. *Journal of Medical Colleges of PLA*. 2007, Vol. 22, 5, pp. 303-311.
68. **Whitters, C.J. et al.** Dental materials: 1997 literature review. *Journal of Dentistry*. 1999, Vol. 27, pp. 401-435.
69. **Zhou, Z.R. and Zheng, J.** Tribology of dental materials: a review. *Journal of Physics: Applied Physics*. 2008, Vol. 41, pp. 1-22.
70. **Maciel, D. et al.** The influence of the composite resins' expiration time on its compression resistance. *Arquivos em Odontologia*. 2005, Vol. 41, 3, pp. 235-241.
71. **Seeley, R. et al.** *Anatomia e Fisiologia*. Third Edition. Lisboa : Lusodidacta, 2001.
72. **Kim, K. H. and Ramaswaswamy, N.** Electrochemical surface modification of titanium in dentistry. *Dental Materials Journal*. 2009, Vol. 28, 1, pp. 20-36.
73. **Santiago, A.S., et al.** Response of osteoblastic cells to titanium submitted to three different surface treatments. *Braz Oral Res*. 2005, Vol. 19, 3, pp. 203-208.
74. **Boyer, R., Welsch, G. and Collings, E.W.** *Materials properties handbook: titanium alloys*. First Edition. USA : ASM International, 1994.
75. **Franchi, M. et al.** Early detachment of titanium particles from various different surfaces of endosseous dental implants. *Biomaterials*. 2004, Vol. 25, pp. 2239–2246.
76. **Zhu, Y. and Watari, F.** Surface Carbonization of Titanium for Abrasion-resistant Implant Materials. *Dental Materials Journal*. 2007, Vol. 26, 2, pp. 245-253.
77. **Iijima, D. et al.** Wear properties of Ti and Ti–6Al–7Nb castings for dental prostheses. *Biomaterials*. 2003, Vol. 24, pp. 1519–1524.
78. **Anusavice, K.J.** *Philips, Materiais Dentários*. Eleventh Edition. s.l. : Elsevier.
79. **Bauer, J.R.O.** Mechanical properties of commercially pure titanium and Ti-6Al-4V alloys casting in different environments. *Universidade de São Paulo*. 2008, Vol. 61.
80. **Kuromoto, N. K., Simão, R. A. and Soares, G. A.** Titanium oxide films produced on commercially pure titanium by anodic oxidation with different voltages. *Materials Characterization*. 2007, Vol. 58, pp. 114–121.
81. **Zhu, X. et al.** Effects of topography and composition of titanium surface oxides on osteoblast responses. *Biomaterials*. 2004, Vol. 25, pp. 4087–4103.

82. **Kasemo, B. and Lausmaa, J.** Metal Selection and Surface Characteristics. [book auth.] P.-I. Branemark, G.A. Zarb and T. Albrektsson. *Tissue-Integrated Prostheses: Osseointegration in Clinical Dentistry*. Sweden : Quintessence Publishing Co., Inc., 1985, 9, pp. 99-116.
83. **Baier, R.E., et al.** Surface properties determining bioadhesive outcome: methods and results. *Journal Biomed. Mater. Res.* 1984, Vol. 18, 4, pp. 337-355.
84. **Albrektsson, T., et al.** Osseointegrated titanium implants. *Acta Orthop. Scand.* 1981, Vol. 52, 2, pp. 155-170.
85. **Therinn, M., Meunier, A. and Christel, P.** A histomorphometric comparison of the muscular tissue reaction to stainless steel, pure titanium and titanium alloy implant materials. *Journal of Materials Science: Materials in Medicine*. 1991, Vol. 2, pp. 1-8.
86. **Tang, G., et al.** Preparation of porous anatase titania film. *Materials Letters*. 2004, Vol. 58, pp. 1857– 1860.
87. **Cai, Z.** Electrochemical characterization of cast titanium alloys. *Biomaterials*. 2003, Vol. 24, pp. 213-218.
88. **Pourbaix, M.** *Atlas of electrochemical equilibria in aqueous solutions*. Second Edition. USA : Nace TX, 1974.
89. **Wolfgang, P.** The characterization of particulate debris obtained from failed orthopedic implants: Chapter 5. [Online] 2000. <http://www.engr.sjsu.edu/WofMatE/projects/srproject/>.
90. **Textor, M.** Properties and biological significance of natural oxide films on titanium and its alloys. [book auth.] D.M. Brunette, et al. *Titanium in Medicine*. s.l. : Springer, 2001, 7, pp. 172-224.
91. **Oliveira, A.L., Malafaya, P.B. and Reis, R.L.** Sodium silicate gel as a precursor for the in vitro nucleation and growth of a bone-like apatite coating in compact and porous polymeric structures. *Biomaterials*. 2003, Vol. 24, 15, pp. 2575-2584.
92. **Hench, L.L., Jones, J.R. and Sepulveda, P.** Bioactive Materials for Tissue Engineering Scaffolds. s.l. : EPSRC, MRC, FAEPE, US Biomaterials Inc., 1996, 1, pp. 3-23.
93. **Marques, C.** *Tratamento de Superfícies de Implantes de Titânio*. Departamento de Ciência e Tecnologia, Instituto Militar de Engenharia. Rio de Janeiro : s.n., 2007.
94. **Depprich, R. et al.** Behavior of osteoblastic cells cultured on titanium and structured zirconia surfaces. *Head & Face Medicine*. 2008, Vol. 4, 29, pp. 1-29.
95. **Ong, J.L., et al.** Effect of surface topography of titanium on surface chemistry and cellular response. *Implant Dent*. 1996, Vol. 5, 2, pp. 83-88.

96. **Byon, E, et al.** Apatite-forming ability of micro-arc plasma oxidized layer of titanium in simulated body fluids. *Surface & Coatings Technology*. 2007, Vol. 201, pp. 5651–5654.
97. **Hanawa, T.** Biofunctionalization of titanium for dental implant. *Japanese Dental Science Review*. 2010, Vol. 46, pp. 93–101.
98. **Hong, M. et al.** A study on osteoblast-like cell responses to surface modified titanium. *J Korean Acad Prosthodont*. 2003, Vol. 41, 3, pp. 300-318.
99. **Koh, J.W., et al.** Biomechanical evaluation of dental implants with different surfaces: Removal torque and resonance frequency analysis in rabbits. *J Adv Prosthodont*. 2009, Vol. 1, pp. 107-112.
100. **Thirugnanam, A., Kumar, T.S.S. and Chakkingal, U.** Bioactivity Enhancement of Commercial Pure Titanium by Chemical Treatments. *Trends Biomaterials and Artificial Organs*. 2009, Vol. 23, 2, pp. 76-85.
101. **Gebran, M.P. and Wassal, T.** Avaliação in vitro da adesão de osteoblasto sobre implantes osseointegráveis com superfície tratada (Titamax II®). *Implant News*. 2007, Vol. 4, 1, pp. 79-84.
102. **Rodriguez, R., Kim, K. and Ong, J. L.** In vitro osteoblast response to anodized titanium and anodized titanium followed by hydrothermal treatment. 2003, pp. 352-358.
103. Electrochemistry. [Online] 1998. <http://cstl-csm.semo.edu/APCHEM/20061012/electrochemistrynotes.htm>.
104. **Feng, B., et al.** Characterization of titanium surfaces with calcium and phosphate and osteoblast adhesion. *Biomaterials*. 2004, Vol. 25, pp. 3421–3428.
105. **Lee, J.M. et al.** Surface Analysis of Titanium Substrate Modified by Anodization and Nanoscale Ca-P Deposition. *J Korean Acad Prosthodont*. 2007, Vol. 45, 6, pp. 795-804.
106. **Zhu, X., Kim, K.H. and Jeong, Y.** Anodic oxide films containing Ca and P of titanium biomaterial. *Biomaterials*. 2001, Vol. 21, pp. 2199-2206.
107. **Cui, X., et al.** Preparation of bioactive titania films on titanium metal via anodic oxidation. *Dental materials*. 2009, Vol. 25, pp. 80–86.
108. **Li, Y., et al.** The biocompatibility of nanostructured calcium phosphate coated on micro-arc oxidized titanium. *Biomaterials*. 2008, Vol. 29, pp. 2025-2032.
109. **Dalby, M.J., et al.** In vitro reaction of endothelial cells to polymer demixed nanotopography. *Biomaterials*. 2002, Vol. 23, pp. 2945–2954.
110. **Oliveira, P.T. and Nanci, A.** Nanotexturing of titanium-based surfaces upregulates expression of bone sialoprotein and osteopontin by cultured osteogenic cells. *Biomaterials*. 2004, Vol. 25, pp. 403–413.

111. **Matsuzaka, K., et al.** The attachment and growth behavior of osteoblast-like cells on microtextured surfaces. *Biomaterials*. 2003, Vol. 24, pp. 2711–2719.
112. **Larsson, C., et al.** Bone response to surface-modified titanium implants: studies on the early tissue response to machined and electropolished implants with different oxide thicknesses. *Biomaterials*. 1996, Vol. 17, pp. 605–616.
113. **Schneider, G.B., et al.** Implant Surface Roughness Affects Osteoblast Gene Expression. *Journal of Dental Research*. 2003, Vol. 82, 5, pp. 372–376.
114. *Effect of Surface Characteristics of Metallic Biomaterials on Interaction with Osteoblast Cells.* **Bren, L. et al.** USA : 7th World Biomaterials Congress, 2004. s.n..
115. **Anselme, K. and Bigerelle, M.** Topography effects of pure titanium substrates on human osteoblast long-term adhesio. *Acta Biomateriali*. 2005, Vol. 1, pp. 211–222.
116. **Das, K., Bose, S. and Bandyopadhyay, A.** Surface modifications and cell–materials interactions with anodized Ti. *Acta Biomaterialia*. 2007, Vol. 3, pp. 573–585.
117. **Chiang, C.-Y.** Formation of TiO₂ nano-network on titanium surface increases the human cell growth. *Dental Materials*. 2009, Vol. 25, pp. 1022–1029.
118. **Stanford, C.M., Keller, J.C. and Solursh, M.** Bone Cell Expression on Titanium Surfaces is Altered by Sterilization Treatments. *Journal of Dental Research*. 1994, Vol. 73, 5, pp. 1061–1071.
119. **Lange, R., et al.** Cell-extracellular matrix interaction and physico-chemical characteristics of titanium surfaces depend on the roughness of the material. *Biomolecular Engineering*. 2002, Vol. 19, pp. 255–261.
120. **Kasemo, B.** Biological surface science. *Surface Science*. 2002, Vol. 500, pp. 656–677.
121. **Macak, J.M., et al.** TiO₂ nanotubes: Self-organized electrochemical formation, properties and applications. *Current Opinion in Solid State and Materials Science*. 2007, 11, pp. 3–18.
122. **D’souza, J. and More, H.N.** *Mercury Intrusion Porosimetry : A Tool for Pharmaceutical Particle Characterization*. s.l. : Pharmainfo.net., 2005.
123. **Rupp, F., et al.** Roughness induced dynamic changes of wettability of acid etched titanium implant modifications. *Biomaterials*. 2004, Vol. 25, pp. 1429–1438.
124. **Zhao, G., et al.** High surface energy enhances cell response to titanium substrate microstructure. *J Biomed Mater Res*. 2005, Vol. 74, A, pp. 49–58.
125. **Kuo, J.** *Electron Microscopy Methods and Protocols*. s.l. : Human Press, 2007. ISBN 13: 978-1-58829-573-6.

126. **Herguth, W.R.** *Applications of Scanning Electron Microscopy and Energy Dispersive Spectroscopy (SEM/EDS) To Practical Tribology Problems*. s.l. : Herguth Laboratories, Inc., 2011.
127. **Goldstein, J., et al.** *Scanning Electron Microscopy and X-Ray Microanalysis*. New York, USA : Springer, 2003. ISBN 978-0-306-47292-3.
128. **Stil.** *Non Contact Measures Solutions*. s.l. : STIL, 2010. E1010.
129. **Bhushan, B.** *Nanotribology and Nanomechanics An Introduction*. s.l. : Springer, 2008. ISBN 978-3-540-77607-9.
130. **Wyant, J.C.** *White Light Interferometry*. Optical Sciences Center, University of Arizona. USA : s.n., 2009. AZ 85721.
131. *White Light Interferometry – a production worthy technique for measuring surface roughness on semiconductor wafers.* **Blunt, R.T.** Canada : s.n., 2006. CS MANTECH Conference. pp. 59-62.
132. **Aderson.** *Scanning White Light Interferometric Microscopy for Surface Topography, Profilometry, and Surface Roughness*. [Web] USA : Anderson Materials Evaluation, Inc., 2007.
133. **Sintef.** *White Light Interferometer (WLI)*. [Web] USA : SINTEF. Inc., 2009.
134. **Hart, R.** Information on Contact Angle. *Ramé-hart Instrument*. [Online] 2011. <http://www.ramehart.com/contactangle.htm>.
135. **Van Oss, C.J.** *Interfacial Forces in Aqueous Media*. 2nd Edition. USA : Taylor and Francis Group, 1994.
136. **Landolt, D. and Mischler, S.** Electrochemical methods in tribocorrosion. *Electrochimica Acta*. 2001, Vol. 46, 24-25, pp. 3913-3929.
137. **Ehrenfest, D.M.D., et al.** Classification of osseointegrated implant surfaces: materials, chemistry and topography. *Trends in Biotechnology*. 2009, pp. 1-9.
138. **Padial-Molina, M. et al.** Role of wettability and nanoroughness on interactions between osteoblast and modified silicon surfaces. *Acta Biomaterialia*. 2011, Vol. 7, pp. 771–778.
139. **Vogler, E.A.** Structure and reactivity of water at biomaterial surfaces. *Adv Colloid Interf.* 1998, Vol. 74, pp. 69–117.
140. **Lim, Y.J. and Oshida, Y.** Initial contact angle measurements on variously treated dental/medical titanium materials. *Bio Med Mater Eng*. 2001, Vol. 11, pp. 325-341.
141. **Kasemo, B. and Lausma, J.** Biomaterial and implant surface: A surface science approach. *Int Journal Oral Maxillofac Implant*. 1988, Vol. 3, pp. 247-259.

142. **Paital, S.R. and Dahotre, N.B.** Calcium phosphate coatings for bio-implant applications: Materials, performance factors, and methodologies. *Materials Science and Engineering R*. 2009, Vol. 66, pp. 1–70.
143. **Bigerelle, M., et al.** Improvement in the morphology of Ti-based surfaces: a new process to increase in vitro human osteoblast response. *Biomaterials*. 2002, Vol. 23, pp. 1563–1577.
144. **Angelis, E.D. et al.** Attachment, proliferation and osteogenic response of osteoblast-like cells culture on titanium treated by novel multiphase anodic spark deposition process. *Journal of Biomedical Materials Research Part B: Applied Biomaterials*. 2009, Vol. 88B, pp. 280-289.
145. **Teixeira, L.J.C. et al.** Cells culture in Oral Implantology: review of literature. *Revista IMPLANTNEWS*. 2009, Vol. 6, 5, pp. 479-483.
146. **Curtis, A.S.G., et al.** Adhesion of Cells to Polystyrene Surfaces. *The Journal of Cell Biology*. 1983, Vol. 97, pp. 1500-1506.
147. **Kim, M.J., et al.** Biological response of osteoblast-like cells to different titanium surface by anodizing modification. *J Korean Acad Prosthodont*. 2005, Vol. 43, 6, pp. 751-763.
148. **Lee, J.M., Lee, J.I. and Lim, Y.J.** In vitro investigation of anodization and CaP deposited titanium surface using MG63 osteoblast-like cells. *Applied Surface Science*. 2010, Vol. 256, pp. 3086-3092.
149. **Lumbikanonda, N. and Sammons, R.** Bone cell attachment to dental implants of different surface characteristics. *Int J Oral Maxillofac Implants*. 2001, Vol. 16, pp. 627-636.
150. **Mendonça, G, et al.** Advancing dental implant surface technology – From micron to nanotopography. *Biomaterials*. 2008, Vol. 29, pp. 3822–3835.
151. **Liu, X., Chu, P.K. and Ding, C.** Surface nano-functionalization of biomaterials. *Materials Science and Engineering R*. 2010, Vol. 70, pp. 275-302.
152. **Gronthos, S, et al.** Integrin expression and function on human osteoblast-like cells. *J Bone Miner Res*. 1997, Vol. 12, pp. 1189-1197.
153. **Hélary, G., et al.** A new approach to graft bioactive polymer on titanium implants: Improvement of MG63 cells differentiation onto this coating. *Acta Biomaterialia*. 2009, Vol. 5, pp. 124-133.
154. **Zhu, X., et al.** Cellular Reactions of Osteoblasts to Micron- and Submicron-Scale Porous Structures of Titanium Surfaces. *Cells Tissues Organs*. 2004, Vol. 178, pp. 13-22.
155. **Ochsenbein, A., et al.** Osteoblast responses to different oxide coatings produced by the sol-gel process on titanium substrates. *Acta Biomaterialia*. 2008, Vol. 4, pp. 1506–1517.

-
156. **Matos, M.A.A. and Sant'ana, F.R.** Identificação da isoenzima óssea de fosfatase alcalina por termoinativação. *Rev Bras Ortop.* 1996, Vol. 31, 3.
157. **Martin, J.Y., et al.** Proliferation, differentiation, and protein synthesis of human osteoblast-like cells (MG 63) cultured on previously used titanium surfaces. *Clin Oral Impl Res.* 1996, Vol. 7, pp. 27-37.